Institut für Wasser und Gewässerentwicklung
Universität Karlsruhe (TH)

River Flood Prediction Systems: Towards Complementary Hydrodynamic, Hydrological and Data Driven Models with Uncertainty Analysis

Rajesh Raj Shrestha

Heft 229

Mitteilungen des Instituts für Wasser und Gewässerentwicklung
-Bereich Wasserwirtschaft und Kulturtechnik-
mit ″Theodor-Rehbock-Wasserbaulaboratorium″
der Universität Karlsruhe (TH)
Herausgeber: Prof. Dr.-Ing. Dr. h. c. mult. Franz Nestmann, Ordinarius

2005

River Flood Prediction Systems: Towards Complementary Hydrodynamic, Hydrological and Data Driven Models with Uncertainty Analysis

Zur Erlangung des akademischen Grades eines

DOKTOR-INGENIEURS

an der Fakultät für
Bauingenieur-, Geo- und Umweltwissenschaften
der Universität Fridericiana zu Karlsruhe (TH)

genehmigte

DISSERTATION

von

M. Sc. Rajesh Raj Shrestha

aus Kathmandu, Nepal

Tag der mündlichen Prüfung: 16.02.2005

Hauptreferent:	Prof. Dr.-Ing. Dr. h.c. mult. Franz Nestmann Universität Karlsruhe (TH)
Korreferent:	Prof. Dr. rer. nat. Dr.-Ing. habil. András Bárdossy Universität Stuttgart

Karlsruhe 2005

ZUSAMMENFASSUNG

Hochwasser sind komplexe dynamische Prozesse, die durch räumliche und zeitliche Variation geprägt sind. Das Verständnis dieser Prozesse und die Fähigkeit, diese in Form von numerischen Modellen nachzubilden sind entscheidend für die Planung und das operationelle Hochwassermanagement. Hydrodynamische und hydrologische numerische Modelle sind bewährte Methoden der Hochwassermodellierung. In den letzten Jahren wurden außerdem Verfahren wie Künstliche Neuronale Netze (KNN), Fuzzy Systeme und genetische Algorithmen zu Werkzeugen weiterentwickelt, die sich für die Hochwassermodellierung eignen. Jedes dieser Modelle basiert auf einer individuellen Philosophie, die sich hauptsächlich in der Modellstruktur, Datenanforderung und Fähigkeiten unterscheiden. Außerdem wohnen den Modellen unterschiedliche Unsicherheiten inne, die aus den Daten und Modellrestriktionen entstehen. Die Unterschiede in den Modellphilosophien und den Unsicherheiten legen nahe, einen sich ergänzenden Modellierungsansatz zu schaffen anstatt die Modelle konkurrierend zu betreiben.

Diese Arbeit wurde angeregt von den Möglichkeiten der verschiedenen ergänzenden Herangehensweisen, die diese Modelle zusammen anbieten. Ziel dieser Arbeit ist es, die verschiedenen Methoden zu identifizieren, zu entwickeln und umzusetzen unter Ausnutzung ihrer individuellen Stärken und unter Berücksichtigung der innewohnenden Unsicherheiten. Motiviert durch die Ergebnisse wurden verschiedene Untersuchungen für den Rhein und den Neckar durchgeführt.

Die Arbeit liefert eine detaillierte Abschätzung der Fähigkeiten von hydrodynamisch-numerischen (HN) und hydrologischen Muskingum-Cunge (MC) Modellen sowie KNN- und Neuro-Fuzzy-Modellen. Die Anwendung der HN-Modelle zeigt die Vielseitigkeit dieser Werkzeuge im Zusammenhang mit der Hochwasser- und Überflutungsflächenvorhersage, insbesondere wenn sie in Kombination mit einem geographischen Informationssystem genutzt werden. Die Abschätzung zeigt außerdem, wie effektiv KNN-, Neuro-Fuzzy- und hydrologische MC-Modelle für nichtlineares Flood-Routing eingesetzt werden können. Diese Verfahren sind besonders effizient, wenn nur die Fließvariablen an den Pegelstellen von Interesse sind.

Jedes dieser Modelle ist jedoch nur mit einer Anzahl von Einschränkungen nutzbar. Es ist bekannt, dass KNN-, Neuro-Fuzzy- und MC-Modelle nur so lange zur zuverlässigen Vorhersage geeignet sind, wie die Eingabedaten innerhalb des Kalibrierungsbereiches bleiben. Zur Beurteilung der Performance von KNN- und Neuro-Fuzzy-Systemen jenseits des Kalibrierungsbereichs wird eine Anzahl von Methoden untersucht. Die Untersuchung

zeigt Möglichkeiten auf, die Vorhersagefähigkeiten dieser Modelle etwas über den Kalibrierungsbereich hinaus zu erweitern.

Weitere Untersuchungen berücksichtigen die Fähigkeit dieser Modelle, Extremereignisse vorherzusagen. Die Ergebnisse des KNN-, des Neuro-Fuzzy- und des MC-Modells wurden mit denen des HN-Modells verglichen. Der Vergleich zeigt beträchtliche Differenzen sowohl in der Größenordnung als auch in der Dauer der Spitzenwerte. Daher betonen die Ergebnisse die Einschränkungen eines einzig auf einem KNN-, Neuro-Fuzzy- oder dem hydrologischen MC-Verfahren basierenden Modells für Vorhersagen jenseits des Kalibrierungsbereichs. In dieser Arbeit wird daher ein Anwendungsbereich für diese Modelle festgelegt.

Die Stärken und Einschränkungen der Modelle sind Grundlage der verschiedenen Kopplungsansätze, die in dieser Arbeit beschrieben werden, bei der sich die Qualitäten der einzelnen Modelle ergänzen. Der erste Ansatz bezieht sich auf die Vorhersage der Wasserstandsganglinien des Rheins. Es wird argumentiert, dass auf Grund der vorliegenden Einschränkungen jedes dieser Modelle die Modellierung mit einem einzigen für eine Hochwasservorhersage nicht ausreichend ist. Beispielsweise können hydrologische, KNN- und Neuro-Fuzzy-Modelle innerhalb des Kalibrierungsbereichs verwendet werden, wo diese leicht anzuwenden sind. Für eine Vorhersage außerhalb des Kalibrierungsbereichs ist das HN-Modell die beste Wahl. Die Nutzung von mehr als einem Modell erhöht außerdem das Vertrauen in die Vorhersage, da die Ergebnisse so gegenseitig validiert und verschiedene Szenarien untersucht werden können.

Die zweite Anwendung bezieht sich auf eine Reihe sich ergänzender Ansätze für die Vorhersage von Hochwasserganglinien und Überflutungsgebieten im Flussgebiet des Neckars. Das HN-Modell kann Ungenauigkeiten aufgrund von Unsicherheiten in den Eingangsdaten (Zuflussganglinien) und dem Fehlen kleinerer seitlicher Zuflüsse aufweisen, insbesondere für Hochwasservorhersagen. Daher wurde in einem kombinierten Ansatz das KNN als Flood Routing Modell und das HN-Modell als Überschwemmungs-Modell genutzt. Das KNN-Modell wird also für die Vorhersage der Durchflussganglinien an den Pegelstellen für ein Hochwasservorhersagesystem genutzt. Die vorhergesagten Spitzenabflüsse können als Eingangswerte für das HN-Modell genutzt werden, welches seinerseits, in Verbindung mit dem digitalen Geländemodell, die Überflutungsbereiche an kritischen Stellen des Flussabschnittes vorhersagen kann.

Diese Arbeit beschäftigt sich außerdem ausführlich mit Unsicherheiten in den Eingabedaten, welche aus Wasserstands-Abflussbeziehungen herrühren. Einige datenorientierte Ansätze werden für das Management, die Analyse und die Fortpflanzung der Unsicherheiten herangezogen. Die Methode des Unsicherheits-Managements umfasst die Beziehung zwischen Wasserstand und Abfluss als Ergebnis der nicht-linearen KNN-Abbildungsmethode als Alternative zu einer klassischen Wasserstands-Abfluss-Beziehung. Dies wird anhand der stark gestreuten, nicht linearen Wasserstands-/

Abflusswerte des Neckars und der geschleiften Wasserstands-Abfluss-Beziehung des Rheins verdeutlicht. Beide Anwendungen zeigen, dass die nicht-lineare, KNN-basierte Abbildungstechnik eine überlegene Alternative zu einer Schlüsselkurve ist. Das Verfahren führt außerdem zu einem seriell ergänzenden Modellierungsansatz. Zum Beispiel kann die nicht-lineare KNN-Abbildungsmethode als Pre- und Post-Prozessor für die Randbedingungen eines Routing-Modells eingesetzt werden.

In dieser Forschungsarbeit werden auch auf dem Fuzzy-Erweiterungsprinzip basierte Methoden für die Analyse und Fortpflanzung von Unsicherheiten als Folge der Wasserstands-Abflussbeziehung betrachtet. Die Fuzzy-Regressions-Analyse wird genutzt, um die oberen und unteren Unsicherheitsgrenzen zu definieren. Diese Analyse definiert Abflüsse als Fuzzy-Zahl zu jedem beliebigen Wasserstand. Der Fuzzy-Alpha-Cut einer Abfluss-Fuzzy-Zahl wird zusammen mit einem HN-Modell genutzt, um die Fortpflanzung von Unsicherheiten in Flussschläuchen und Überflutungsflächen zu bestimmen. Die Arbeit stellt einen Ansatz vor, bei dem sich Fuzzy-Erweiterungsprinzip-basierte Methoden und HN-Modelle seriell ergänzen. Die Ergebnisse zeigen, dass Unsicherheiten im Durchfluss zu entscheidenden Unsicherheiten bezüglich der Wasserstände und der Überflutungsflächen führen können.

Diese Arbeit zeigt die sich ergänzenden Modellierungsansätze für die Hochwasservorhersage sowie eine Unsicherheitsanalyse. Die Anwendung dieser sich ergänzenden Modellierungsansätze wird zu einer verlässlicheren Hochwasservorhersage führen und bessere Entscheidungen für das Hochwasser-Management ermöglichen.

SUMMARY

River floods are complex dynamic processes characterised by spatial and temporal variations. The understanding of these processes and the capabilities to encapsulate them in terms of numerical models are of crucial importance for planning and operational management of river floods. The hydrodynamic and hydrologic numerical models provide such capabilities and represent conventional approaches to river flood modelling. In the recent years, data driven models such as artificial neural networks (ANNs), fuzzy systems and genetic algorithm have also emerged as viable tools for river flood modelling. Each of these models is based on entirely different philosophy, with major differences in model structure, data requirement and capabilities. There are also inherent uncertainties in the application of these models that arise from data and model limitations. The differences in model philosophies and the inherent uncertainties raise the possibility of a complementary modelling approach instead of using them in competitive ways.

This thesis is motivated by the possibilities of different complementary approaches that these models offer together. The main objective of this research is to identify, develop and implement complementary methods, with a focus on combining their individual strengths and managing the related uncertainties. Driven by these objectives, several studies are undertaken using the cases of the Rhine and the Neckar Rivers.

The research makes a detailed assessment of the capabilities of a hydrodynamic numerical (HN) model, a Muskingum-Cunge (MC) hydrological model and an ANN and a neuro-fuzzy system based data driven models. The application of the HN models exhibit versatility of these tools in the context of river flood forecasting and prediction of inundation extent, especially when used in combination with geographic information system. The assessment also shows the effectiveness of the ANN, neuro-fuzzy and MC hydrological models for nonlinear flood routing. These approaches are particularly efficient when only the flow variables at the gauging stations are of interest.

However, each of these models is also affected by a number of underlying limitations. It is well known that the data driven and MC models are only predictive as long as the inputs stay within the calibration range. Uncertainties may arise when they are used beyond the range of training datasets. A number of methodologies are explored to assess the performance of the ANN and neuro-fuzzy models beyond the training data range. In particular, the effect of data normalisation range, different activation functions for the ANNs and membership functions for the neuro-fuzzy systems are considered. The assessment shows the possibilities of extending the prediction capabilities of these models to a certain range beyond the training datasets.

Further assessment considers the ability of these models to forecast extreme events. For this purpose, the results of the ANN, neuro-fuzzy and MC models are compared with the HN model results. The comparisons show considerable differences in magnitudes and durations of peaks. The results hence underline only a limited ability of the ANN, neuro-fuzzy and MC hydrological models to forecast beyond the range of training datasets. Therefore, the range of applicability of these models are defined.

The strengths and limitations of these models are in fact the basis for several complementary modelling approaches considered in this research. The first approach deals with a parallel complementary approach for the prediction of water level hydrographs in the Rhine River. It is argued that due to the underlying limitations of each of these models, it may not be sufficient to use a single model for flood forecasting purpose. As an example, the hydrological and data driven models can be used to forecast within the calibration range, where these models offer ease of use. The HN model is the best option available for forecasting beyond calibration. The use of more than one model also increases the confidence of forecasts as the results can be cross validated and different scenarios can be tested.

The second application considers a series complementary approach for the prediction of flood hydrographs and inundation areas in the Neckar River reach. The HN model may be affected by the imprecision in the input data or the absence of minor tributaries and lateral inflows, especially for flood forecasting purpose. In the series approach, the ANN is used as a flood routing model and the HN model is used as inundation model. Hence, in the flood forecasting system the ANN predicts the discharge hydrographs at gauging stations. The predicted peak discharges can be used as inputs to the HN model, which in combination with the digital terrain model can predict inundation extents at critical sections in the river reach.

This thesis also makes an extensive assessment of data uncertainties that arise out of stage discharge relationship. A number of data driven approaches are considered for the management, analysis and propagation of uncertainties. The method of uncertainty management includes the transformation of stage to discharge using an ANN nonlinear mapping method as an alternative to the rating curve. This is demonstrated using the cases of a highly scattered nonlinear relationship in the Neckar River and a looped stage discharge relationship in the Rhine River. Both the applications show that the ANN based nonlinear mapping technique provides a superior alternative to the single value relationship curve. The method also leads to a possibility of the series complementary modelling approach. For instance, the ANN nonlinear mapping method can be used as pre-processor and post-processor of the boundary data for a flood routing model.

The research further considers fuzzy extension principle based methods for the analysis and propagation of uncertainties due to the stage discharge relationship. The fuzzy regression analysis is used to define the upper and the lower uncertainty bounds of the

relationship. The analysis expresses discharges in terms of fuzzy numbers corresponding to any measured water level. The fuzzy alpha cut of a discharge fuzzy number together with an HN model is used to analyse the propagation of uncertainties in river channels and floodplains. The application constitutes a series complementary approach between the fuzzy extension principle based methods and the HN model. The results indicate that uncertainties in discharges can lead to significant uncertainties in the simulation of water levels and inundation areas.

The thesis hence demonstrates the complementary modelling approaches for river flood prediction and uncertainty analysis. Therefore, application of these complementary methods will lead to more reliable flood prediction and facilitate in making better flood risk management decisions.

ACKNOWLEDGEMENTS

I would like to express my deep sense of gratitude to Prof. Dr.-Ing. Dr. h. c. mult. Franz Nestmann for providing me opportunity and financial support for this research. I am most grateful for his invaluable guidance and suggestions throughout the period of this study.

I would like to convey my gratitude to Prof. Dr. rer. nat. Dr.-Ing. habil. András Bárdossy for his guidance. His invaluable comments and ideas helped me to consolidate my research and bring it to the present shape.

I also take this opportunity to extend my thanks to everybody, especially my colleagues at IWK, who have directly or indirectly helped me during this research. I am grateful to Dr.-Ing. Stephan Theobald for his support and suggestions during our technical discussion. I am also thankful to Dr.-Ing. Peter Oberle for his support, providing me all the data. I am grateful to my colleagues Mrs. Kay Dittner and Dip.-Ing. Swentje Thomas for helping me in English and German corrections. My special thanks goes to present and past staffs of Resources Engineering for their friendship and help in day to day life throughout my stay in Karlsruhe.

I am also grateful to Dr. Shie-Yu Liong from the National University of Singapore for his comments and sharing with me his insights in neural networks.

I would also like to express my deep appreciation to all my family members for the support and understanding during my study in Germany. An important credit for the successful completion of this work goes to my wife Dibyashree Shrestha, for her patience, understanding and encouragement during this long and difficult journey.

CONTENTS

CHAPTER 1

BACKGROUND

1.1 Introduction

River floods are natural phenomena that occur recurrently in a hydrological time scale. The phenomenon is characterised by increased water levels in river channels, overspilling of natural banks or artificial embankments and subsequent inundation of the surrounding floodplains. The floodplains are amongst the most intensely utilised and densely populated areas throughout the world and their inundation can cause extensive damage. With increasing social and economic development bringing pressure on land use within the floodplains, potential for flood damage is increasing on many rivers [White, 2000].

It has almost become a regular phenomenon that several areas in the world suffer from floods every year. In the last decade there has been catastrophic flooding in China, India, Bangladesh, Germany, Poland, Mozambique and the United States [ISDR, 2004]. Asia represents one of the worst flood affected areas in the world, with the countries like Bangladesh, China, India, Vietnam and Nepal being severely affected by floods in a regular basis. The 2002 floods in Elbe, Moldau and Danube rivers were some of the worst floods to hit Central Europe causing losses of billions of Euros in parts of the Czech Republic, Germany and Austria. Other notable flood events in Germany include the Rhine River flood of 1993 and 1995 and the Odra River flood of 1997.

The consequences of floods to the society go far beyond the economic costs. When severe flood occur in the inhabited areas, they bring natural disaster involving loss of life, property plus serious disruption of the ongoing activities in urban and rural communities [Smith and Ward, 1998]. Flood disasters account for about a third of all natural catastrophes by number and economic losses and are responsible for more than half of the fatalities [Berz, 2000].

Traditionally, flood management has essentially been problem driven: usually after a severe flood event a project would be quickly implemented without giving any thought to the impact such solutions would have on upstream and downstream areas [APFM, 2004]. The research in the past few decades has led to a better understanding of different processes and sub-processes of river flooding and their interactions with the surroundings. As a result there is now a shift in paradigm towards a broader integrated approach to manage the recurrent cycle of flood disasters in a more effective manner. The United Nations guidelines for reducing flood losses [ISDR, 2004] describes the flood

disaster management as an end-to-end process for recognizing the risks through a suite of planned actions which include: (i) pre-disaster – preventive measures and preparedness; (ii) during the flood – disaster relief, response and mitigative actions; and (iii) post disaster – rehabilitation, reconstruction, economic recovery, and efforts to assess and fine tune the preventive measures.

Integrated flood management should hence investigate each of these actions in every phase of disaster management. Systematic analysis and management tools are essential for the evaluation of these broad range of parameters and planning for the alternative course of actions. Furthermore, flood management contains a number of semi-structured and non-structured problems, which require a modelling capability to grasp and manage flood damage reduction systems [Simonovic, 1998]. In this regard, modern data acquisition, management and dissemination systems together with the numerical models have significant roles to play.

1.2 Flood Risk and Management

A proactive management of flood risks requires the development of strategies to reduce the risks and policies and programmes to put these strategies into effect [ISDR, 2004]. Flood risk results from a combination of the associated probability of a flood event and potential consequence. Ideally, the flood risk management should take into consideration both the elements probability and consequence.

Plate [1998] described the flood risk management in terms of risk assessment and risk mitigation. The risk assessment consists of evaluating the hazard of a flood event and the potential damage if the specified hazard event were to occur. Gendreau and Gilard [1998] presented an approach that divides the flood risk assessment into the factors of vulnerability and hazard assessments. Accordingly, the vulnerability is characterised by the sensitivity of specific land use to the flood phenomenon, whereas the hazard is characterised by physical parameters of the flood flow such as frequency, depth, discharge, duration and velocity.

The risk mitigation is achieved through altering either or both the hazard and the vulnerability, through risk reduction prior to a flood and emergency response during and after a flood [White, 2000]. The flood mitigation measures can be broadly classified as structural and non-structural measures (Figure 1.1). The structural measures represent the traditional approach to flood management focussed on the containment of flood by employing engineering and abatement methods. Typical examples of the structural measures include levees and storage reservoirs. The structural measures affect the hydraulic behaviour of the river and mainly interfere with the hazard component of the flood risks [Gendreau and Gilard, 1998].

In the recent years, there has been a growing emphasis on the non-structural measures. The non-structural measures are based on the strategy of living with the floods rather than controlling them. These measures recognise the occurrence of floods as part of natural processes and aim to limit losses by means of loss sharing and loss reduction methods. The non-structural measures mainly affect the vulnerability component of flood risk [Gendreau and Gilard, 1998]. There is seldom a unique structural or non-structural solution to reduce and manage risks. In many cases, a combination of both the measures might bring an optimum solution.

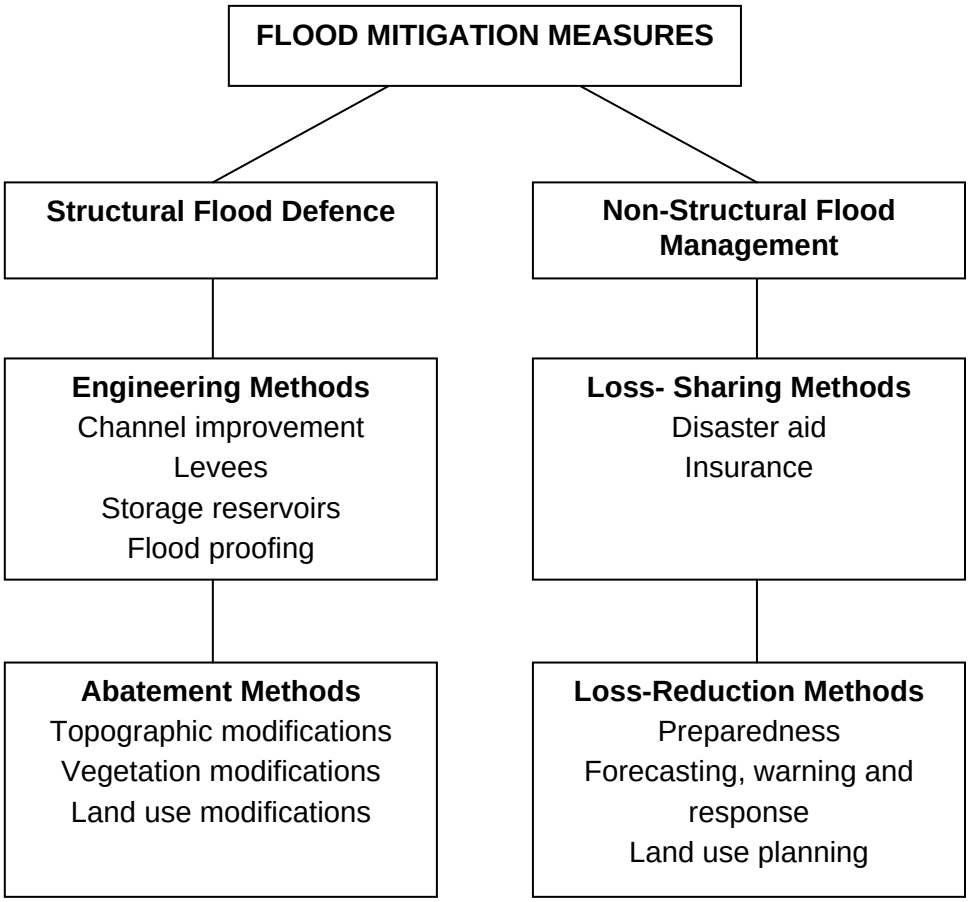

Figure 1.1. Flood mitigation measures
Adapted from Smith and Ward [1998]

1.3 Flood Modelling and Forecasting Systems

The operational flood management comprising of the integrated flood forecasting, warning and response system is an important component of the non-structural flood management. The flood forecasting systems must be sufficiently accurate in order to promote the confidence of communities. The greatest benefits of an effective flood warning system occur when flooding is severe, widespread and/or sudden and communities and organisations are prepared to mitigate impacts [ISDR, 2004].

It is only with the integrated processes in all stages of operational flood management that an optimum level of flood protection is ensured [Nestmann and Emmermann, 2003]. The implementation of the integrated system requires data handling, communication, forecasting, decision support and dissemination tools together with the management of coordination and response activities (Figure 1.2).

The technologies for the operational flood management consisting of numerical models and geographic information system (GIS) are vital components of the integrated system. The numerical models provide tools to forecast the likely magnitude, extent and duration of the flood events, while the GIS tools facilitate the integration and spatial analysis of data, and depiction of the likely inundation extents.

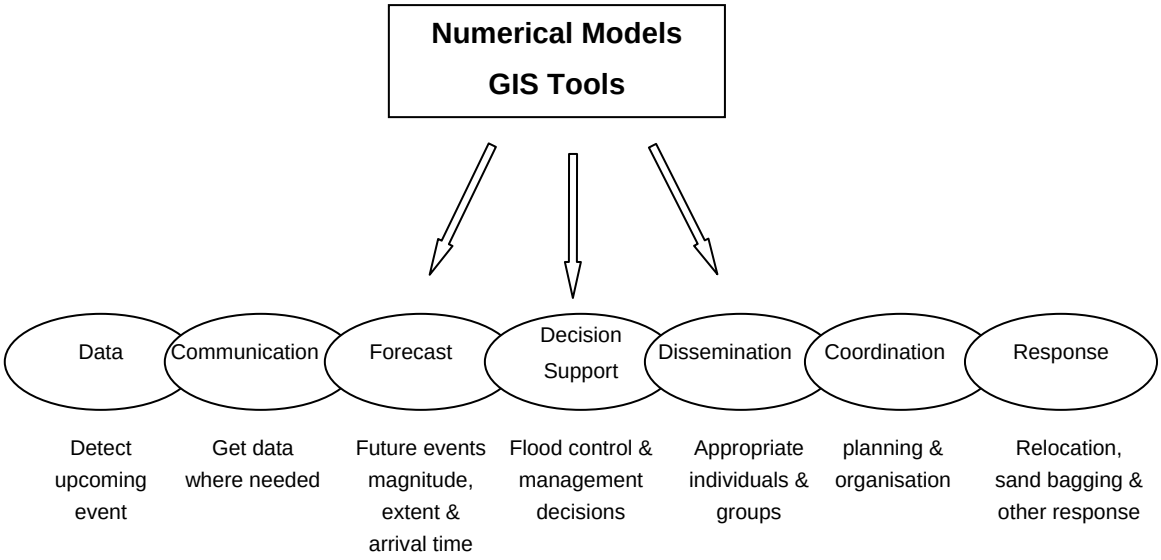

Figure 1.2. Integrated flood forecasting, warning and response systems
Adapted from ISDR [2004]

A typical integrated flood forecasting system consists of a number of subsystems that include precipitation forecasts, rainfall runoff models, flood routing and inundation models. For instance, a prototype European flood forecasting system developed by a collaboration of researchers across Europe consisted a number of components: (i) global numerical weather prediction models, (ii) a regional numerical weather prediction model for downscaling of global precipitation, (iii) a catchment hydrological model comprising a flood simulation model, and (iv) a flood inundation model [De Roo *et al*., 2003]. Each chain in the integrated system adds lead time to the forecasts, which is vital for effective coordination and response activities.

Prediction of flood flows in river channels and floodplains is an important component of the integrated flood forecasting system. The system comprising of the flood routing and inundation models provides means of predicting the likely magnitude, arrival time as well

as extent of inundation of an upcoming flood event. *The scope of this thesis is limited to the river flood prediction component of the flood forecasting system. The discussion on flood forecasting herein, will be limited to river flood prediction.*

1.4 River Flood Prediction Systems

River flood prediction generally requires the forecast of flood hydrographs at the gauging stations and calculation of water levels at critical locations in a river reach. The former, commonly known as flood routing, involves the prediction of the temporal and spatial variations of the flow wave as it moves from upstream to downstream. The latter involves the computation of the relationship between peak discharge and water levels.

A large number of numerical modelling tools are available for the solution of the river flood prediction problems. The rapid advancement of the computing technologies together with sophisticated algorithms to solve numerical problems have led to the development of a large number of efficient and reliable computer models. The modelling tools for river flood prediction can be grouped into three distinct classes consisting of physically based hydrodynamic models, hydrological models and data driven models.

The physically based hydrodynamic numerical (HN) models are based on sound conservation principles of mass and momentum and are capable of simulating both the flood hydrographs and water levels. The system domain of the HN models is discretized in terms of finite space – time grids. For instance, a one-dimensional (1D) HN model consists of the spatial discretization in terms of river cross sections, structural elements like barrages, storage cells, etc., and temporal discretization in terms of time steps. This makes the HN models data intensive to set up and operate. However, the HN model is also capable of making predictions of the flow parameters such as discharge, water levels and velocities at every spatial grid point of the model. In addition, the HN model in combination with a digital terrain model (DTM) can also predict the likely inundation extents. Due to this reason, the HN model is considered a powerful and versatile tool for flood prediction.

The hydrological flood routing models, on the other hand, constitute a reach by reach prediction of discharge hydrographs based on the response of the reach to the inflows. They are only capable of simulating the outflow hydrographs from a river reach, which is considered as a function of inflow and storage. The parameters of the hydrological models may be determined empirically (for example: Muskingum method) or ‘physically based’ coefficients (for example: Muskingum-Cunge method). Although less versatile than the HN models, the hydrological models are important tools in flood forecasting because of their simplicity, limited data requirement and ease in setting up and operating.

In the recent years, the application of data driven models such as artificial neural networks (ANNs), fuzzy rule-based models, neuro-fuzzy systems, genetic programming, and

support vector machines etc., are gaining in popularity. The structures of data driven models do not explicitly take into account the physical processes inside a system but constitute universal approximation of the input and output signals. Physical insight into the system is however necessary to understand the dependencies and correlation between the datasets. The data driven approaches are capable of simulating any variables that they have been trained for. For example, in the context of river flood prediction the data driven approaches can be used to forecast downstream flow parameters based on upstream flows from the main river and tributaries. The data driven models are relatively easy to set up and are advantageous because of their capability to handle highly nonlinear data in dynamic systems.

1.5 Uncertainties in River Flood Prediction Systems

River flood prediction is affected by a number of inherent uncertainties. Imperfect knowledge about the procedures and data generates uncertainty in the forecasts of floods [Maskey, 2004]. The uncertainties in the river flood prediction can be broadly classified into the data, model and parameter uncertainty.

The accuracy of the data is an important factor that affects the performance of the river flood prediction systems. As discussed in section 1.4, the basic data required for a river flood prediction system include the flow and topographical data. The flow data may be measured or predicted values from another component of the flood forecasting system. The measured data too may be based on direct measurement or derivation. For instance, the water levels are directly measured values and the discharges are usually derived from a stage discharge relationship curve. The uncertainties in the relationship curve in particular may be considerable, which can lead to incorrect discharges with potentially large errors, influencing flood forecasting, statistical estimation of flood flows for design and decisions to promote flood defence schemes [Samuels *et al*., 2002].

The uncertainty in flow data will also affect the capability of the prediction models. For instance, an HN model set up and calibrated with uncertain flow data, or a data driven model trained with the uncertain data will lead to uncertainty in forecasts. The amount of data available is also a major factor in considering the prediction capability of the model. The availability of large amount of data will not only lead to better calibration/training of the model, but also to better model verification, thus enhancing the generalisation capability of the model.

The accuracy of the topographical data will also have a significant effect on the reliability of the river flood prediction models. An HN model with inadequate topographic representation will not have good prediction capabilities, even with excellent calibration [Abbot *et al*., 2001]. Similarly, the accuracy of the digital terrain model affects the capability of the model to predict realistic inundation areas.

On the other hand, the uncertainties in the model elements will also lead to the uncertainties in predictions. Every model is indeed a model of reality, which includes a number of simplifying assumptions and inevitably produces inaccuracies [Babovic *et al*., 2001]. In an integrated flood forecasting system consisting of chain of forecast models the uncertainty in each forecast models will propagate through the system, hence affecting the uncertainty of the entire system. Each chain in the forecasting system will not only add vital lead time to the forecast, but also add to the level of uncertainty.

The uncertainties specific to the river flood prediction models relate to the simplification of a highly complex phenomenon of flood wave propagation and inundation. A major source of uncertainty arises in the approximation of the complex flows in river channels and floodplains. The one-dimensional assumption of the multi-dimensional flow inevitably leads to uncertainty. The assumption may be sufficient when flows are predominantly one-dimensional and problems such as flood routing. But it will lead to uncertainties in the case of complex flow in floodplains and prediction of the inundation areas. The multi-dimensional solution of the problem however will add to the complexity of the model and make it expensive in terms of data requirement and computing power. Hence, it is important to strike a balance in view of the model uncertainty and specific problem under consideration.

The model parameters such as the Strickler coefficient in a hydrodynamic model also give rise to the model uncertainties. The calibration of the HN model is usually an over-parameterised problem, with more parameters available than the supporting data for the model calibration [Cunge, 1998]. Therefore, considerable uncertainty arises in the model, particularly in the region where no calibration data is available.

The range of applicability of the model is another important factor to be considered. Usually, only a certain range of datasets is available for model calibration and validation. So, the application of model for the prediction of extreme events, where no datasets are available for calibration, will lead to uncertainty. This factor is especially critical in the application of the data driven models as they are generally considered only valid within the range of training (calibration) datasets.

1.6 Research Needs

The research and applications with regard to river flood prediction have taken three different directions. As discussed in the section 1.4, hydrodynamic, hydrological and data driven models are the three distinct classes of models available for this purpose. Each of these models is based on an entirely different philosophy, although the end result might be the same. The data requirement to develop each of these models and their capabilities varies a lot too. For instance, an HN model is capable of making simulations at every

cross sections. The hydrological and data driven models in contrast can only predict at the model output boundary.

The different philosophy of the model development and their inherent capabilities raises the potentials of complementary modelling as opposed to using them in a competitive way. The complementary nature of their advantages and disadvantages lead to a notion that they can be effectively used together in an optimal manner [Abebe, 2004]. It is therefore, important to assess the strengths and limitations of each of the modelling approaches. Such an assessment will help in identifying the potential of combination of the strengths of these approaches.

The river flood prediction also needs to be considered from a perspective of managing the uncertainties inherent in it. For example, the data uncertainty due to the stage discharge relationship curve may potentially constitute a dominant source of uncertainty. This may affect the capability of the models to make reliable prediction needed for real time operations. In addition, the uncertainty makes it difficult to identify suitable options for flood risk management.

It is therefore imperative to develop methodologies for identifying, quantifying, managing and propagating uncertainties in river flood predictions. In this context, too, the data driven models based on the fuzzy sets and ANNs can complement the HN and hydrological models. Flexible data driven tools based on fuzzy numbers and nonlinear mapping can handle the uncertainties and nonlinear relationships and provide methods for the quantification, management and propagation of the uncertainties.

1.7 Objectives of the Present Research

The overall objective of this research is to identify, develop and implement complementary physically based and data driven models with regard to river flood prediction and uncertainty analysis. The specific objectives of the study are outlined below:

- To assess the strengths, limitations and range of applicability of the hydrodynamic, hydrological and data driven models in the context of river flood prediction.
- To investigate the possibilities of complementing the hydrodynamic models with hydrological and data driven models.
- To develop the methodologies for complementary modelling with regard to the parallel and series complementary approach.
- To assess the uncertainties of the stage discharge relationship and apply methods of managing, quantifying and propagating the uncertainties in the context of river flood prediction.

1.8 Structure of the Thesis

The thesis is organised in 7 chapters consisting of background (chapter 1), basic concepts (chapters 2 and 3), applications (chapters 4, 5 and 6) and conclusions and perspective (chapter 7). An outline of the thesis is given below.

Chapter 2 gives an overview of the basic concepts of the hydrodynamic and hydrological models. This chapter includes the fundamental equations, methods of solution and a discussion on the applications of the unsteady flow and the steady flow hydrodynamic model together with the Muskingum and the Muskingum Cunge hydrological models.

Chapter 3 reviews the basic concepts of artificial neural networks and fuzzy systems. It describes different neural network architectures and activation functions used in this study. There is also a discussion on the practical aspects of the ANN model construction. The chapter also describes basic concepts of fuzzy systems in the context of data driven flood modelling and uncertainty analysis. Important methods based on fuzzy sets such as extension principle, alpha level cut and adaptive network based fuzzy inference system used in this thesis are described. There is also a review of applications of the ANNs and fuzzy systems, with reference to river flow prediction and related uncertainty analysis.

Chapter 4 presents a contribution of this research in the context of complementary hydrodynamic, hydrological and data driven models for river flood prediction. The application of hydrodynamic, hydrological, ANNs and neuro-fuzzy systems are described. There is a discussion on the strengths and limitations of each of these models and a complementary modelling approach is considered so that the strength of one model can complement the other.

Chapter 5 presents a combined hydrodynamic and artificial neural networks model for flood routing and mapping inundation extents. The application assesses the limitations of the hydrodynamic model in flood routing, which arise from imprecision in the input data and need to estimate lateral inflows. An alternate approach is considered with the application of the ANN model for the prediction of discharge hydrographs at the gauging stations and the HN models in small sections for the prediction of the inundation areas.

Chapter 6 considers uncertainties in discharges due to the stage discharge relationship and methods of managing and analysing the uncertainties. The uncertainty management method includes the nonlinear mapping of the relationship using the ANNs. The uncertainty analysis includes the application of fuzzy regression to define the range of uncertainty of the relationship. In addition, the propagation of the uncertainties to the river channel and floodplains is considered with an application of the extension principle based fuzzy alpha cut technique in combination with a hydrodynamic numerical model.

Chapter 7 summarises the important conclusions of this thesis and gives perspectives for further research in the area of river flood prediction and uncertainty analysis.

CHAPTER 2

HYDRODYNAMIC AND HYDROLOGICAL MODELS

This chapter provides background information on hydrodynamic and hydrological models for unsteady flow simulation in rivers. The fundamental equations of a full one-dimensional hydrodynamic model including energy loss coefficients and dimensionless numbers are described. A brief discussion on a method of solution and stability criteria of the numerical schemes of the hydrodynamic model is given. The basic concepts of floodplain mapping using a steady flow simulation of one-dimensional hydrodynamic model in combination with geographic information system (GIS) are discussed. In the case of hydrological model, this chapter outlines the basic principles of the Muskingum Cunge simplified distributed model. The method of solution and stability criteria of the Muskingum Cunge model are included. The chapter also discusses a number of recent applications of the hydrodynamic and hydrological models for flood routing. There is a brief description of the flood extent mapping and flood risk assessment methods.

2.1 Physically Based Hydrodynamic Numerical Models

The physically based river modelling system is an important component of flood forecasting and risk assessment system. As the name suggests, the physically based models are based on the mathematical representation of physical system and processes in it. For instance, in the physically based hydrodynamic numerical (HN) models, the system domain is defined by river geometry and the underlying processes are described in terms of numerical equations.

The importance of the physically based HN model in a flood prediction system can be attributed to its ability to simulate different variables such as discharges, water levels, and velocities at every grid point in the model domain. In addition, the HN model can also be used for the routing of the flood wave from upstream to downstream location in a river reach.

The physical domain of the modelling system can be described in terms of one-dimensional (1D) or the multidimensional formulations. The general form are the Navier – Stokes equations which describe the unsteady flow of viscous incompressible fluid in a three-dimensional (3D) space. In the two-dimensional (2D) formulation, depth averaged form of the governing equations are used. The 1D formulation considers the flow variation only in the axial direction of flow.

Both sufficiency and the applicability of these formulations depend upon a number of specific parameters of river flow that needs to be analysed. This thesis mainly takes into consideration the simulation of flow and water level at the gauging station and inundation mapping at certain sections in the river reach. The scope of this thesis is limited to 1D description of flows in the river channel and a network of 2D cells in the floodplains. The inundation extents are also defined by the 1D HN model in the river channel, with subsequent spatial projection of water levels into the floodplains using the GIS.

2.1.1 Saint Venant Equations

The 1D HN model is the most commonly used tool for the flood routing and water level simulation. The 1D HN model is based on the Saint Venant equations, which is derived from the principles of mass and momentum conservation in open channel flow. The terms used in the definition of the equation are illustrated in Figure 2.1.

The Saint Venant equations can be expressed as the continuity equation (2.1) and the momentum equation (2.2) [Cunge *et al.*, 1980]:

$$\frac{\partial y}{\partial t} + \frac{1}{b}\frac{\partial Q}{\partial x} = 0 \tag{2.1}$$

$$\frac{\partial Q}{\partial t} + \frac{\partial}{\partial x}\left(\frac{Q^2}{A}\right) + gA\frac{\partial h}{\partial x} + gA\left(S_f - S_o\right) = 0 \tag{2.2}$$

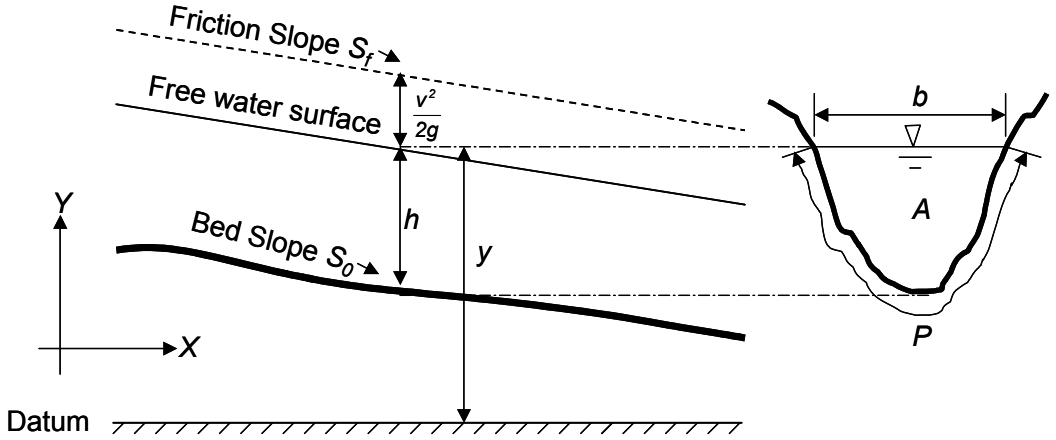

Figure 2.1. Definition sketch of Saint Venant equation
Adapted from Henderson [1966]

where

y = water surface elevation [m]

h = depth of flow [m]

Q = discharge [m^3/s]

b = top width of flow [m]

A = active cross sectional area of flow [m^2]

g = gravitational acceleration [m/s^2]

S_f = friction slope

S_0 = bed slope

x = distances along the channel [m]

t = time [s]

The magnitude of each of the terms in the momentum equation plays a significant role in the hydraulics of the system. Chow *et al*. [1988] defined the terms in the momentum equation (2.2) as:

$\frac{\partial Q}{\partial t} =$ Local acceleration term

$\frac{\partial}{\partial x}\left(\frac{Q^2}{A}\right) =$ Convective acceleration term

$\frac{\partial h}{\partial x} =$ Pressure slope term

S_f = Friction slope term

S_0 = Gravity slope term

The pressure slope may be expressed as:

$$\frac{\partial h}{\partial x} = \frac{\partial y}{\partial x} + S_0 \qquad (2.3)$$

where

$\frac{\partial y}{\partial x} =$ Water surface slope

The Saint Venant equations of unsteady flow are based upon a number of assumptions [Cunge *et al*., 1980]. These include: (i) the velocity is uniform over the channel cross section, (ii) vertical accelerations are negligible, (iii) boundary friction and turbulence can

be modelled by resistance laws analogous to steady state flow and (iv) the slope of the channel is small, such that the cosine of the angle between the plane of the channel bottom and the horizontal plane is essentially unity.

Based on the assumption (iii), the friction slope can be taken as the slope of the energy grade line in steady flow. This is given by:

$$S_f = \frac{Q|Q|}{K^2} \tag{2.4}$$

where

K = conveyance of the channel section with same dimension as discharge [m^3/s].

The momentum equation (2.2) can be expressed in terms of water surface slope as:

$$\frac{\partial Q}{\partial t} + \frac{\partial}{\partial x}\left(\frac{Q^2}{A}\right) + gA\frac{\partial y}{\partial x} + gA\frac{Q|Q|}{K^2} = 0 \tag{2.5}$$

The equation (2.2) may also be expressed in the following non-conservative form from which simplified forms of the momentum equation can be derived [Chow *et al*., 1988]:

$$\frac{\partial v}{\partial t} + v\frac{\partial v}{\partial x} + g\frac{\partial h}{\partial x} + g\left(S_f - S_0\right) = 0 \tag{2.6}$$

Kinematic wave

Diffusion wave

Dynamic wave

where

v = mean velocity in the channel [m/s]

Here, the kinematic wave model neglects local acceleration, convective acceleration and pressure terms. The diffusion wave model neglects local acceleration and convective acceleration terms. The dynamic wave model considers all the terms of the momentum equation.

2.1.2 Energy Loss Coefficient

The energy losses in the river channel can be evaluated in terms of Gauckler–Manning-Strickler equations:

$$Q = KS_f^{1/2} \tag{2.7a}$$

$$K = k_{st} A R^{2/3} \tag{2.7b}$$

$$v = k_{st} R^{2/3} S_f^{1/2} \tag{2.7c}$$

where

k_{st} = Strickler coefficient [$m^{1/3}/s$]

R = hydraulic radius, defined as the ratio of flow area A to wetted perimeter P [m]

The Manning coefficient expressed as a reciprocal of Strickler coefficient is used in English speaking countries:

$$K = \frac{1}{n} A R^{2/3} \tag{2.8}$$

where

n = Manning resistance coefficient [$m^{-1/3}s$]

The Strickler or Manning coefficient contains a number of factors, and not just the channel friction as generally assumed. The value is highly variable and depends upon a number of factors including: surface roughness, channel irregularities, channel alignment, size and shape of channel, scour and deposition, vegetation, obstructions, stage and discharge, seasonal change, temperature, suspended materials and bedload [Chow, 1959]. There are several references available listing the typical values [Chow, 1959; Henderson, 1966].

Sometimes the Chezy equation is used instead of the Strickler or the Manning equation for the representation of energy loss in the open channel. The Chezy equation can be expressed as:

$$v = C\sqrt{RS} \tag{2.9}$$

where

C = Chezy coefficient [$m^{1/2}s^{-1}$]

The Strickler or the Chezy coefficient is the main parameter for the calibration of hydrodynamic numerical models. The coefficients are calibrated within a range of values so as to obtain a good match between the observed and simulated flow variables. The range of values can be established based on the site conditions. In general, it is acceptable to calibrate the coefficient within a known range of variations than to try to calibrate a model by attributing unrealistic values to these coefficients [Abbott *et al*., 2001].

2.1.3 Dimensionless Numbers

The dimensionless flow parameters define flow characteristics and give the possibility to generalise the flow situation. Mishra and Singh [2002] described the dimensionless numbers in relation to the momentum equation (2.2).

2.1.3.1 Froude Number

The effect of gravity on the state of flow is defined by the square root of the ratio of inertial force to gravitational force as the dimensionless Froude Number. The dimensionless Froude number (*Fr*) may be expressed as:

$$Fr = \frac{v}{\sqrt{gL}} \tag{2.10}$$

where

L = characteristics length [m]

In open channel flow, the characteristics length (L) is often taken as the hydraulic depth (D), which is defined as active cross sectional area of flow (A) divided by the top width of flow of free surface (b).

Depending on the magnitude of the Froude number, the state of flow is subcritical, critical or supercritical. When the Froude number is less than 1, the effect of gravitational force is less than the inertial force and the state of flow is referred to as subcritical flow. When the inertial and gravitational forces are equal, the Froude number is equal to unity and the flow is at the critical. When the inertial force exceeds the gravitational force, the Froude number is greater than 1, the state of flow is referred to as supercritical flow.

The inertial term in the momentum equation (2.2) is represented by the convective acceleration term and the gravitational force is given by bed slope (S_0) [Mishra and Singh, 2002]. The Froude number also represents an important criterion in the solution of the Saint Venant equations. When the state of flow is subcritical, the state of flow is controlled by channel characteristics at the downstream end of the river reach. In the case of supercritical flow, the flow is governed by the upstream end of the river reach. Hence, the boundary conditions for the model based on the Saint Venant equation has to be set appropriately based on the state of flow.

2.1.3.2 Reynolds Number

The Reynolds number (*Re*) is defined as the ratio of inertial force to viscous force. It can be mathematically expressed as:

$$Re = \frac{vD}{\nu} \tag{2.11}$$

where

D = hydraulic depth [m]

ν = Kinematic viscosity [m^2/s] (defined as ratio of viscosity μ to the fluid density ρ)

The Reynolds number is often used to describe the characteristics of flow. Generally, the flow is said to be in laminar state for $Re < 2300$, transitional state for $2300 \leq Re \leq 4000$ and turbulent state for $Re > 4000$. The flow is considered completely turbulent only for $Re > 10^5$. The significance of the Reynolds number in the Saint Venant equation is not directly apparent although the inertial term is represented by convective acceleration term of the momentum equation (2.2). The Saint Venant equations does not directly have the viscosity term, but is included indirectly as shown below.

The friction factor f in pipe flow is the function of the Reynolds number for the laminar and transitional zone of the Moody diagram. The friction factor may be expressed by the Darcy–Weisbach formula as:

$$f = \frac{8gRS_f}{v^2} \tag{2.12a}$$

which leads to:

$$v = \sqrt{\frac{8g}{f} RS_f} \tag{2.12b}$$

Comparing equations (2.7c), (2.9) and (2.12b), the Chezy and Strickler coefficient can be related to the friction factor as [Nestmann, 1998]:

$$C = k_{st} R^{1/6} = \sqrt{\frac{8g}{f}} \tag{2.13}$$

It is to be noted that in a complete turbulent flow through fully rough zone in a pipe, the friction factor f and hence the Chezy coefficient C (in a Moody diagram) becomes independent of Reynolds number Re [Henderson, 1966]. In natural channels, this energy loss takes place either internally if the medium is viscous, through turbulence if the channel boundaries are rough, or if the flow converts from supercritical to subcritical, or in combination thereof. The convective acceleration term in equation (2.2), in particular, represents the magnitude of turbulence through velocity change, leading to the formation of eddies or vortices that dissipate energy [Mishra and Singh, 2002].

2.1.4 Numerical Solution of Saint Venant Equation

The solution of one-dimensional Saint Venant equations is usually based on the finite difference approximation schemes. The finite difference schemes can be further classified into explicit or implicit. In the explicit schemes, the flow variables at one time level could be expressed as the function of values of the dependent variables at an earlier time step. In the implicit finite difference schemes, the Saint Venant equations are transformed into a set of algebraic equations, which must be solved simultaneously for all grid points in the river reach at a given time step. Although explicit schemes are easier to implement, implicit schemes are generally preferred due to the numerical stability considerations [Fread, 1992].

2.1.4.1 Implicit Finite Difference Scheme

The implicit finite difference scheme is based on the solution the Saint Venant equations (2.1) and (2.5) in a system of partial differential forms. Numerous mathematical methods and corresponding numerical schemes exist for the solution of these partial differential equations. Of the various schemes, the Preissmann weighted four point scheme is one of the most popular. The scheme has been described in a number of literatures [Fread, 1974; Cunge *et al*., 1980; Abbott, 1992]. Numerous applications of the Preissmann scheme have been reported in river modelling systems such as CARIMA [SOGREAH, 1978], UNET [USACE, 1997] and FLDWAV [Fread and Lewis, 1998].

In the weighted four point implicit scheme, the continuous space-time grid system as shown in Figure 2.2 depicts the region in which the solution of the flow equations is sought. An *x-t* plane is a convenient means of representing relationships among the variables within the time increment Δt and space increment Δx, with ψ space weighing factor and θ time weighing factor.

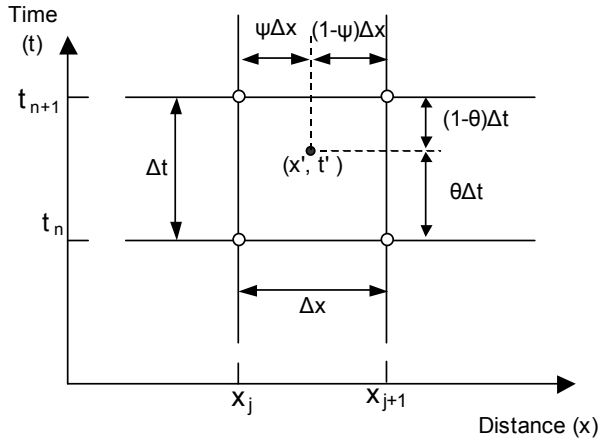

Figure 2.2. Space – time discretization of the implicit finite difference scheme

The temporal and the spatial derivatives by forward-difference quotient at point (*x′, t′*) can be expressed as follows:

$$\frac{\partial f}{\partial t} \approx \frac{\left(f_{j+1}^{n+1} + f_j^{n+1}\right) - \left(f_{j+1}^{n} + f_j^{n}\right)}{2\Delta t} \tag{2.14}$$

$$\frac{\partial f}{\partial x} \approx \frac{\theta\left(f_{j+1}^{n+1} - f_j^{n+1}\right) + (1-\theta)\left(f_{j+1}^{n} - f_j^{n}\right)}{\Delta x} \tag{2.15}$$

where, *f* represents any dependent variable or functional quantity (such as *Q* and *y*) and the space weighing coefficient ψ = 0.5. The time weighing coefficient is assigned in the range $0 \le \theta \le 1$.

The application of the Preissmann scheme to the derivatives in equations (2.1) and (2.5) yield the following equations (2.16) - (2.20) [Cunge *et al*., 1980]:

$$\frac{\partial y}{\partial t} \approx \frac{\left(y_{j+1}^{n+1} + y_j^{n+1}\right) - \left(y_{j+1}^{n} + y_j^{n}\right)}{2\Delta t} \tag{2.16}$$

$$\frac{\partial Q}{\partial t} \approx \frac{\left(Q_{j+1}^{n+1} + Q_j^{n+1}\right) - \left(Q_{j+1}^{n} + Q_j^{n}\right)}{2\Delta t} \tag{2.17}$$

$$\frac{\partial Q}{\partial x} \approx \frac{\theta\left(Q_{j+1}^{n+1} - Q_j^{n+1}\right) + (1-\theta)\left(Q_{j+1}^{n} - Q_j^{n}\right)}{\Delta x} \tag{2.18}$$

$$\frac{\partial}{\partial x}\left(\frac{Q^2}{A}\right) \approx \frac{\theta}{\Delta x}\left(\frac{\left(Q_{j+1}^{n+1}\right)^2}{A_{j+1}^{n+1}} - \frac{\left(Q_j^{n+1}\right)^2}{A_j^{n+1}}\right) + \frac{(1-\theta)}{\Delta x}\left(\frac{\left(Q_{j+1}^{n}\right)^2}{A_{j+1}^{n}} - \frac{\left(Q_j^{n}\right)^2}{A_j^{n}}\right) \tag{2.19}$$

$$\frac{\partial y}{\partial x} \approx \frac{\theta\left(y_{j+1}^{n+1} - y_j^{n+1}\right) + (1-\theta)\left(y_{j+1}^{n} - y_j^{n}\right)}{\Delta x} \tag{2.20}$$

Adapting a convention all dependent variables are defined at time level $(n+1)\Delta t$ such that:

$$f_j^{n+1} = f_j^{n} + \Delta f \tag{2.21}$$

Substituting the values of partial derivatives from equations (2.16) - (2.20) to Saint Venant equations (2.1) and (2.5), the following system of equations emerge:

$$A\Delta y_{j+1} + B\Delta Q_{j+1} + C\Delta y_j + D\Delta Q_j + G = 0 \tag{2.22}$$

$$A'\Delta y_{j+1} + B'\Delta Q_{j+1} + C'\Delta y_j + D'\Delta Q_j + G' = 0 \tag{2.23}$$

The system of equations (2.22) and (2.23) for *N* grid points lead to a total of *2(N-1)* equations with *2N* unknowns. Two boundary conditions provide two additional equations required for the system of equations to be determinate. These equations are all solved simultaneously for all grid points at a certain time step. All the variables at time step *n* are known and time step *n+1* are unknown. Using the known values of y_j^n and Q_j^n the coefficients *A, B, C ,….., G'* can be determined and the linearised system of equations (2.22) and (2.23) for *N* points can be solved giving the new approximation of the unknowns at new time step *(n+1)Δt.* The simultaneous solution of *2(N-1)*2(N-1)* system of equations requires an efficient matrix technique such as the Newton iteration method [Cunge *et al*., 1980].

2.1.4.2. Stability Criteria

The implicit schemes can generally be considered unconditionally stable for different time and distance steps [Cunge *et al*., 1980]. An important stability criteria for the implicit scheme is given by the time weighing factor *θ*. The Preissmann scheme considered in this chapter is unconditionally, linearly stable for $\theta \geq 0.5$. The solution become fully implicit for $\theta = 1$, and fully explicit for $\theta = 0$. The scheme is most stable at $\theta = 1$ and most accurate at *θ* approaches 0.5. Usually, the weighing factor $\theta = 0.6$ can be used to minimise the loss of accuracy and avoid the stability problem [Fread, 1992].

Useful criteria for the selection of appropriate computational distance *Δx* and time step *Δt* is given by Fread and Lewis [1993]:

$$\Delta x \leq \frac{cT_r}{20} \tag{2.24}$$

$$\Delta t \leq \frac{T_r}{20} \tag{2.25}$$

where

T_r = minimum time of rise of hydrograph of upstream boundary condition [s]

In practical problems, a number of other criteria may also contribute to the appropriate selection of *Δx*. These include the considerations of dramatic change channel cross sectional properties, changes in channel slope and hydraulic structures such as levees, bridges, culverts weirs and spillways [USACE, 1997].

2.1.5 Steady Flow Simulations

Flow in open channel can be considered steady if depth, discharge and mean velocity of flow at a particular location do not change with time or can be assumed constant during a time period. The steady flow equations are usually expressed in terms of classical

continuity and energy equations, as given in the references such as Chow [1959] and Henderson [1965]. The differential form of the steady flow equations can also be obtained from the unsteady flow equation (2.2) by assuming Q = constant and $\partial Q/\partial t = 0$:

$$\frac{\partial}{\partial x}\left(\frac{Q^2}{A}\right) + gA\frac{\partial h}{\partial x} + gA\left(S_f - S_o\right) = 0 \tag{2.26}$$

The numerical solution of the classical steady flow equations (continuity and energy) is usually undertaken using the standard step method, where numerical computations proceed on steps from cross section to cross section [Chow, 1959]. The finite difference unsteady flow modelling systems can also be used to obtain the steady flow simulations if the boundary conditions are fixed and initial perturbations are allowed to dissipate out of the system [Cunge *et al*., 1980].

The analysis of the propagation of the flood wave through a river channel generally requires full unsteady flow equations. The steady flow computations are useful in unsteady flow simulations in cases such as the calculations of initial conditions. The main areas of applications of steady flow computations include water surface profile computations for hydraulic design problems like dikes and backwater effects of construction of structures. Steady flow computations are also widely used in combination with geographical information systems for mapping inundation extents.

2.2 Hydrological Flow Routing Models

A number of simplified hydrological models have been developed for the unsteady flow routing in a river reach. The hydrological models, in general, constitute a reach by reach prediction of discharge hydrographs based on the response of the reach to the inflow and storage. From the principle of mass conservation the difference between the inflow Q_j and the outflow Q_{j+1} in a river reach can be expressed as the rate of change of storage S [Fread, 1992]:

$$Q_j\left(t\right) - Q_{j+1}\left(t\right) = \frac{dS}{dt} \tag{2.27}$$

The solution of the equation (2.27) for the outflow Q_{j+1}, with approximation of the storage S leads to a lumped flow routing. Amongst different lumped models used for flood routing in rivers, the Muskingum model is one of the most popular methods. The model can accommodate looped relationships between storage and outflow existing in natural rivers. It is a simple method requiring only inflow and outflow from the reach. The following empirical linear storage equation defines this relationship:

$$S_j^n = K\left[XQ_j^n + (1-X)Q_{j+1}^n\right] \tag{2.28}$$

where

S_j^n = storage in the routing reach at time n [m^2]

Q_j^n = inflow at time n [m^3/s]

Q_{j+1}^n = outflow at time n [m^3/s]

K = storage time coefficient with same dimension as travel time [s]

X = dimensionless weighing factor, ranging between 0 to 0.5.

For the routing interval Δt the continuity equation takes the following finite difference form.

$$Q_{j+1}^{n+1} = C_1 Q_j^n + C_2 Q_j^{n+1} + C_3 Q_{j+1}^n \tag{2.29}$$

The routing coefficients C_1, C_2 and C_3 are defined in terms of Δt, K and X:

$$C_1 = \frac{\Delta t + 2KX}{2K(1-X) + \Delta t} \tag{2.30a}$$

$$C_2 = \frac{\Delta t - 2KX}{2K(1-X) + \Delta t} \tag{2.30b}$$

$$C_3 = \frac{2K(1-X) - \Delta t}{2K(1-X) + \Delta t} \tag{2.30c}$$

$$C_1 + C_2 + C_3 = 1 \tag{2.30d}$$

The Muskingum model as defined by equations (2.28), (2.29) and (2.30) are based on parameters K and X, expressed in terms of C_1, C_2 and C_3. During the solution of these equations, parameter K is estimated from the travel time of the flood wave through the river reach. The value of parameter X is evaluated using a trial and error procedure.

Cunge [1969] modified the lumped Muskingum model into a distributed model by combining it with the diffusion wave analogy (equation 2.6). The modified equation also includes the lateral inflow:

$$Q_{j+1}^{n+1} = C_1 Q_j^n + C_2 Q_j^{n+1} + C_3 Q_{j+1}^n + C_4 \tag{2.31}$$

The terms C_4 can be obtained from average lateral inflow q_l:

$$C_4 = \frac{q_l \Delta t \, \Delta x}{2K(1-X) + \Delta t} \tag{2.32}$$

Cunge [1969] obtained the routing parameters *K* and *X* by forcing the numerical diffusion to match the hydraulic diffusion as follows:

$$K = \frac{\Delta x}{c} \tag{2.33}$$

$$X = \frac{1}{2}\left(1 - \frac{Q}{BS_o c \Delta x}\right) \tag{2.34}$$

where c is the wave celerity, which can be obtained as:

$$c = \frac{dQ}{dA} \tag{3.35}$$

2.2.1 Method of Solution

The Muskingum Cunge (MC) flood routing is carried out by the solution of equation (2.31). A simple finite difference solution as schematised in Figure 2.3 is used for the solution of the equations. The coefficients C_1, C_2, C_3 and C_4 are based on parameters *K* and *X* which can be obtained from the equations (2.33) – (2.34). The only unknown in these equations is the slope parameter S_0, which can be obtained from the Gauckler–Manning-Strickler equations (2.7a and 2.7b). However, the parameters *K* and *X* are also the functions of Q_{j+1}^{n+1} and require its initial estimate. This may be obtained from $Q_{j+1}^{n+1} = Q_j^{n+1} + Q_{j+1}^n - Q_j^n$, requiring the subsequent iterations if the estimated and predicted value differ by an unacceptable amount [Price, 1985]. Since the parameters *K* and *X* are slowly varying functions of *Q*, the first estimate is usually sufficient. The stability criteria as outlined in the section 2.3.2 are a necessary condition for the solution of Muskingum Cunge equations.

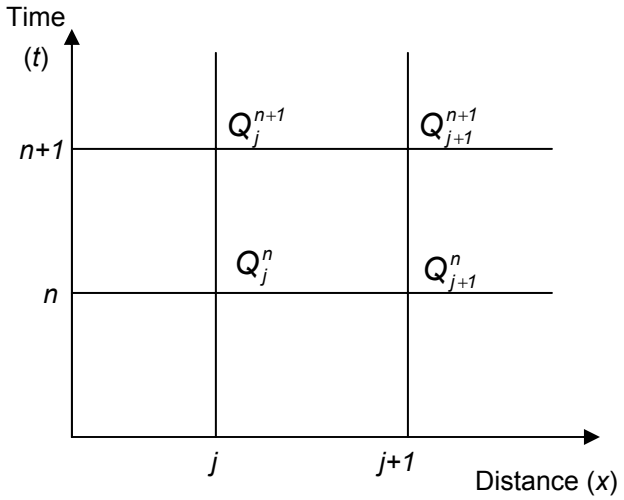

Figure 2.3. Finite difference discretisation of the Muskingum Cunge equation

2.2.2 Stability Criteria

In the Muskingum Cunge (MC) method, the selection of appropriate intervals of *Δx* and *Δt* is an important criterion for the stability of the scheme. Two dimensionless numbers are frequently used for description of the stability criteria. These are the Courant number *Cr*, and the cell Reynolds number *D*.

The Courant number is defined as the ratio of physical wave celerity c to grid celerity (Δx/Δt) [Mishra and Singh, 2002]:

$$Cr = c\frac{\Delta t}{\Delta x} \tag{2.36}$$

In general, the Courant number *Cr* is the limiting criteria for the explicit schemes (*Cr ≤ 1*). For the optimal solution of the MC method, temporal and spatial resolution should be selected such that *Cr ≈ 1*. For smoothly rising hydrographs, the criteria for the temporal resolution is recommended as [Ponce, 1994]:

$$\Delta t \le \frac{T_r}{5} \tag{2.37}$$

There are no definite criteria for the spatial resolution *Δx.* The combined criteria of the Courant number and the cell Reynolds number give a practical consideration for the selection of *Δx*. Ponce [1994] defined the cell Reynolds number *D* as the ratio of hydraulic diffusivity to grid diffusivity as:

$$D = \frac{Q}{BS_o c\Delta x} \tag{2.38}$$

The combined Courant number and cell Reynolds number criteria for the determination of the temporal and spatial resolution is given by [Ponce, 1994]:

$$Cr + D \ge 1 \tag{2.39}$$

2.3 Review of Applications

A review of applications of hydrodynamic and hydrological model with reference to flood routing, floodplain mapping and flood risk assessment is given in the following paragraphs.

2.3.1 Flood Routing

The transmission of the flood wave in a river channel is characterised by filling and emptying of floodplain storage area. The 1D HN model in a simple configuration does not

take this effect into account. A relatively simple way of considering the storage effect is to use a quasi 2D model consisting of a full 1D equation for flows in river channels and a 2D network of cells in the floodplains [Cunge *et al*., 1980]. The 2D cell networks are represented by series of interconnected cells in the inundation area. The flow exchange between the two cells is represented by hydraulic discharge formula such as weir, orifice and Strickler law etc.

Using this approach attenuation of the flood wave due to the storage effects can be adequately represented. A number of recent applications have shown the quasi 2D approach as an effective tool for the representation of the attenuation effects [Min Thu, 2002; Willems *et al*., 2002].

The hydrological routing approach provides a simple alternative to the full 1D HN models. However, the hydrological routing models are limited by factors such as backwater effects and floodplain effects. The modified Muskingum Cunge model has an advantage over the lumped Muskingum model. It has only the friction loss coefficient as the model parameter which can be obtained from the equation (2.7) or (2.8). The model is considered as the nonlinear coefficient method and does not require the outflow hydrograph as downstream boundary condition. The model relies upon physical characteristics such as rating curves and channel cross sections [Ponce, 1994]. However, it cannot handle the downstream disturbance that propagates upstream [Chow *et al*., 1988]. The method starts to diverge from the completely unsteady flow situation when affected by backwater effects and rapidly rising hydrographs [USACE 1994].

2.3.2 Floodplain Mapping and Flood Risk Assessment

In the case of floodplain mapping and flood risk assessment problems, the ability to predict the spatial inundation extent of a flood event is an important criterion. A number of methods have been developed in the recent years to support this prediction. The available methods include the use of 1D HN model in the river channel with subsequent spatial projection in the floodplain using geographic information system (GIS) [Oberle, *et al*., 2000; Shrestha *et al*., 2002; Tate *et al*., 2002]. The alternative to use of the spatial projection is a 1D representation of flow in the channel and a 2D representation in the floodplains [Bates and De Roo, 2000; Dhondia and Stelling, 2002].

A number of applications of the fully 2D flow models have been reported in the recent years. In contrast to 1D flow models, which are based on the finite difference schemes, the 2D models include the application of finite element [Bates *et al*., 1996; Aronica *et al*., 1998; Tucciarelli and Termini, 2000] or the finite volume methods [Beffa and Connell, 2001; Connell et al., 2001].

A number of researchers have made the comparisons of the 1D and 2D approaches of river flood inundation. Horritt and Bates [2002] mainly used satellite borne flood extent

observations for the calibration of a 1D and 2D models. The models produced similar levels of performance despite their different dimensionalities. Oberle [2004] made a detailed analysis of the inundation extent from an integrated system of an 1D model and GIS with a full 2D model. The analysis showed a very good match between the models with less than 5 cm water level difference in 51 percent of the areas and less than 10 cm difference in 78 percent of the areas.

The scope of this thesis for prediction of the inundation extents is limited to the application of 1D HN model in the river channel with subsequent spatial projection of water levels in the floodplain using GIS. In a typical application the steady flow simulation is performed in a relatively short river reach using peak flood discharges. The model is calibrated with the observed flood marks in the river. The calibrated model is then used for the computations of water surface profiles for peak floods of different return periods.

The computed water surface profiles can be integrated with the GIS technology for the depiction of inundation areas. This usually requires the development of a raster (grid) based digital terrain model (DTM), which is the representation of the topographical surface in terms of regularly spaced *x, y* and *z* coordinates. The DTM can be developed from the vector data such as river cross sections, contours and spot elevations. A number of methods for conversion of the vector data into the raster based DTM are available such as inverse distance interpolation. Alternatively, the vector data can first be interpolated to a triangulated irregular network (TIN), which is a surface representation, derived from interconnected and non-overlapping triangles. The TIN can then be converted to the raster based DTM. The DTM can also be prepared from high resolution Laser induced Detection and Ranging (LiDAR) data.

The water surface profiles from the HN model can be combined with the DTM for floodplain modelling. The process of floodplain modelling usually consists of a number of steps. The detailed description of this process is available in Shrestha [2000], Oberle *et al*. [2000], Tate *et al*. [2002] and Oberle [2004]. A brief description is given below.

i. The steady flow water surface profiles from the HN models are imported to the GIS environment.

ii. Water surface TIN are formed based on water surface profiles and converted to water surface grids.

iii. The water surface grids are subtracted from the digital elevation model to obtain the difference model.

iv Inundation areas are obtained from the difference model in terms of vector polygons.

The process is usually automated by a user interface between the hydrodynamic modelling system and the GIS such as HEC-GeoRAS [USACE, 2002]. For this purpose, the Institute of Water Resources Management, Hydraulic and Rural Engineering (IWK), University of Karlsruhe has developed a GIS-supported flood management system

[Oberle *et al*., 2000]. It consists of a structured graphical user interface for steady flow computation. The cross sections of the HN model were linked with lines of equal water surface elevation in the GIS. Based on the steady flow simulations and in combination with the digital terrain model at the sections, inundation grids and polygons can be depicted.

The methodology can be extended further to undertake risk assessment by dividing it into the components of hazard and vulnerability [Gilard, 1996; Shrestha *et al*., 2002]. The general structure of the floodplain mapping and flood risk assessment model is shown in Figure 2.4.

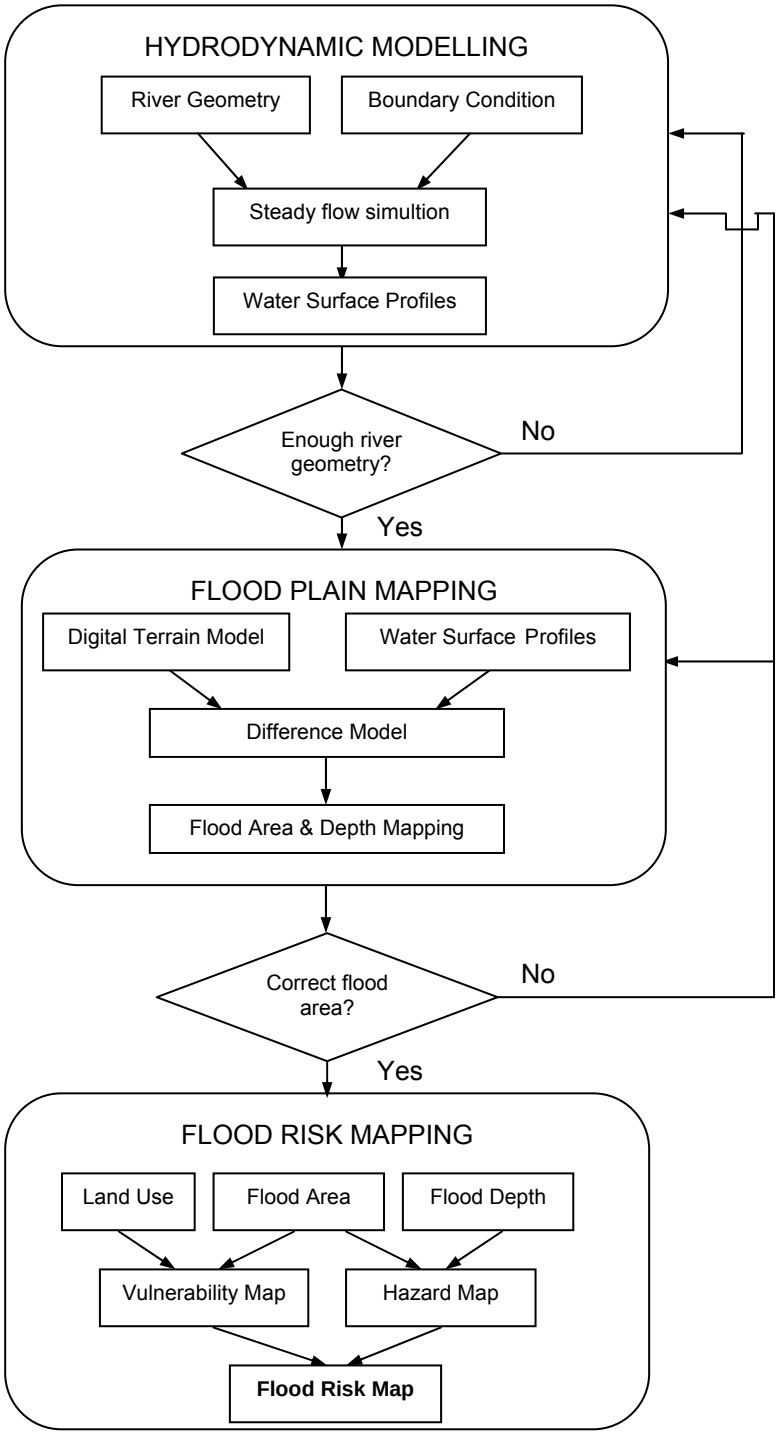

Figure 2.4. Structure of the flood plain mapping and flood risk assessment model
Adapted from Shrestha *et al*. [2002]

CHAPTER 3

DATA DRIVEN MODELS: ARTIFICIAL NEURAL NETWORKS AND FUZZY SYSTEMS

This chapter describes basic concepts of artificial neural network (ANN) and fuzzy systems in the context of data driven river flood modelling and uncertainty analysis applied in this thesis. The chapter starts with the general definition of the ANN and different constituents of a neuron of the ANN. An outline of a number of activation functions and different network architectures used in this study is given. The chapter also discusses practical aspects of the ANN model construction.

Similarly, a general definition of the fuzzy systems is given together with an outline on a number of fuzzy numbers. The important principles for uncertainty analysis such as extension principle and alpha level cut are described. The chapter also includes a discussion on fuzzy rule based model and adaptive network based fuzzy inference system. A review of applications of the neural networks and fuzzy systems, especially with reference to river flow prediction and related uncertainty analysis are also included.

3.1 Data Driven Modelling

The notion of developing models from data has been a subject of significant research interest in water resources systems. Such models are mainly based on the artificial intelligence methods and can be broadly classified as data driven models. The rapid advancement in the information processing technologies together with availability of low cost computers have also brought these methods to hydrology and hydraulics. As a result, there has been a widespread application of artificial intelligence based data driven methods such as artificial neural networks, fuzzy logic, genetic algorithm, support vector machines etc., to solve water related problems.

The application of data driven modelling in water resources systems can also be viewed in the framework of hydroinformatics systems, which has been described as an electronic knowledge encapsulator that models (part of) the real world for the simulation of physical, chemical and biological processes in water systems [Abbott, 1991]. The systems bring together computational hydraulics and hydrology, knowledge based systems, artificial intelligence based data driven methods, information and commutation systems including web-based technologies. In this context, this thesis considers hydraulic, hydrological and data driven models as complementary methods.

The data driven modelling constitute a universal approximation of the input and output signals, without explicitly taking into account the physical processes inside a system. These models are able to make abstractions and generalisation of the processes and physical insight into the system is necessary to understand the dependencies and correlation between the different data signals. The data driven methods provide fast and relatively easy means of model development for highly complex, nonlinear and dynamic systems. They are also capable of handling noise and uncertainties in data and can complement the physically based models, especially when underlying physical processes are not well understood and/or affected by uncertainties.

The artificial neural networks (ANNs) and fuzzy systems based data driven methods have individually reached a degree of maturity where they are being applied to real world problems [Tsoukalas and Uhrig, 1997]. In this chapter, these methods are considered in more detail.

3.2 Artificial Neural Networks

Artificial neural networks (ANNs) are inspired by the capability of human brains to learn from highly complex nonlinear information in a parallel distributed network. They have the capability to learn from experiences and rapidly solve hard computing problems. This human brain inspired connectionist computing paradigm has been a subject of scientific investigation since the early days of computers. First introduced by McCulloch and Pitts, [1943], the rapid development of computer technology in the recent years has led to the advancement of this computing paradigm. Within the last decade it has experienced a huge resurgence due to development of more sophisticated algorithms and emergence of powerful computational tools [ASCE, 2000a]. In the recent years, the ANNs have emerged as practical technology with successful applications in many fields [Bishop, 1999]. Consequently, the ANNs have become one of the most popular data driven techniques with applications in diverse field such as modelling dynamical systems and time series forecasting, control systems and classification problems.

The ANNs can generally be defined as parallel interconnected networks capable of identifying complex and non-linear systems. A number of alternative definitions of the ANNs are available. Haykin [1995] described a neural network as a massively parallel distributed processor that has a natural propensity of storing experimental knowledge and making it available for use. Knowledge is acquired by the network through a learning process. Interneuron connection strengths known as synaptic weights are used to store the knowledge.

Schalkoff [1997] provided a generic definition of an ANN as a structure (network) composed of a number of interconnected units (artificial neurons). Each unit has an input/output characteristic and implements a local computation or function. The output of

any unit is determined by its characteristic, its interconnection to other units, and (possibly) external inputs. The network develops an overall functionality through training.

A typical neuron of the ANN consists of the following features.

- **Input**: Propagates input signals to the neuron
- **Synaptic weights**: Interneuron connection that weighs their respective input signals.
- **Bias**: Threshold that has an effect of either increasing or decreasing the net input.
- **Summing Junction**: An adder for summing the input signals weighted by respective synaptic weights and bias.
- **Activation function**: Modifies the signal from the summing junction using some given function.
- **Output**: Provide the output signal of the neuron.

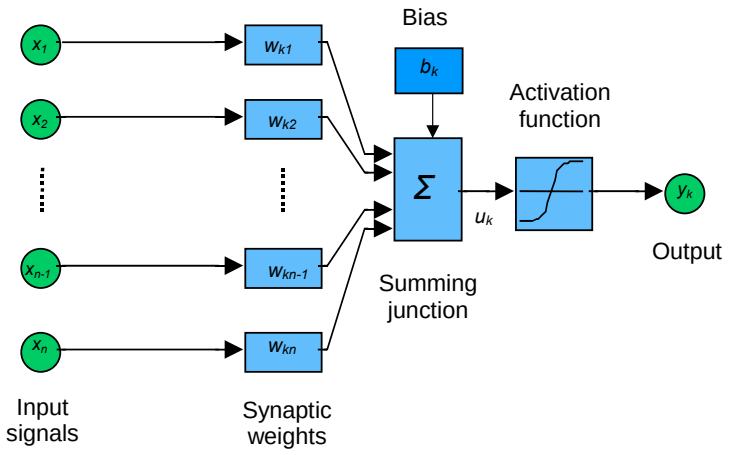

Figure 3.1. Structure of a neuron of an artificial neural network
Adapted from Haykin [1994]

The architecture of a neuron is defined by the connection of inputs, weights and bias together with the activation function. As shown in Figure 3.1, the neuron inputs x_1, x_2,.....x_n are connected to a neuron by weights w_{k1}, w_{k2},..... w_{kn}. All the weighted signals in the neuron are summed up in a junction to produce a net value u_k. The net value may be increased or decreased by employing a bias b_k. The activation function transforms the signal using some given function of u_k. The input and the output in the neuron k may be expressed in the mathematical terms as follows:

$$u_k = \sum_{j=1}^{n} w_{kj} x_j + b_k \tag{3.1}$$

$$y_k = f(u_k) \tag{3.2}$$

3.2.1 Activation Functions

Activation functions constitute an important component of the neural network architecture, as it defines the output from a neuron. The commonly used activation functions and their modified forms used in this study are given below.

i**. Linear function**: The function returns the neuron's output simply as a sum of all the weighted inputs of x_k and bias. This may be modified by a factor k to provide different limiting amplitudes. This function is defined as:

$$y_k = ku_k \tag{3.3}$$

ii. **Sigmoidal function**: The function produces an output in the range of 0 to +1. This function is of the form:

$$y_k = \frac{1}{1+exp(-u_k)} \tag{3.4}$$

iii. **Hyperbolic tangent function**: It is mathematically equivalent to $tanh(u_k)$ and produces an output in the range of -1 to +1. This function is given by:

$$y_k = \frac{2}{1+exp(-2u_k)} - 1 \tag{3.5}$$

iv. **Hyperbolic tangent + linear function**: It can be used to combine non-linearity of the hyperbolic tangent function with the linear function using the weighing factor α. This function has of the form:

$$y_k = \left(\frac{2}{1+exp(-2u_k)} - 1 \right) \alpha + (1-\alpha) u_k \tag{3.6}$$

Figure 3.2 shows these four different activation functions for the data range of –2 to +2. It can be seen that the sigmoidal function and linear function provides lowest and highest limiting amplitudes respectively of the functions considered. The limiting amplitude range of the asymptotes of the sigmoidal and the hyperbolic tangent functions produce a 'squashing effect' to the input signals. The effect limits the value of output of an ANN to values between the two asymptotes, which is useful in keeping the output of a neuron within a reasonable dynamic range [Tsoukalas and Uhrig, 1997]. If the output layers use sigmoidal or hyperbolic tangent functions, the outputs are restricted to a small range of values. The application of the linear function at the output layer makes it possible for the network to take any value.

The hyperbolic tangent and the sigmoidal functions are most commonly used in the hidden layers. The main advantage of these functions is differentiability, which is an important criterion for training neural network using gradient based algorithm.

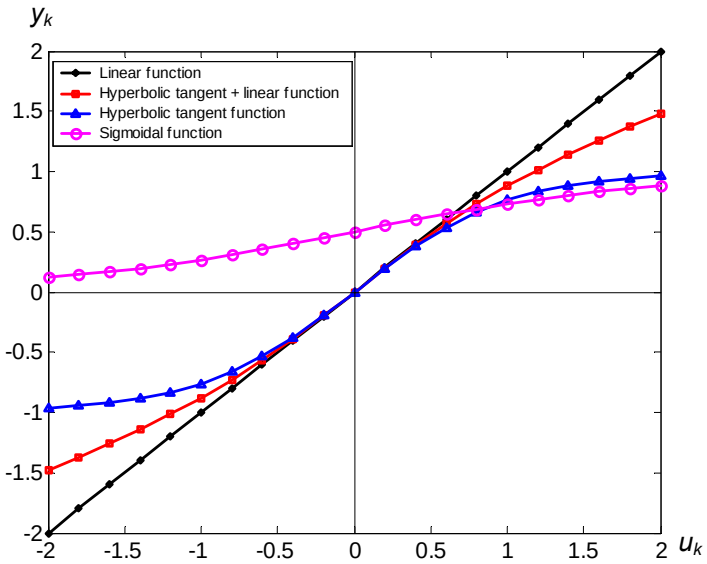

Figure 3.2. Activation functions

3.2.2 Multilayer Perceptrons

The multilayer perceptrons (MLPs) are one of the most widely used types of neural networks, which can be trained in a supervised manner to solve highly non-linear problems. The structure of the MLPs may consist of a number of hidden layers between the input and output layers, each consisting of one or more nodes. The nodes in the consecutive layers are connected but not within the same layer. The output of a node in a layer is only dependent on the inputs it receives from the previous layer, the corresponding weights and bias and the activation function. Thus, there is a uni-directional flow of information from the input to the output layer and the MLPs are also often called multilayer feedforward networks. Figure 3.3 shows a typical MLP network consisting of one input layer, one hidden layer and one output layer.

An MLP model exhibits nonlinearity given by a smooth nonlinear activation function (Haykin, 1994). The presence of a nonlinear activation function is an important characteristic, otherwise the MLP reduces to a linear model. The MLP usually consists of nonlinear functions such as sigmoidal or hyperbolic tangent functions at the hidden layers and linear activation function at the output layer.

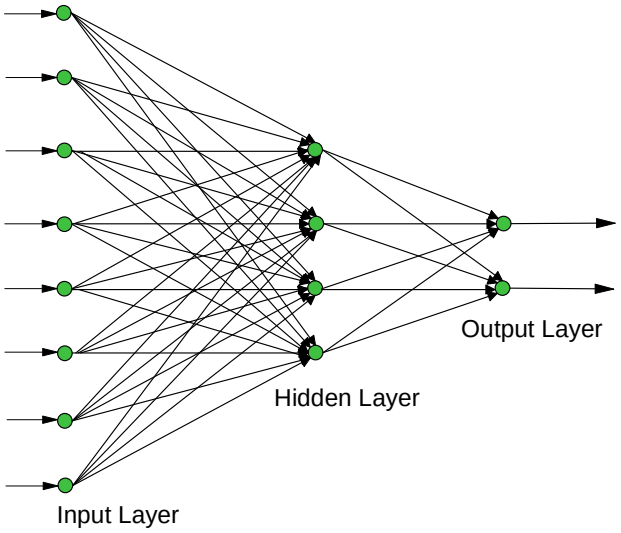

Figure 3.3. Structure of the multilayer perceptron neural network

3.2.3 Dynamic Neural Networks

In static problems such as pattern recognition the input vector *x* can be trained to output vector *y* independent of time. However, in the real world dynamic problems, input and output vectors are no longer independent of time. For instance, in the river hydrodynamics temporal variation from upstream to downstream is an important consideration.

While the standard MLP is popular in many areas of applications they lack the capability to learn the temporal patterns in dynamic systems. The capability of the MLPs in modelling such dynamic systems can be enhanced in a number of ways. In a simple configuration, the standard feedforward network may be used with a sequence of vectors in the input layer at certain time delays. This provides a memory kernel that stores past values in the input signal and the temporal pattern is converted to the spatial pattern. A tap delay operator can be used to provide the memory, which functions as an input pre-processor when used only in the input layer. The tap delay operator may be further extended to the hidden and the output layers in the network, using multiple inputs of the same vector replicated across time. This produces very sophisticated neural topologies, which are useful for time series prediction and system identification. Such networks are commonly known as time delay neuron networks. An example of the temporal neural networks with time delays in the input layer is shown in Figure 3.4.

Recurrent Networks also belong to the class of temporal networks, and consist of feedback loop in the network topology (Figure 3.5). The information from the output of a neuron is circulated back in the network using a feedback loop subjected to time delays. The feedback allows the network to recirculate signals from the past, providing dynamic states to the network. A recurrent ANN maps the signal from state to state, the network

input is the initial state and the mapping is through one or more states to form the network output [Schalkoff, 1997].

The feedback may circulate information through the same level of neuron (local feedback) or through neurons in preceding layers (global feedback). Partially recurrent networks recirculate past outputs of a neuron with a feedback loop to the current or previous layers. For example the first layer outputs of a feedforward network can be recirculated to the same layer inputs. Such networks are usually referred to as Elman networks. The recurrent connection allows the Elman network to both detect and generate time varying patterns. If the network uses totally interconnected recurrent network topology, the network is often referred to as Hopfield net. Input vectors are used as initial conditions to the network, which recurrently updates until it reaches stable output vector [Demuth and Beale, 2004].

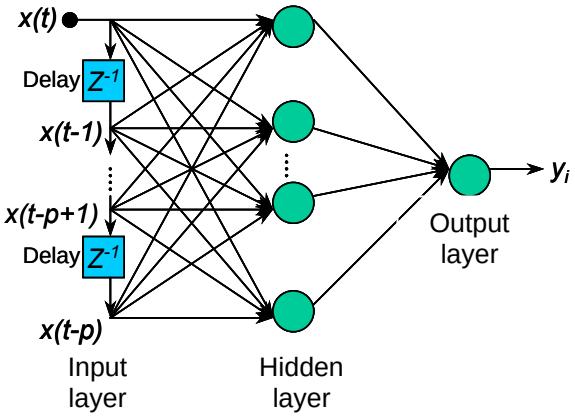

Figure 3.4. Time delay neural network

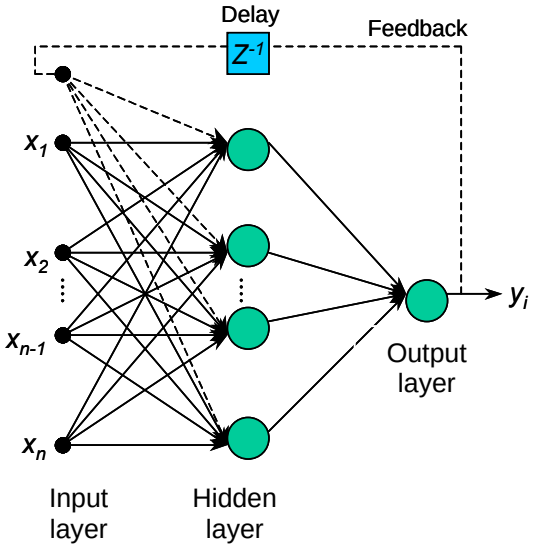

Figure 3.5. Recurrent neural network

3.2.4 Radial Basis Function Networks

The radial basis function network (RBFN) is related to a feedforward network with a modified hidden layer and training algorithm, which may be used for mapping purpose [Schalkoff, 1997]. The network has a three layer architecture consisting of one input layer, one hidden layer and one output layer. The hidden layer of the RBFN consists of Gaussian activation function and the output layer consists of linear activation function. The structure of a RBFN network is schematised in Figure 3.6.

The hidden nodes are the most important processing elements of the RBFNs, which are radially symmetrical and consist of a radial centre vector, and a distance measure. The most common form of the Gaussian activation function in the hidden layer of the RBFNs can be expressed as:

$$u_k = \left\| \left(x_j - w_{kj} \right) \right\|^2 \tag{3.7a}$$

$$y_k = e^{-u_k / 2\sigma^2} \tag{3.7b}$$

where, w_{kj} is the weight vector corresponding to the input vector x_j of the network and σ is the parameter to control the spread of the function.

In contrast to the MLP, the weight vectors are not connected to the input vectors but are used to calculate the distance of the input space from the radial centre. These weights are used in conjunction with the Gaussian function to determine the centre of the units receptive field.

The approximation of the input-output relationship is based on obtaining a suitable number of nodes in the hidden layer and by positioning them in the input space where the data is mostly clustered. The RBFN design and training consists of the determination of the RBFN unit centres and hidden layer weights. The number of nodes in the hidden layer is determined during training process such that the output of the neuron attains a design goal.

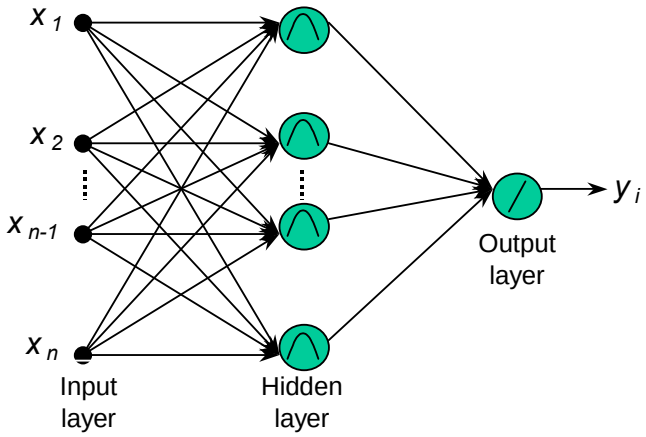

Figure 3.6. Structure of radial basis function network (RBFN)

3.2.5 Neural Network Training

The training process of the ANN involves the adjustment of weights and biases until the specified performance criteria is met. This is similar to the idea of calibration, which is integral part of hydrological and hydrodynamic modelling. The main difference is that the parameters of the hydrological or hydrodynamic models have a physical or conceptual meaning, which is lacking in the case of weights and biases of the neural networks.

The ANN training may consist of unsupervised or supervised methods. The unsupervised training consists of organising the data in terms of suitable classes or clusters. The self-organizing feature maps, also known as Kohonen maps [Kohonen, 1990] use unsupervised learning method. In supervised training, the network performance is judged by comparing the desired outputs corresponding to the target vector with the actual network outputs. There are a number of algorithms available for supervised training. The most popular algorithm for training ANNs are the methods based on the backpropagation algorithm. More details on the some of the training algorithm are given in Appendix A.

3.2.6 ANN Model Construction

The construction of an ANN based model is an iterative process which consists of selection and preprocessing of input and output variables, designing the ANN architecture, training, cross validation and testing. There are no fixed rules for developing an ANN, however, general framework can be based on previous successful applications in engineering [ASCE, 2000a]. The basic framework for the ANN model construction is shown in Figure 3.7.

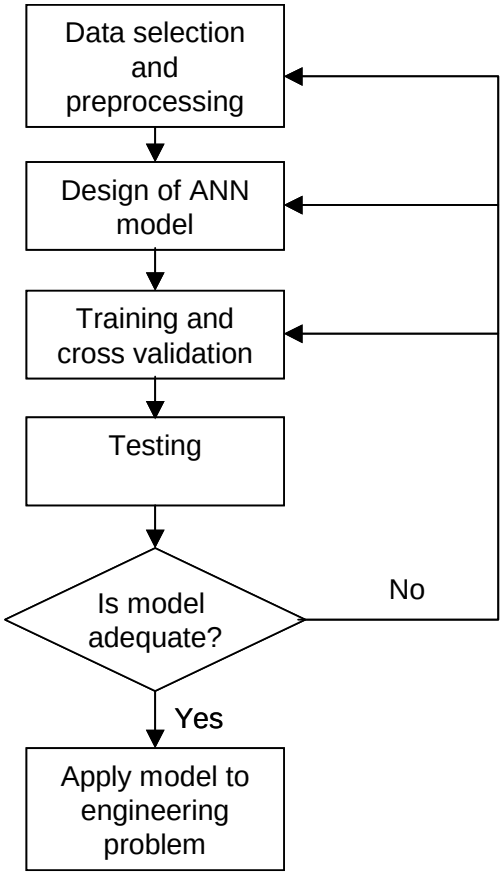

Figure 3.7. ANN model construction
Adapted from Gautam [2000]

3.2.6.1 Data Selection and Pre-processing

The selection of appropriate input and output datasets is an important consideration in the ANN modelling. For the ANN model to be able to generalise the system, it is important that the set of data contains different conceivable events. Although an ANN does not consider the physical basis of the system, it is necessary to understand different physical processes and sub-processes occurring inside the system. The physical insight into the system helps in understanding the dependencies of different datasets, leading to a better selection of input variables. This helps in including key variables into the training process and preventing inclusion of unnecessary and irrelevant information. For instance, a large number of unnecessary inputs will lead to a complex model, and drastically slow down the training process. In such a situation, a more efficient training can be performed when the input variables that do not have significant effects on the performance of the ANN are removed.

Statistical analysis of the input and output spaces can also be performed to identify the underlying relationship of the variables like linear trends, seasonality, outliers etc. For example, cross correlation analysis may be performed between the input and output spaces to identify the corresponding lag times. When the input vectors are highly correlated and redundant, principle component analysis may be performed to reduce the dimension of the input space.

Data normalisation is another important step in pre-processing. Typical data normalisation is in the range between [0 – 1.0] or [-1.0 – 1.0]. If the ANN is to be used for extrapolation, alternative normalisation ranges between [0.1 - 0.9] or [0.2 – 0.8] is suggested [Imrie *et al*., 2000; Dawson *et al*., 2002]. The activation function also provides the 'squashing effect' to the inputs and the effect is higher for the higher data range compared to lower data range. Due to this effect, the ANN may underpredict when the data in the excess of training range are used for model simulation. The lower normalisation range can accommodate the data that are in excess of training datasets and helps in limiting the squashing effects of the activation functions.

3.2.6.2 Design of an ANN Model

The design of an ANN model consists of the selection of appropriate network architecture and training algorithm. Typical applications involve the training of suitable network architectures such as multilayer perceptron, or recurrent networks using the backpropagation or the Levenberg Marquardt algorithm. The design of the network architecture also requires specification of factors, such as the number of neurons in the different layers, the number of hidden layers, and the type of activation functions. An optimum ANN model can be considered as the one with the best performance while retaining simple and compact network architecture. However, the design of optimum

network architecture with number of layers and neurons is a tedious procedure, which usually involves trials and errors. A network with too few neurons cannot approximate the functional relationship between the input and output. An excessive number of neurons may cause a problem called overfitting. The overfitting leads a network that performs very well for the training dataset but becomes unable to generalise new situations (Figure 3.8). A useful strategy is to start with a simple network architecture with minimum number of layers and neurons. The number of layers and neurons can be increased to improve the performance.

3.2.6.3 Training, Cross Validation and Testing

The training of ANNs involves the presentation of inputs and targets to the network and adjusting weights until the desired network performance is achieved. However, the training process should approximate the functional relationship between the input and output and avoid overfitting. For this purpose the available data is generally partitioned into three parts for training, cross validation and testing. The validation sets are used during the training process to monitor the generalisation capability. Normally, the errors of the validation datasets decrease during the initial training iterations but start to rise as the network overfits the training data (Figure 3.9). When the validation errors increase for a number of iterations in a criteria specified by 'early stopping', the training process is stopped and the iteration with the least validation error is used. The test sets are independent sets of data for evaluation of the performance of the trained networks.

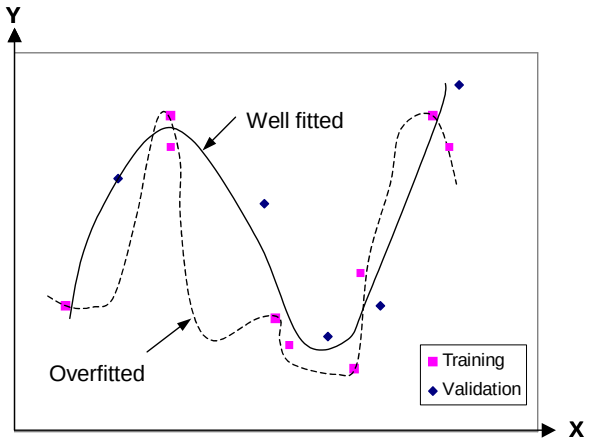

Figure 3.8. Well fitted and overfitted trainings

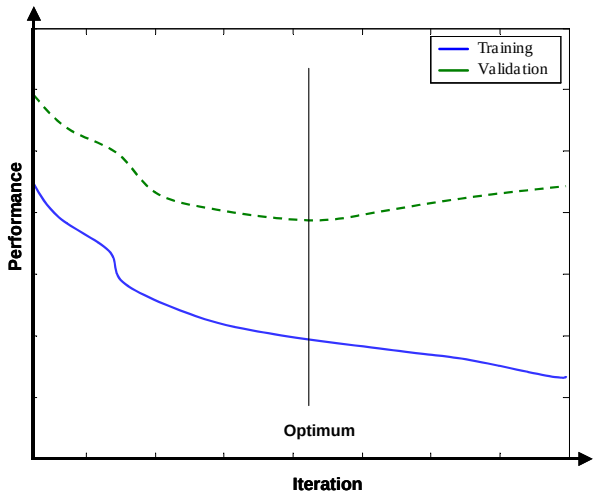

Figure 3.9. Performance of training and validation sets

3.3 Fuzzy Systems

Fuzzy systems such as fuzzy sets and fuzzy logic are based on the concept of 'partial truth', often encountered in the real world problems. In contrast to the classical set theory, defined as either belong to or does not belong to a set, the boundary of a fuzzy set is vaguely defined to take into consideration of the partial truth. Zadeh [1965] introduced the fuzzy set as a class of object with a continuum of grades of membership. Hence, the classical notion of binary membership has been modified for the representation of uncertainty in data.

Fuzzy sets are used to describe the uncertainty and imprecision in a non-probabilistic framework [Bárdossy and Duckstein, 1995]. The transition between the membership and non-membership can therefore be gradual due to imprecisely and vaguely defined boundaries of the fuzzy sets. This property makes the fuzzy set theory viable for the representation of uncertainty in a non-probabilistic form [Maskey, 2004].

Since, the pioneering work of Zadeh [1965], the fuzzy systems have emerged as powerful tools with wide range of applications. Fuzzy systems represent one of the most influential concepts in engineering and operational research such as in the representation of uncertainty, system modelling and data analysis [Wolkenhauer, 2001].

3.3.1 Membership Functions

The membership functions are the essence of fuzzy sets, as they offer flexible means of defining the degree of belongingness to a set. The degree of belongingness or membership may take any value between and including 0 and 1, with no membership at 0 and full membership at 1. The interval between 1 and 0 contains infinity of numbers, which represent partial membership to a given set. In mathematical terms, assuming X as a universe set of x values (elements), then A as a fuzzy subset of X, in ordered pairs is given by:

$$A = \left\{ \left(x, \mu_A(x) \right); x \in X, \mu_A(x) \in [0,1] \right\} \tag{3.8}$$

where, $\mu_A(x)$ is the grade of membership of x in the fuzzy subset A.

A membership function can be of any shape depending on the type of a fuzzy set it belongs to. The only condition a membership function must satisfy is it should vary between 0 and 1.

3.3.2 Fuzzy Numbers

Fuzzy numbers are normal and convex fuzzy sets, whose numerical values in the domain are assigned by specific grades of membership. While Boolean operations such as union

and intersection can be carried out on any fuzzy sets, the fuzzy numbers can be used to perform arithmetic operations such as addition, subtraction, multiplication and division. The commonly used fuzzy numbers are given below and shown in Figures (3.10)-(3.13).

i. **Triangular fuzzy number:** It is based on fuzzy number $A = (a, b, c)$ with $a \le b \le c$. The interval (a, c) is the support of the triangular fuzzy number. This membership function is given by:

$$\mu_A(x) = \begin{cases} 0 & \text{if } x \le a \\ \dfrac{x-a}{b-a} & \text{if } a \le x \le b \\ \dfrac{c-x}{c-b} & \text{if } b \le x \le c \\ 0 & \text{if } x \ge c \end{cases} \tag{3.9}$$

ii. **Trapezoidal fuzzy number:** The function is based on fuzzy number $A = (a, b, c, d)$, where $a \le b \le c \le d$. The interval (a, d) is the support of the trapezoidal fuzzy number. This membership function is given by:

$$\mu_A(x) = \begin{cases} 0 & \text{if } x \le a \\ \dfrac{x-a}{b-a} & \text{if } a \le x \le b \\ 1 & \text{if } b \le x \le c \\ \dfrac{d-x}{d-c} & \text{if } c \le x \le d \\ 0 & \text{if } x \ge d \end{cases} \tag{3.10}$$

iii. **Generalised bell fuzzy number:** It is based on fuzzy parameters (a, b, c), where, b is usually positive and c locates the centre of curve. This membership function is given by:

$$\mu_A(x) = \frac{1}{1 + \left| \dfrac{x-c}{a} \right|^{2b}} \tag{3.11}$$

iii. **Gaussian fuzzy number:** The function based on fuzzy parameters (c, σ), where, c locates the centre of the curve and σ represents the spread. This membership function is given by:

$$\mu_A(x) = e^{\frac{-(x-c)^2}{2\sigma^2}} \tag{3.12}$$

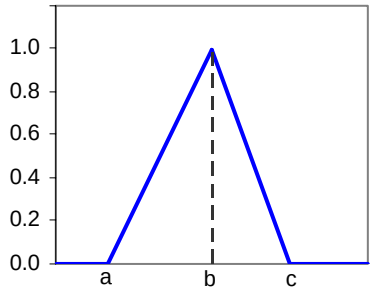

Figure 3.10. Triangular fuzzy number

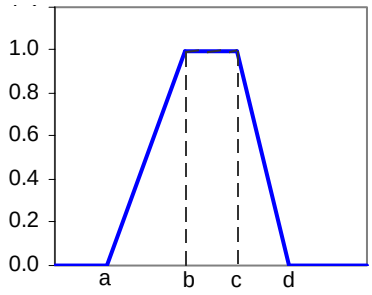

Figure 3.11. Trapezoidal fuzzy number

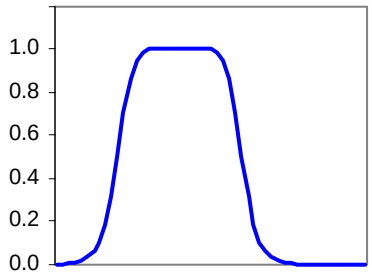

Figure 3.12. Generalised bell fuzzy number

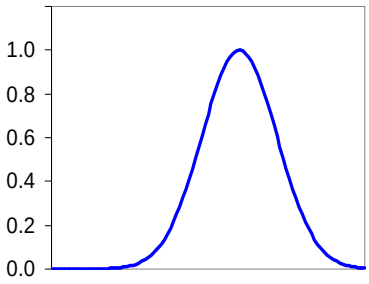

Figure 3.13. Gaussian fuzzy number

The linear function used in the definition of the triangular fuzzy numbers may be replaced by a monotonic function. This is called Left-Right or *L-R* representation of fuzzy numbers [Dubois and Prade, 1980]. According to the modified definition [Bárdossy *et al*., 1990], a fuzzy set *A* of the set of real numbers is called *L-R* fuzzy number if the membership of *x* is calculated as follows (Figure 3.14):

$$\mu_A(x) = \begin{cases} L\left(\dfrac{m - x}{\alpha}\right) & \text{for } x \le m,\ \alpha > 0 \\ R\left(\dfrac{x - m}{\beta}\right) & \text{for } x > m,\ \beta > 0 \end{cases} \tag{3.13}$$

where, m is the central value and α and β are the left and right spreads respectively. L and R are the left and right references (Figure 3.15), given by continuous strictly decreasing functions defined on [0, 1] and:

$$L(z) = R(z) = \begin{cases} 1 & \text{if } z \le 0 \\ 0 & \text{if } z > 1 \end{cases} \tag{3.14}$$

The fuzzy set can be written as:

$$A = (m, \alpha, \beta)_{LR} \tag{3.15}$$

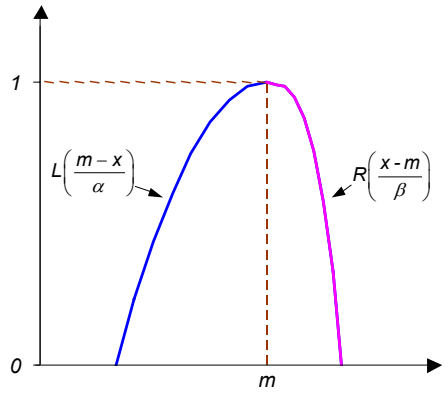

Figure 3.14. L-R fuzzy number

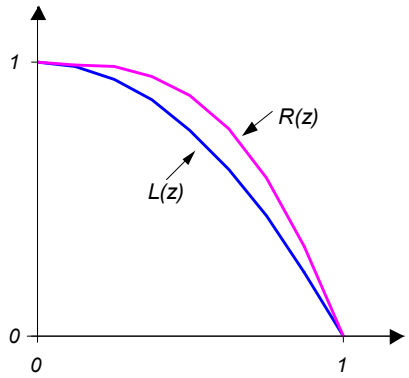

Figure 3.15. L-R fuzzy functions

3.3.3 Extension Principle

The extension principle provides a general method for extending crisp mathematical operations in order to deal with the fuzzy quantities. The mathematical definition of the extension principle from Bárdossy and Duckstein [1995] is as follows.

Let X and Y be two sets, and f a point to point mapping from X to Y.

$$f : X \to Y \quad \text{for every } x \in X \quad f(x) = y \in Y \tag{3.16}$$

The operator f can be extended to operate the fuzzy subset of X. Let A be the fuzzy subset of X with membership function $\mu_A(x)$, then the image of A in Y is the fuzzy subset B with the membership function.

$$\mu_B(x) = \begin{cases} sup\{\mu_A(x);\ y \in f(x),\ x \in X\} \\ 0 \quad \text{if there is no } x \in X \text{ such that } f(x) = y \end{cases} \tag{3.17}$$

where *sup* is the supremum operator (the supremum is the least upper bound).

3.3.4 Alpha Level Cut

The alpha level cuts (α – level cuts) are based on the extension principle and can be used for resolving the fuzzy sets in terms of crisp sets. Parameterisation of the shape of a fuzzy number by α levels offer a convenient way of transforming fuzzy arithmetic into simple arithmetic operations [Tsoukalas and Uhrig, 1997]. When the membership function of a fuzzy set is normal and convex, the interval arithmetic can be used to horizontally cut the fuzzy membership function at a finite number of α - levels between 0 and 1.

Mathematically, let A be the fuzzy subset of X with membership function $\mu_A(x)$. Then, alpha cut (A_α) of the fuzzy subset A is the set of elements, which have at least a membership value greater than or equal to α.

$$A_\alpha = \{x \in X,\ \mu_A(x) \geq \alpha\} \tag{3.18}$$

Figure 3.16 shows an example of fuzzy membership function with α – level cut and its support. Let an α - level cut intersects at two points corresponding to x_1 and x_2 $(x_1, x_2 \in X)$, respectively. Then the set A_α contains all possible values of the variable X including and between x_1 and x_2 and are referred as lower and upper bounds of the α – level cut.

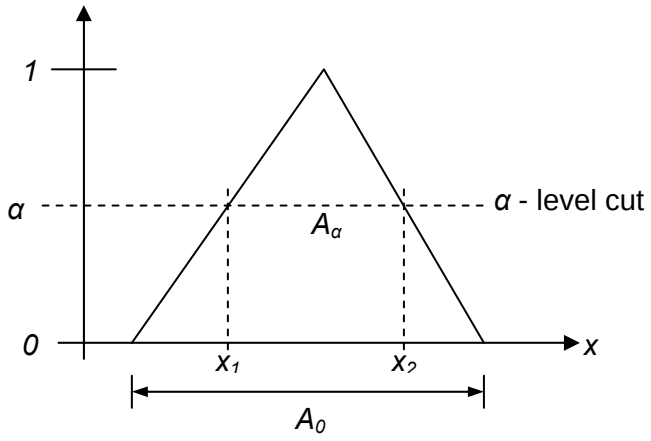

Figure 3.16. Fuzzy membership function and α level cut

3.3.5 Fuzzy Rules

Fuzzy rules are conditional statements that describe the dependence of one variable on another that comprise of fuzzy logic. The fuzzy rules are constructed in the form of 'if-then' statements such as 'if x is A', 'then y is B', where x and y are the variables defined on the values A and B respectively. The 'if x is A' is the antecedent part of the rule and the 'then y is B' is the consequent part of the rule. In general form, a set of arguments $A_{i,k}$ in the form of fuzzy sets with membership functions $\mu_{Ai,K}(x)$ and a consequent B_i may be expressed in the following form:

$$IF\ a_1 \text{ is } A_{i,1} \square\ a_2 \text{ is } A_{i,2} \square \ldots \square\ a_k \text{ is } A_{i,k} \text{ THEN } B_i \tag{3.19}$$

In the above statement, a_k represents the crisp inputs to the rule and the operator $\square$ stands for AND or OR or XOR. In contrast to the crisp rule, fuzzy rules allow partial and simultaneous fulfilment of rules [Bárdossy and Disse, 1993]. The verbal rules are often

translated into fuzzy rules consisting of linguistic variables. The linguistic variables offer a complementary language to the analytical approaches [Tsoukalas and Uhrig, 1997]. The linguistic variables of the fuzziness may be of the forms such as LOW, MEDIUM, HIGH, POOR, SATISFACTORY, FAIR, GOOD, EXCELLENT etc. For example, the fuzzy rule consisting of linguistic variables may be expressed in the following form.

IF inflow is HIGH AND reservoir level is FULL, THEN outflow is HIGH (3.20)

3.3.6 Fuzzy Rule Based Model

A fuzzy rule-based model (FRBM) consists of mapping the relationship between causative and resultant data using a collection of fuzzy rules. The process of formulating the input output mapping using fuzzy logic is referred to as the fuzzy inference. The FRBM also known as the fuzzy inference system consists of membership functions, fuzzy rules and fuzzy operators. An important advantage of the FRBM is, that the physical processes can be expressed in the form of linguistic variables and rules. The FRBM is most suitable where there is very little information or the available information is highly ambiguous [Aronica *et al*., 1998]. The formulation of fuzzy rule based models consists of the following steps.

i. **Fuzzification of the input variables**: The input variables are subjected to fuzzification, which is the process of determining the degree to which the inputs belong to a fuzzy set in terms of membership function. The input variables are compared with the membership functions on the premise part to obtain the membership values of each linguistic label (in the interval between 0 and 1).

ii. **Application of fuzzy operators**: In contrast to the traditional rule-based systems where crisp rules are used, fuzzy rules are satisfied to varying degrees of weights measured on the continuous scale [0,1] depending on the conditions of the rule. The truth value corresponding to the fulfilment of the conditions of the rule for a given premise is called the degree of fulfilment (DOF) of the rule [Bárdossy and Duckstein, 1995]. The DOF is determined based on the membership values of the arguments and logical connector used.

iii. **Combination of rule responses**: Normally several logical rules of the 'IF – THEN' form are partially satisfied producing several associated fuzzy consequences. The overall response from a rule system can be derived from the combination of the relevant individual rule responses. The commonly used combination methods are minimum, maximum and additive methods.

iv. **Defuzzification**: The combined rule consequence is converted to a crisp set, using a process of transforming a fuzzy consequence into a crisp consequence called

defuzzification. The commonly used defuzzification methods include mean of maxima and centroid of area.

The two commonly used fuzzy inference methods include Mamdani type and Sugeno type methods. The Mamdani type inference system uses a fuzzy output membership function. After the application of an implication method, the fuzzy sets from the output variables need to be defuzzified. The Sugeno type inference system uses a nonfuzzy membership function in the output part, in terms of either constant or linear function. The nonfuzzy output makes this method suitable for optimisation and adaptive techniques [The Mathworks Inc., 2004a].

3.3.7 Rule Construction

Rule construction is the most important part in the process of developing fuzzy rule based models. Fuzzy rules may be constructed based on the available knowledge about the system or the available data. There are basically the following ways to obtain the fuzzy rules:

i. The rules are defined by expert knowledge directly.

ii. The rules are assessed based on the combination of expert knowledge and available input/output data.

iii. The rules are derived only from the available input/output data of the system.

In simple systems, the rules, which are the building blocks of a FRBM, can be obtained from expert knowledge. In cases where input/output data are available, it may be more efficient to obtain rules from the available datasets. Analogous to neural networks training, the fuzzy rules can be formulated from the historical data using training sets. Bárdossy and Duckstein [1995] proposed three techniques to obtain fuzzy rules based on training datasets. These include the counting algorithm, the weight counting algorithm, and the least square algorithm. Jang [1993] proposed the adaptive network based fuzzy inference system that identifies parameter of the network through a hybrid learning rule combining the backpropagation gradient-descent with least square method. This method is briefly described in the following subsection.

3.3.8 Adaptive Network Based Fuzzy Inference System

Adaptive network based fuzzy inference system (ANFIS) is a fuzzy inference system implemented in the framework of adaptive networks [Jang, 1993; Jang and Sun, 1995]. The network structure consists of nodes and directional links through which nodes are connected. The part or all of the nodes are adaptive, which means the parameters pertaining to the nodes can be adjusted to minimise the errors. The network architecture

of the ANFIS is similar to the feedforward neural network with supervised learning capabilities. Similar to the adjustment of weights and biases in the neural networks, the premise parameter of the input membership function and the consequent parameters of the output membership functions are adapted in the ANFIS.

Fundamentally, ANFIS is a network representation of a Sugeno-type fuzzy system, endowed with neural network learning capabilities [Tsoukalas and Uhrig, 1997]. In a Sugeno-type fuzzy system, the 'if then rule' of the system is expressed as the output of each rule in a linear combination of input variables a_k plus a constant term p_k:

$$\text{IF } a_1 \text{ is } A_{i,1} \text{ and } a_2 \text{ is } A_{i,2} \text{ and } \ldots \text{ and } a_k \text{ is } A_{i,k} \text{ THEN } f = p_0 + p_1 a_1 + p_2 a_2 + \ldots + p_k a_k \tag{3.21}$$

ANFIS can construct a network for the realization of these rules based on the input-output datasets. The structure of the ANFIS consists of five layers special network topology [Jang, 1993; Jang and Sun, 1995]. The structure of the ANFIS as shown in Figure 3.17 is described below.

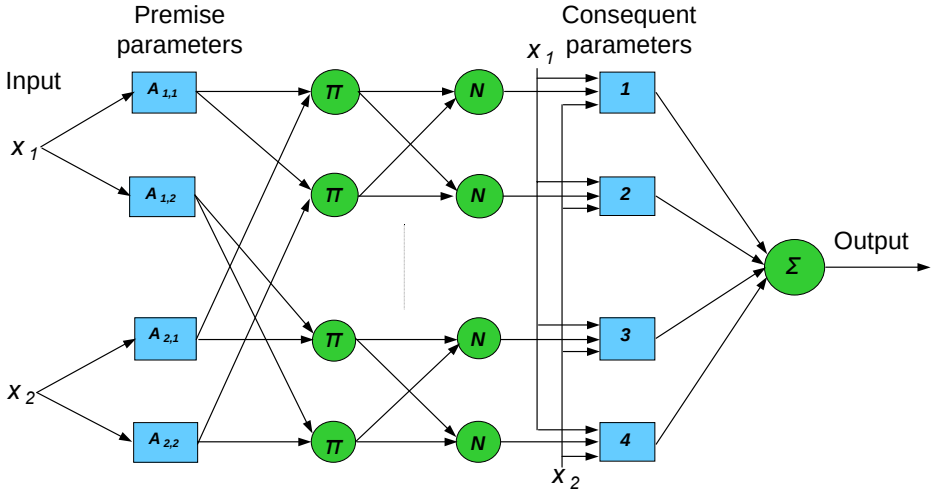

Figure 3.17. Structure of ANFIS
Adapted from Jang [1993]

Layer 1: The layer is the adaptive (square) node consisting of a membership function with a node function. The outputs of this layer are the membership values of the premise part. Membership functions commonly used include generalized bell, Gaussian, triangular and trapezoidal fuzzy numbers.

Layer 2: It consists of a fixed (circle) node denoted by π. Each node in this layer calculates the degree of fulfilment, ν_i by multiplication:

$$\nu_i = \mu_{A_{i1}}(x) * \mu_{A_{i2}}(x) * \ldots\ldots * \mu_{A_{ik}}(x), \quad i = 1:k \tag{3.22}$$

Layer 3: The layer also consists of a fixed (circle) node, each node represented by *N*. The i^{th} node in this layer calculates the normalized DOF as the ratio of the i^{th} rule's DOF to the sum of all rules DOF:

$$\overline{\nu_i} = \frac{\nu_i}{\nu_1 + \nu_2 + ... + \nu_k}, \quad i = 1:k \tag{2.23}$$

Layer 4: It consists of an adaptive (square) node with a node function given by:

$$O_i = \overline{\nu_i} * f_i = \overline{\nu_i}\left(p_0 + p_1 x_1 + p_2 x_2 + ... + p_k x_k\right) \tag{3.24}$$

where $\overline{\nu_i}$ is the output of layer 3 and (p_0, p_1, p_2 ..... p_k) are the parameter sets referred to as consequent parameters.

Layer 5: It consists of a single node that aggregates the overall output as the summation of all incoming sets:

$$y = \sum_i \overline{\nu_i} * f_i \tag{3.25}$$

The ANFIS thus formulated needs to be trained for the mapping of input output datasets. The training consists of the tuning of the premise and consequent membership function parameters. Optimisation algorithms like backpropagation and least square algorithm may be used for the tuning of membership functions parameters of the ANFIS.

The ANFIS implementation in the MATLAB Fuzzy logic toolbox [The Mathworks Inc., 2004a] makes use of backpropagation to learn the premise parameters and least mean square estimation to determine the consequent parameters. The learning procedure has two parts: in the forward pass the functional signals go forward till layer 4 and the consequent parameters are identified by least mean square procedure. In the backward pass, the errors propagate backwards and the premise parameters are updated by gradient descent [Jang, 1993]. The hybrid learning procedure is iterated until the errors reach the specified tolerance limit [The Mathworks Inc., 2004a].

3.4 Review of Applications

In the recent years, there has been a wide range of application of artificial neural networks and fuzzy systems in hydrology and hydraulics. Some of the applications with reference to river flood prediction are given in the following subsections.

3.4.1 ANN Applications

The application of ANN based models has been gaining in popularity in recent years in the field of hydrology and hydraulics. A review of the application of ANNs in hydrology can be found in the ASCE Task Committee on Application of Artificial Neural Networks in Hydrology [ASCE, 2000b]. Typical applications involve the training of two to three layer networks using suitable network architectures like multilayer perceptron, radial basis function networks or recurrent networks. The performances of the ANNs have been found to be comparable with other data driven modelling approaches [Lekkas *et al*., 2001; Sivakumar *et al*., 2002].

Several researchers have demonstrated the application of the ANNs for rainfall-runoff modelling [Minns, 1996; Dawson and Wilby, 1999; Gupta *et al*., 2000; Solas *et al*., 2000; Shamseldin *et al*., 2002]. Most of the applications in this area involve training of runoff from a catchment based on the observed precipitation data. Frequently, supplementary information such as temperature, snowmelt have been added. The results of the studies show that the ANNs provide efficient tools for modelling rainfall runoff processes.

Another popular area of application of the ANNs is the streamflow simulation without involving precipitation as input. A typical application in the streamflow simulation involves the prediction of flows or water levels at a downstream location in a river reach based on the flows or water levels at upstream locations [Thirumalaiah and Deo, 1998; Imrie *et al*., 2000; Liong *et al*., 2000; Lekkas *et al*., 2001; Sivakumar *et al*., 2002]. Frequently, inflows from the tributaries are also added and the ANNs are used to make predictions based on the travel time from upstream to downstream location in a river reach. The results of the studies indicate that the ANNs can provide quick and reliable forecasts, particularly when they are desired over a certain range of values.

There are a number of applications of the ANNs in modelling the nonlinear relationship between the stage and discharge values [Tawfik *et al*., 1997; Bhattacharya and Solomatine, 2000; Jain and Chalisgaonkar, 2000; Sudheer and Jain, 2003]. The applications involve the training of ANNs for discharges based on the water levels. The results of the applications show that the ANNs are superior to single value stage discharge relationship.

Hybrid modelling by integrating neural networks with numerical models has also been a theme of several studies. The outline of different approaches of integrating the numerical models and ANN has been given by van den Boogaard and Kruisbrink [1996]. The approaches include; (i) the training of the ANNs based on the observations and/or simulated results from the numerical models, (ii) with priori knowledge such as continuity equations as constraints, (iii) updating of output variables of numerical models (error correction), (iv) as a pre-processor for numerical models, and (v) ANNs embedded into the numerical schemes.

The recent applications of the integrated ANNs and numerical models include encapsulation of the numerical models [Dibike *et al*., 1999] and the simulation of two-dimensional flow [Dibike and Abbot, 1999]. There are also a number of applications of the ANNs for updating the output variables of the numerical model [Abebe and Price, 2000; Babovic *et al*., 2001; Wright and Dastorani, 2003]. The application of ANNs embedded into numerical schemes include the generation of wave equation from hydraulic data, and an ANN learning scheme that mimic the numerical scheme for the simple cases of one and two dimensional flow problems [Dibike, 2002].

An important criterion in application of ANNs for flood flow simulation is the prediction of flows beyond the range of training datasets. Minns [1996] applied ANNs to both real and theoretical catchments and found that the peak flows were considerably underestimated. Thirumalaiah and Deo [1998] used ANNs for river stage forecasting and found that although lower water levels were predicted fairly accurately, higher water levels were underestimated. Solas *et al*. [2000] used average, dry and wet years mean annual precipitation in a rainfall-runoff modelling application of ANNs and observed that high flows were overestimated for the wet years.

The reasons that the ANNs underestimate or overestimate extreme flows may lie in the network structure used and range of training datasets. Thirumalaiah and Deo (1998) suggested that this could be due to a smaller number of training patterns for higher water levels. Minns [1996] emphasised the need to ensure that the training datasets actually contain all conceivable events.

A number of methodologies useful for making predictions beyond calibration range are outlined in Imrie *et al*. [2000] and Shrestha *et al*. [2005]. This includes the scaling of the input and output datasets and the use of different activation functions at the hidden layers. In the ANN applications the inputs data are generally normalised in the range such as [0 – 1.0] or [-1.0 – 1.0]. In order to accommodate the data beyond training range, alternative normalisation ranges have been suggested. The scaling of training data in a range between [0.1 - 0.9] or [0.2 – 0.8] as compared to the range [0.0 – 1-0] have been reported to be effective means of improving generalisation [Imrie *et al*., 2000; Dawson *et al*., 2002]. This can accommodate validation and test datasets in excess of training datasets.

The upper and the lower limits of activation functions such as [0,1] or [-1,1] also provide a limiting amplitude to the datasets and affect the generalisation capability of the ANNs. Imrie *et al*. [2000] investigated the effects of different output activation functions for improving generalisation using cascade correlation network building strategy. Shamseldin *et al*. [2002] examined the significance of different nonlinear activation functions for the hidden and the output layers in the context of overall performance of the multilayer feedforward networks. An alternative approach is the application of a nonlinear activation function at the hidden and the linear function at the output layers. The application of linear

activation in the output layers enables the network to take any range of values [Demuth and Beale, 2004].

3.4.2 Fuzzy Systems Applications

The application of fuzzy systems in hydrology has been gaining in popularity in the recent years. There are a number of applications of fuzzy rule based models in field of hydrology in general and river flow forecasting in particular. Bárdossy [1996] used the FRBM for the description of elements of the hydrological cycle consisting of infiltration, surface runoff and unsaturated flow. In this application, the fuzzy rules derived according to the expert-specified structure using synthetical datasets were found to provide a robust tool, which could handle non-linearities, without requiring a prescribed functional structure.

Bárdossy [2000] used the fuzzy rules for flood forecasting problem. Fuzzy rules were derived from observed flood events using a combinatorial optimization technique for forecasting peak discharges and daily discharge are in two catchments. Stüber *et al*. [2000] used the FRBM to develop a streamflow simulation model. The model included the upstream flows as inputs and rules are colloquially formulated based on the expert knowledge for the prediction of downstream flows. The study further looked at an automated generation of fuzzy rule rainfall-runoff model in combination with the optimisation algorithm.

One of the main advantages of using the fuzzy systems is their ability to handle the uncertainty in data and model parameters. Maskey [2001] used a fuzzy set theory based method to quantify the uncertainty in a flood forecasting model. The method uses experts' judgements on quality and importance of uncertain parameters using linguistic variables. Maskey [2004] used a probability theory-based Monte Carlo method and the fuzzy set theory-based extension principle method to analyse uncertainties in a flood forecasting model. The disaggregation of the precipitation time series was used for the analysis of the uncertain temporal distribution of precipitation. The study found that output uncertainty due to the temporal distribution can be significant as compared to the uncertainty from precipitation magnitude. Abebe [2004] used the FRBM to characterise the overall prediction uncertainty of a physically based model. The errors between model predictions and corresponding historical observations are used to define extract anticipatory fuzzy rules that relate the expected prediction errors.

Calibration is an important process in the application of hydrological and hydrodynamic models. Aronica *et al*. [1998] used the fuzzy rules for the calibration of a hydrodynamic model to address the problem of uncertainty in data. They expressed the model performance criteria such as peak discharge, in terms of 'if/then' fuzzy rules to derive the likelihood measure. Yang *et al*. [2004] applied the fuzzy multiobjective function for a distributed rainfall-runoff model calibration using only three important features of a hydrograph (time to peak flow, peak flow, and total runoff volume). The fuzzy

multiobjective function describes the acceptability level ranging from 0 to 1 for ‘‘good’’ to ‘‘bad’’, the multiobjective function were minimised during model calibration.

Many of the hydrological applications involve the use of statistical regression analysis of the independent and dependent variables. The variables are quite often characterised by uncertainties and the fuzzy regression analysis provides an alternative tool for the definition of the uncertainties. Bárdossy *et al*. [1990] proposed the application of fuzzy regression as an alternative to statistical regression analysis, when the relationship between the variables is imprecise, data are uncertain and sample size is insufficient. The paper also outlined a number of areas of applications of fuzzy regression in hydrology including discharge curves, water quality parameters and soil hydraulic permeability. Özelkan and Duckstein [2000] used a multi-objective fuzzy regression modelling of conceptual rainfall runoff processes. The study concluded that the multi-objective fuzzy regression has an excellent potential for rainfall runoff modelling for the general problem of reducing possible model error in the case of uncertain data.

There are also a number of applications of the neuro-fuzzy system in river flow forecasting. Gautam [2000] used the autoregressive exogenous input fuzzy inference system (ARXFIS) for the rainfall runoff modelling. The ARXFIS is a Sugeno type dynamic fuzzy system obtained by subtractive clustering of data. The ANFIS was used to fine tune the parameters. Bazartseren *et al*. [2003] compared the performance of ANNs and neuro fuzzy system for the short term water level prediction. The result of the study showed both the ANNs and neuro-fuzzy systems performed comparably well, explicitly outperforming the linear statistical models for the prediction horizon.

CHAPTER 4

COMPLEMENTARY HYDRODYNAMIC, HYDROLOGICAL AND DATA DRIVEN MODELS

This chapter considers a parallel complementary approach of hydrodynamic, hydrological and data driven models for river flow prediction. The methodologies discussed in chapters 2 and 3 are used to develop hydrodynamic, hydrological and data driven models independently. The hydrodynamic numerical (HN) model used in this study includes a physically based one-dimensional (1D) model. The hydrological model consists of a simplified distributed Muskingum Cunge model. The data driven models considered in this study include the artificial neural network (ANN) and the adaptive network based fuzzy inference system (ANFIS).

A reach of the Rhine River from Maxau to Worms gauging stations together with the Neckar River from Heidelberg station to Rhine confluence is taken as the study area. All four models are separately developed to predict water levels at a downstream gauging station at Worms. The performances of each of these independently developed models are assessed and the strengths and limitations of each of these approaches are considered in detail. The important aspects considered include data requirement, forecast horizon and time required to develop each of these models. In addition, the capabilities of these models to predict beyond the range of calibration datasets are assessed. A complementary modelling approach is discussed, so that the strength of one model can complement the other.

4.1 Study Area

The study is conducted in the section of the Rhine River in South - Western Germany in the region of Heidelberg, Karlsruhe, Mannheim and Ludwigshafen. The area consists of a reach of about 80 km length from the gauging station Maxau (Rhine km 362.30) to the gauging station Worms (Rhine km 443.40) as shown in Figure 4.1. The reach lies in the upper Rhine section from Basel (Rhine km 170) to Bingen (Rhine km 530), which flows through the plain between the mountains of the Black Forest and the Vosges. This section of the Rhine River receives a major tributary the Neckar River at Mannheim (Rhine km 428.20). Hence, the 26 km reach of the Neckar River from the gauging station Heidelberg (Neckar km 26.10) to confluence is also included in the study. The catchment area of the Rhine River at the Worms station and the Neckar River at the Heidelberg station are

68827 km^2 and 13783 km^2 respectively [LFU, 2000]. There are no major tributaries in either of the reaches. The Rhine river reach does not consist of any structures, while the Neckar reach consists of a number of barrages and navigation canals.

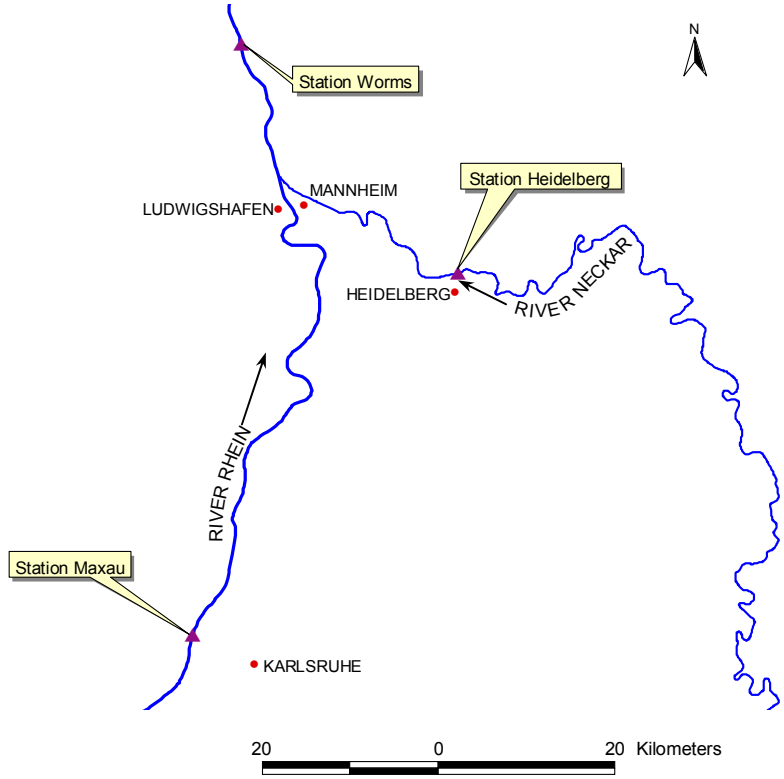

Figure 4.1. Study reach of the Rhine and Neckar River

4.2 Available Data

The basic data required for the physically based models are flow time series and river cross sections. Similarly, only time series data are required for the data driven modelling approaches. The river cross sections consist of river channels and floodplains at 100 m intervals. The cross section data are obtained from the following sources:

- State Office for Land Survey Baden – Württemberg (*Landesvermessungsamt Baden – Württemberg*)
- Federal Waterways Engineering and Research Institute (*Bundesanstalt für Wasserbau BAW*), Karlsruhe
- Water and Navigation Office (*Wasser und Schifffahrtsamt*), Heidelberg

The flow data are obtained from the Water and Navigation Administration (*Wasser und Schifffahrtsdirektion*) South-West, Mainz. The data consists of flow and water level time series at one hour intervals from the gauging stations Maxau, Worms and Heidelberg for

the 1988, 1990, 1993 and 1994 flood events. The statistical characteristics of the data are summarised in the Table 4.1.

Table 4.1. Statistical characteristics of the flow data

Gauging Station	Year	No. of records	Maximum flow (m^3/s)	Minimum flow (m^3/s)	Mean flow (m^3/s)	Standard deviation (m^3/s)
Maxau	1988	1440	4079	843	2083	785
	1990	348	4200	752	2044	938
	1993	490	3007	1014	1844	554
	1994	696	2393	1178	1530	232
Worms	1988	1440	5268	1093	2791	1075
	1990	348	4734	933	2558	1052
	1993	490	4765	1289	2567	914
	1994	696	3940	1410	2020	555
Heidelberg	1988	1440	1945	224	619	462
	1990	348	2299	224	547	523
	1993	490	2706	246	710	556
	1994	696	2341	224	453	415

The available flow and stage data are plotted against each other for all four years of records. Figures 4.2, 4.3 and 4.4 depict the stage discharge plot for the Maxau, Worms and Heidelberg gauging stations respectively. It is obvious that the flow data from all three stations have been derived from a single value stage discharge curve. However, due to unsteady flow in the rivers, the relationship may be characterised by hysteresis, depicting different stage discharge relationships for the rising and the falling limbs of a hydrograph. A more detailed treatment in this respect is given in chapter 6. As the water levels are directly measured values and the discharges values are derived from the curve, the water level times have better accuracies compared to discharges. Hence, it is decided to use the water levels at the Worms station for the calibration of the hydrodynamic and hydrological models and as targets for the training and validation of data driven models.

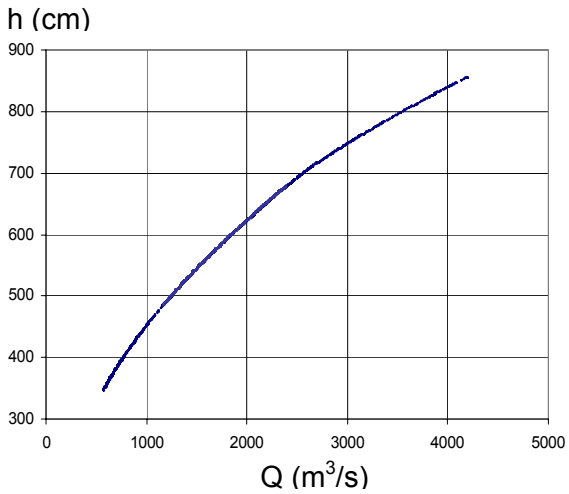

Figure 4.2. Stage discharge relationship for the Maxau station

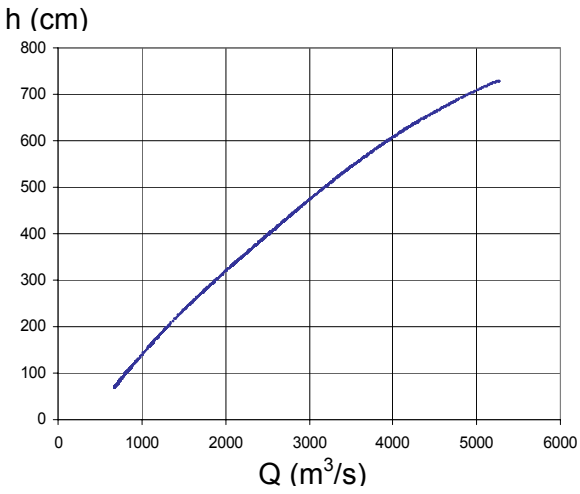

Figure 4.3. Stage discharge relationship for the Worms station

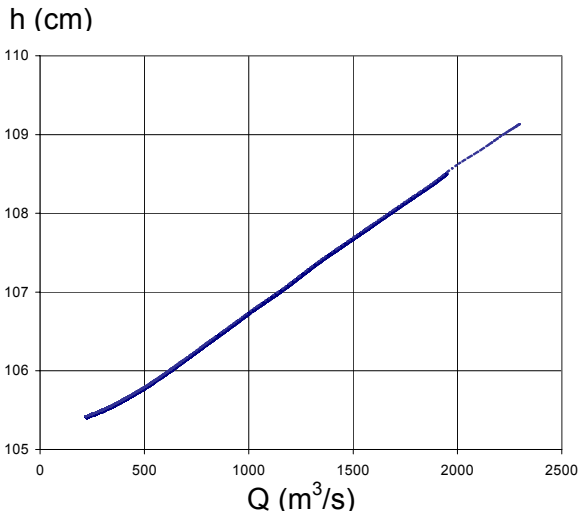

Figure 4.4. Stage discharge relationship for the Heidelberg station

4.3 Hydrodynamic Numeric Model

As a first modelling option for the study area a one dimensional (1D) hydrodynamic numerical (HN) model is used. This study is only concerned with the flow and water level at the gauging stations. Since, the transverse flow and stage variations are not of specific interest, the 1D assumption is adequate [USACE, 1993]. Due to this limited scope, the use of multidimensional models such as 2D model is ruled out.

The HN is set up using the 1D modelling system CARIMA from SOGREAH [1978]. The CARIMA is a generalised hydrodynamic numerical modelling system based on full one-dimensional Saint-Venant equations. The solution of these equations is based on the

Preissmann implicit finite difference method, which is generally considered unconditionally stable for all Courant numbers [Cunge *et al.*, 1980]. The CARIMA modelling system is capable of handling a complex network of channels and structures like weirs and bridges. As the system is based on the full Saint Venant equations, it is also capable of representing the backwater influence of tributaries such as in the Rhine - Neckar confluence. A wide range of applications of the CARIMA has been reported in Cunge *et al.* [1980] and it has been used comprehensively in the Institute of Water Resources Management, Hydraulic and Rural Engineering, University of Karlsruhe [Theobald, 1999; Minh Thu, 2002; Oberle, 2004].

4.3.1 Model Implementation

The HN model is applied to the study area with a computational grid size of Δx = 100 m and Δt = 1 hour, which satisfies the stability criteria of equations (2.24) and (2.25). The time weighing factor θ = 0.6 is used. The model geometry is defined by cross sections consisting of channel bed and floodplains at 100 m interval in both the Rhine and the Neckar sub-reaches. The number of cross sections is 811 in the Rhine sub-reach from Maxau to Worms and 298 in the Neckar sub-reach from Heidelberg to the confluence. The schematisation of the reaches in the HN model is shown in Figure 4.5.

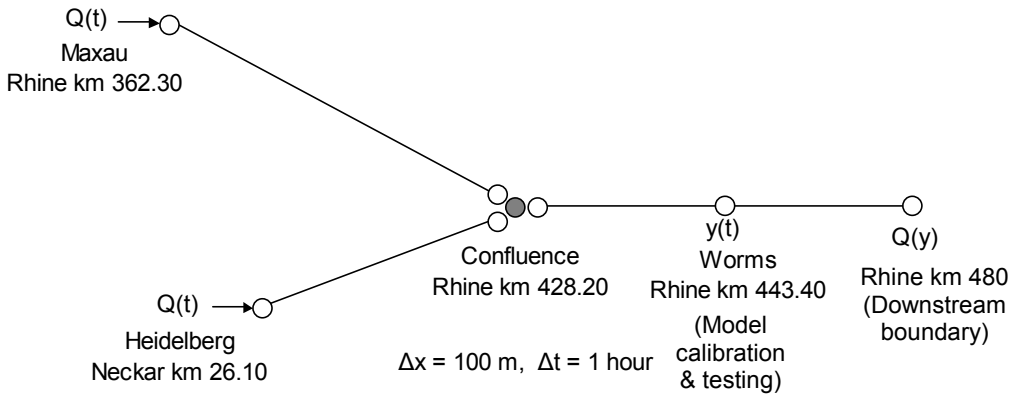

Figure 4.5. Schematisation of the reaches in the HN model

The flow hydrographs $Q(t)$ from the gauging stations at Maxau (Rhine) and Heidelberg (Neckar) are used as upstream boundary conditions. Although the stage hydrograph is available at the downstream boundary of the Worms station, it will not be available if the model is used for flood forecasting purpose. In such a situation, a single value stage discharge relationship $Q(y)$ is more convenient to use as the downstream boundary condition. However, due to the unsteady flow situation in nature, the relationship is not a single valued condition, but takes a looped form. The application of a single valued condition causes the unsteady character of the flow to be perturbed along a certain distance upstream. Therefore the downstream boundary condition should be located

sufficiently downstream from the station being used for calibration [Cunge *et al.*, 1980]. Because of this reason, the downstream boundary $Q(y)$ is extended to a further distance of 36.6 km. The initial conditions of the model are set up using a steady flow calculation.

The unsteady flow calibration is done by adjusting the model parameter (Strickler coefficient) in such a way that a good match can be obtained between the observed and simulated time dependent hydrographs. The stage hydrograph at the Worms station is used for the calibration of the model. Different values of the Strickler energy loss coefficients at the main channel and the floodplains are used. This consists of 10 different values of the Strickler coefficient in the range of 25 to 40 $m^{1/3}/s$ in the river channel and 4 different values from 15 to 25 $m^{1/3}/s$ in the floodplains. The Neckar reach has been calibrated using the steady flow water surface profiles as described in section 5.2 and therefore no further calibration is done. The biggest flood event consisting of the 1988 datasets is used as calibration datasets and 1990, 1993 and 1994 as test datasets.

4.3.2 Results and Discussion

The comparison of observed and HN-simulated results for the 1988 flood event (calibration) is depicted in Figure 4.6. The comparisons for the test datasets (1990, 1993 and 1994 floods events) are shown in Figures 4.7, 4.8 and 4.9. The performance of the HN model is assessed using the statistical criteria of the coefficient of determination (R^2), and the root mean square error (RMSE). In addition, the peak error (PE) and the maximum absolute error (MAE) in water levels are also considered. The detail description on these criteria is given in Appendix B. The results of the statistical analysis are summarised in Table 4.2.

The performance of the HN model for the 1988 flood event (calibration datasets) is found to be very good, considering both the phase and amplitude portraits of the flood wave. The HN model overestimates the peak of the 1990 flood event (test dataset). The 1990 model results also consist of a phase error leading to an incorrect arrival time of the flood peak. However, the performance of the HN model in the cases of the 1993 and 1994 flood events (test datasets) are quite reasonable. There are good matches for the flood wave phases, with correct simulations of the arrival time of the peak water levels. However, the initial low water levels for both of the flood events are overpredicted.

Table 4.2. Statistical performance of the HN model results

Flood Event	R^2	RMSE (m)	PE (m)	MAE (m)
1988	0.9937	0.16	-0.04	0.32
1990	0.9611	0.38	0.32	0.46
1993	0.9842	0.21	0.08	0.22
1994	0.9820	0.17	0.14	0.41

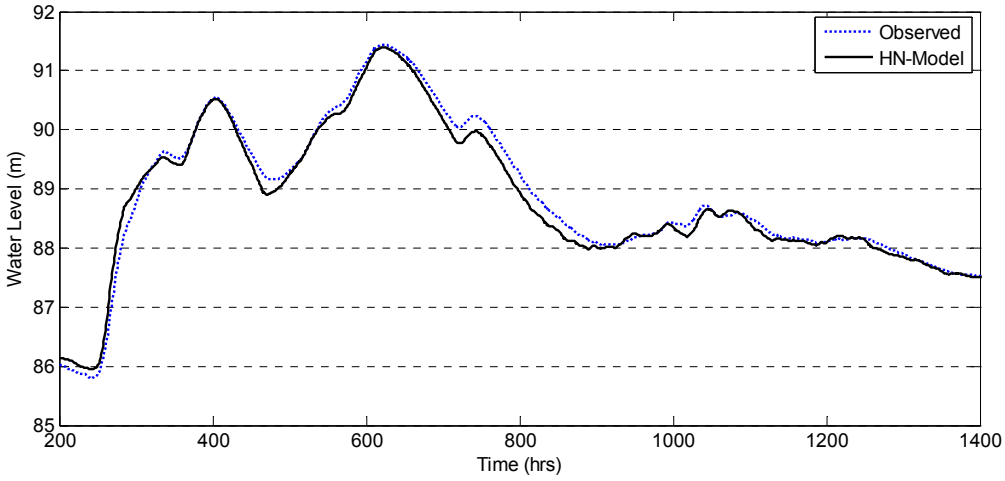

Figure 4.6. Observed and HN model results at the Worms station (1988 calibration datasets)

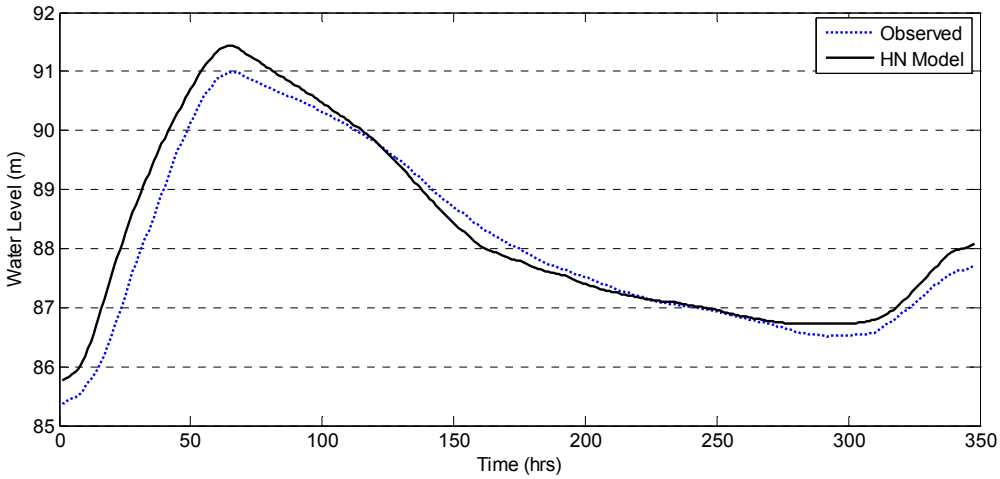

Figure 4.7. Observed and HN model results at the Worms station (1990 test datasets)

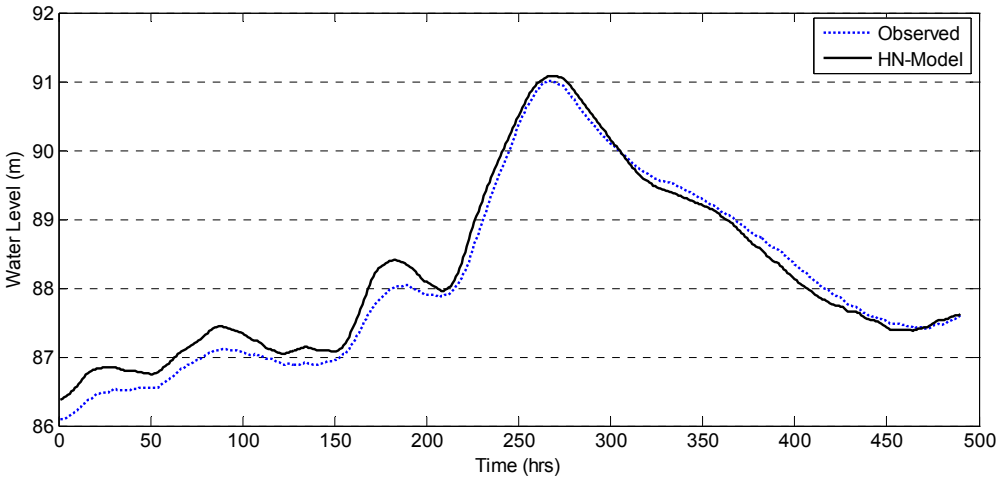

Figure 4.8. Observed and HN model results at the Worms station (1993 test datasets)

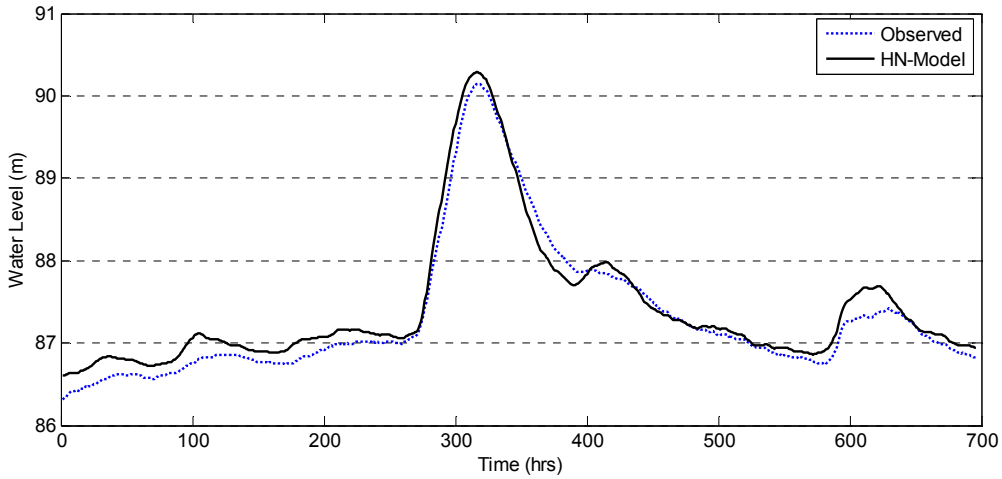

Figure 4.9. Observed and HN model results at the Worms station (1994 test datasets)

4.4 Muskingum Cunge Hydrological Model

A Muskingum Cunge (MC) simplified distributed hydrological model is the second model applied to the study reach. The model as shown in Figure 4.10 consists of three reaches: Maxau – confluence, Heidelberg – confluence and confluence – Worms. The space time grid is defined by the stability criteria of the equations (2.36) – (2.39). The time step (Δt) of 1 hour is chosen, which satisfies the stability criteria for Δt considering the minimum time of rise of upstream hydrograph of 36 hours (1993 and 1994 flood events). Similarly, the grid space (Δx) is chosen to get the average Courant number close to 1 according to the equation (2.36). Hence, model reaches are further divided into seven sub-reaches (j) between Maxau – confluence, three between Heidelberg - confluence and two between confluence – Worms. A simple algebraic summation is used for the addition of flows at the confluence as given by the equation (4.1).

$$Q_{confluence} = Q_{out(Worms-Confluence)} + Q_{out(Heidelberg-Confluence)} \tag{4.1}$$

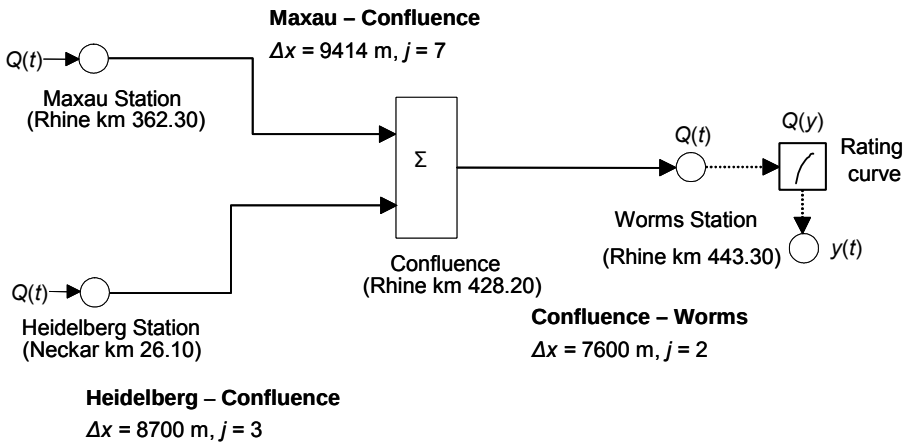

Figure 4.10. Schematisation of the reaches in the Muskingum Cunge based model

4.4.1 Model Implementation

The MC based routing model is developed using the interactive MATLAB/Simulink environment. The river reaches are represented by subsystem blocks in the Simulink as shown in Figure 4.11. There are further subsystems under each reach subsystem consisting of computational elements of the model. The finite difference schemes given by the equation (2.29) are formulated using feedback loops and time delays. The river cross sections at Maxau, Heidelberg and Worms are used to define the river geometry. Lookup tables are used to define the time varying relationship such as stage and discharge (rating curve), and stage and cross section variables: flow area, flow width and wetted perimeter. Hence, the cross section parameters together with the Strickler coefficients are used to obtain the coefficient values C_1, C_2, and C_3 from the equations (2.30a), (2.30b) and (2.30c).

The MC model does not require a downstream boundary condition and the available downstream water levels can be used for the model calibration. For the same reason described in section 4.2.1 the water levels time series are used in preference to the flow time series for the calibration. The MC model calibration is done by adjusting the model parameter (Strickler coefficient). In this case too, the 1988 datasets are used for the model calibration and the 1990, 1993 and 1994 for model testing. The water levels at the Worms station are obtained by transforming the output discharge time series using a depth discharge lookup table (rating curve). Best results are obtained with the Strickler energy loss coefficients coefficient: 38 $m^{1/3}s^{-1}$ in the Rhine reach and 35 $m^{1/3}s^{-1}$ in the Neckar reach. The average values of the Courant number obtained are 0.74, 1.35 and 1.04 for the Maxau – confluence reach, the Neckar-confluence reach and the confluence-Worms reach respectively.

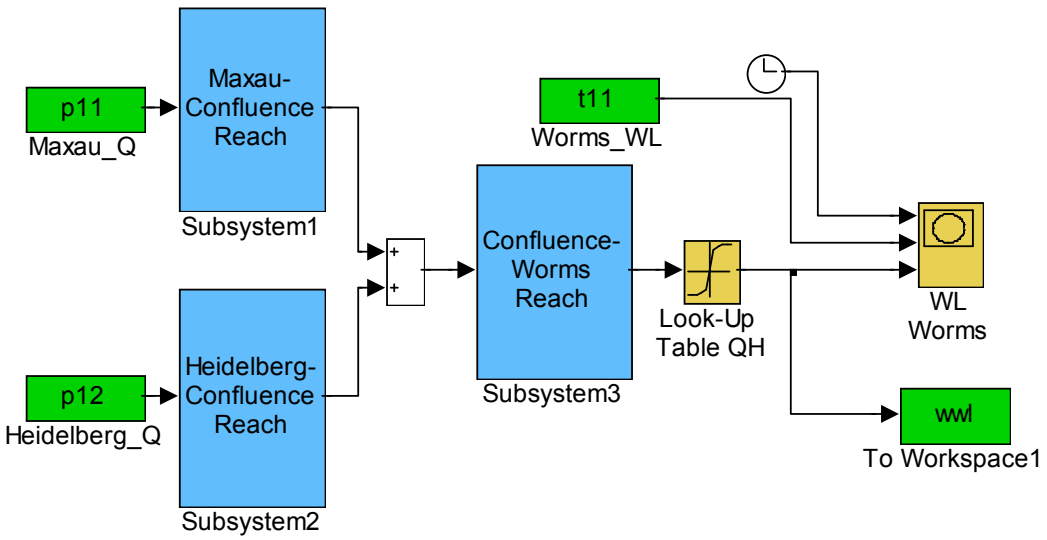

Figure 4.11. Schematisation of the model in Simulink

4.4.2 Results and Discussion

The comparison of observed and MC model simulated results for the 1988 flood event (calibration) is depicted in Figure 4.12. The comparisons of the model simulation for the 1990, 1993 and 1994 floods events (test datasets) are shown in Figures 4.13, 4.14 and 5.15. The statistical performance of the model results is given in Table 4.3.

The overall performance of the MC model is found to be good for both the calibration and the test datasets. In the case of the 1988 flood event (calibration datasets) there is some underprediction in the first peak. However, the MC model depicts better performance for the 1990, 1993 and 1994 test datasets. There are very good fits of the amplitude and phase portraits of the 1993 and 1994 datasets. In this case also, there is an overprediction of the 1990 flood peak. In comparison to the HN model, the MC model has a better performance in terms of the R^2 and RMSE criteria for all three test datasets. The model predicts the flood peaks very well with the peak error (PE) less than 30 cm. The maximum absolute error (MAE) in the water level is about 50 cm.

Table 4.3. Statistical performance of the Muskingum Cunge model results

Flood Event	R^2	RMSE (m)	PE (m)	MAE (m)
1988	0.9931	0.18	0.10	0.52
1990	0.9823	0.15	0.30	0.48
1993	0.9962	0.08	0.14	0.22
1994	0.9927	0.09	0.09	0.26

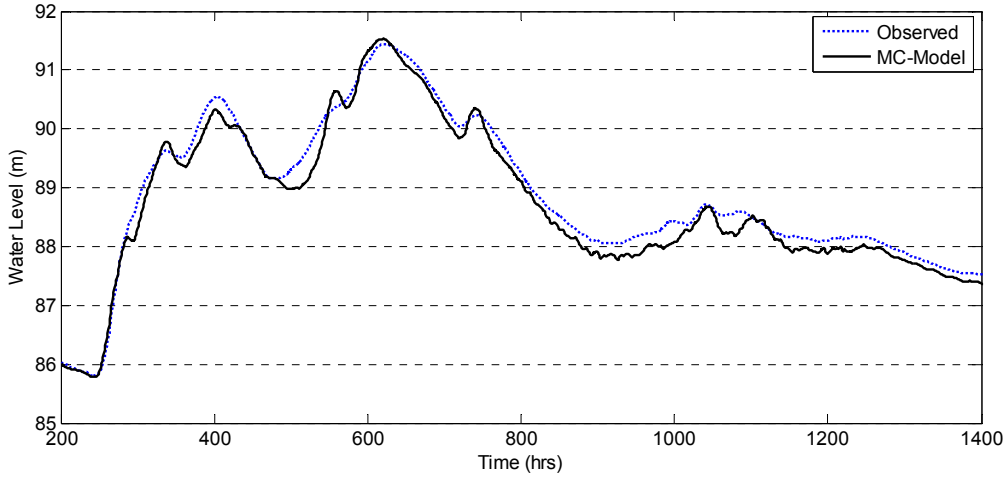

Figure 4.12. Observed and Muskingum Cunge model results at the Worms station (1988 calibration datasets)

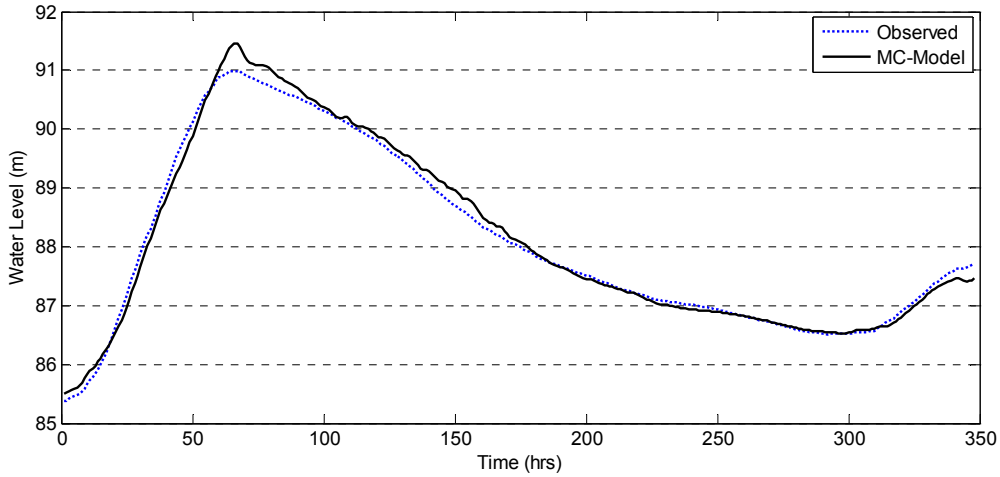

Figure 4.13. Observed and Muskingum Cunge model results at the Worms station (1990 test datasets)

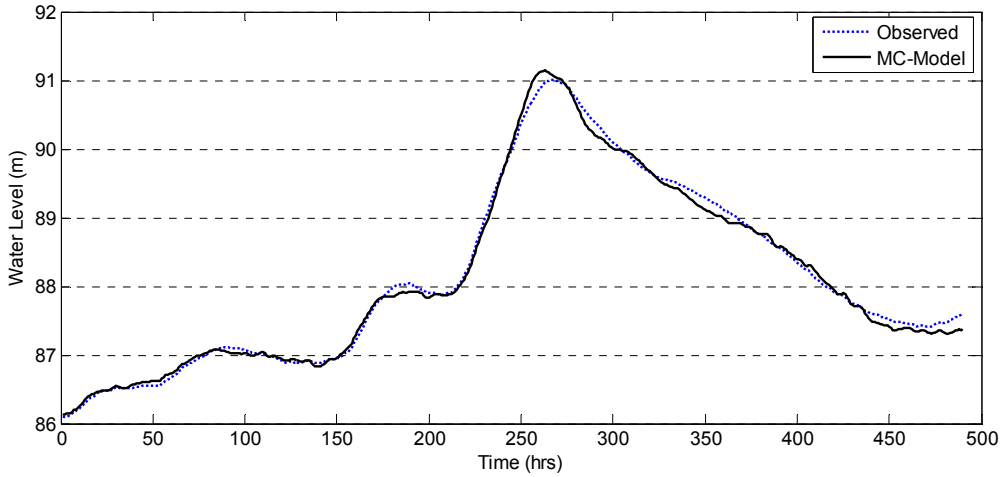

Figure 4.14. Observed and Muskingum Cunge model results at the Worms station (1993 test datasets)

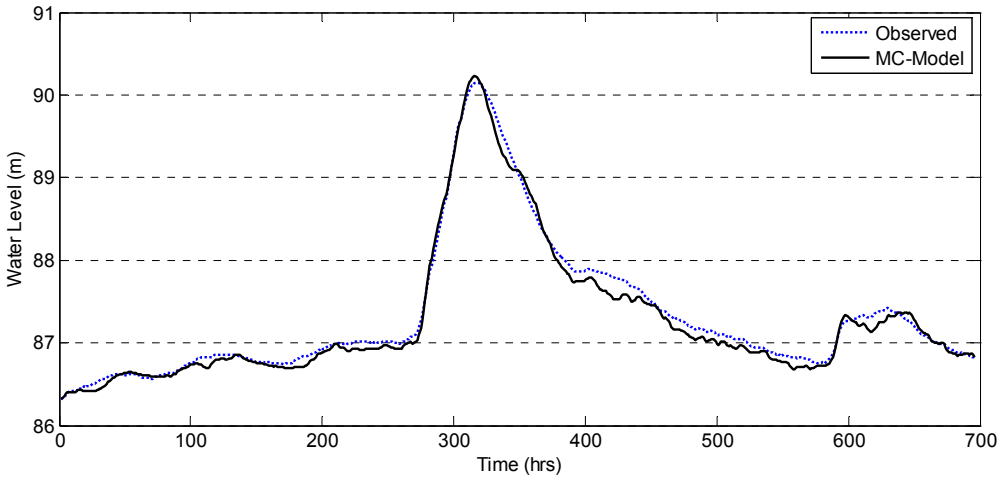

Figure 4.15. Observed and Muskingum Cunge model results at the Worms station (1994 test datasets)

4.5 Data Driven Models

The third part of this study considers two data driven methods for the study reach. The methods include the artificial neural network (ANN) and the adaptive network based fuzzy inference system (ANFIS) models. Since both the modelling approaches are quite similar, they are considered together.

The first step in developing the ANN and the ANFIS based model is the selection of appropriate model architecture and the model inputs and outputs. The ANN architecture selected consists of a recurrent network, which can be trained in a supervised manner to solve time varying non-linear problems. The architecture of the ANFIS model consists of a grid partitioned structure, with the domains of the antecedent variables partitioned into a specified number of membership functions.

The inputs and outputs to the both data driven models are deliberately taken the same as the HN and the MC models, so that the direct comparison of the results can be made. Hence, the flow time series from the Maxau stations in the Rhine River and the Heidelberg station in the Neckar River are taken as the model inputs. The water level time series at the Worms station is taken as the targets. It is to be noted that the data driven models can also be trained for flow time series based on the upstream flow time series or water level time series based on the upstream water level time series.

4.5.1 Model Implementation

As both the ANN and the ANFIS models are based on direct mapping of input output datasets, they perform best when the inputs are shifted based on the appropriate time lags between the inflows and the outflows. The cross correlation analysis is usually done to find the appropriate lag time between upstream and downstream [Imre *et al.*, 2000; Gautam, 2000]. However, such an analysis did not yield a uniform lag time as the flow at the Worms station is influenced by the flow from the Neckar River. Hence, the lag time is carefully examined based on peak flows at all three stations. From the examination, 24 hours lag time from Maxau to Worms and 8 hours lag time from Heidelberg to Worms are adapted. The inputs and outputs of the data driven models are shown in Figure 4.16.

The training sets for both the data driven models are taken as the 1988 flood events data, which is the same data used for HN and MC models calibration. The flood event data from 1990 is used for validation and 1993 and 1994 as test datasets. The inputs and outputs are normalised between –1 and 1.

The structure of the ANN consists of 2 neurons in the input layer, 16 neurons in the first hidden layer, 10 neurons in the second hidden layer and 1 neuron in the output layer. It is observed during initial trainings that the use of recurrent feedback in the output layer enhances the performance of the ANN. Hence, the recurrent networks are used for all the

network trainings, although it slowed down the training process considerably. The network consists of hyperbolic tangent activation functions in the hidden layers and linear activation function in the output layer. The ANN model is developed using the procedure of the MATLAB Neural Network Toolbox [Demuth and Beale, 2004]. The backpropagation algorithm with Bayesian regularisation of the Levenberg-Marquardt approximation is used for the trainings. Early stopping criteria provided by the validation datasets are used to prevent overtraining. The test datasets are used independently for the evaluation of the model performance.

The ANFIS model is developed using the procedures of the MATLAB Fuzzy logic toolbox [The MathWorks Inc., 2004a]. The structure of the ANFIS model consists of a Sugeno type fuzzy system with generalised bell input membership functions and a linear output membership function. The network consists of 2 inputs each with 3 input membership functions, 9 rules and 1 output membership function. The training algorithm consists of the backpropagation and least squares estimation for the adjustment of premise and consequent parameters of the ANFIS respectively. In this case too, early stopping criteria provided by the validation datasets are used to prevent overtraining and the test datasets are used for the independent evaluation of the model performance.

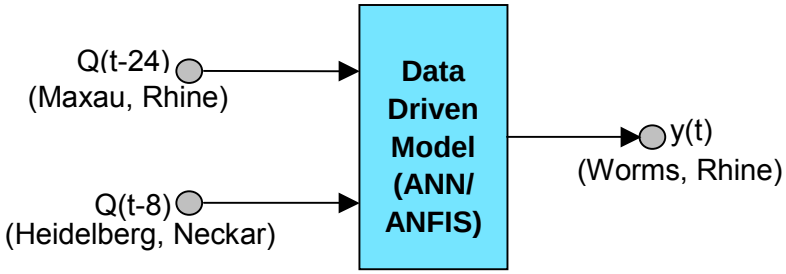

Figure 4.16. Input and output of the data driven models

4.5.2 Results and Discussion

The comparison of the observed water levels with the simulated results from the ANN and ANFIS for the 1988 (training) and 1990 (validation) flood events are given in the Figures 4.17 and 4.18 respectively. The comparisons for the 1993 and 1994 (test) floods events are shown in Figures 4.19 and 4.20. The statistical performances of the ANN and ANFIS model results are summarised in Table 4.4 and Table 4.5.

The overall performance of both the ANN and the ANFIS models are found to be quite close to each other for the training, validation and test datasets. In the case of the 1988 training dataset, results of both the ANN and the ANFIS models have a good match with observations. The 1990 (validation) dataset show overprediction of peak water levels with the errors of 0.62 and 0.68 m for the ANN and ANFIS models respectively. It is to be

noted, that the HN and the MC models also overpredict the peak water levels for the 1990 datasets. However, both the ANN and ANFIS performed reasonably well for the 1993 test datasets with a good fit of the peak water levels. The performances of the ANN and the ANFIS are similar for the 1994 test datasets. The statistical performance of the ANN in terms of R^2, RMSE, PE and MAE parameters are found to be slightly better in comparison to the ANFIS model.

Table 4.4. Statistical performance of the ANN model results

Datasets	R^2	RMSE (m)	PE (m)	MAE (m)
Training (1988)	0.9956	0.12	0.03	0.52
Validation (1990)	0.9886	0.22	-0.62	0.74
Test (1993)	0.9919	0.10	0.04	0.43
Test (1994)	0.9883	0.07	-0.11	0.40

Table 4.5. Statistical performance of the ANFIS model results

Datasets	R^2	RMSE (m)	PE (m)	MAE (m)
Training (1988)	0.9938	0.12	-0.14	0.50
Validation (1990)	0.9848	0.24	-0.68	0.77
Test (1993)	0.9902	0.10	-0.04	0.41
Test (1994)	0.9839	0.08	-0.02	0.52

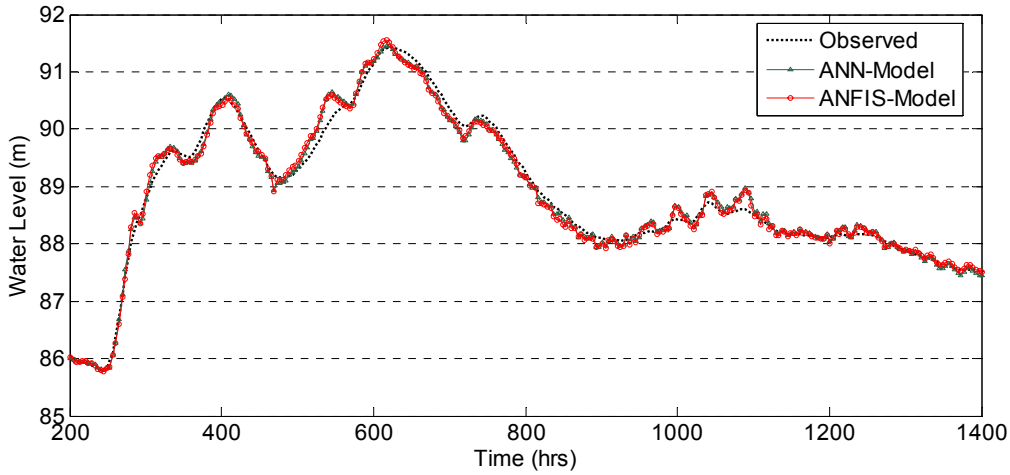

Figure 4.17. Observed, ANN and ANFIS results the at Worms station (1988 training datasets)

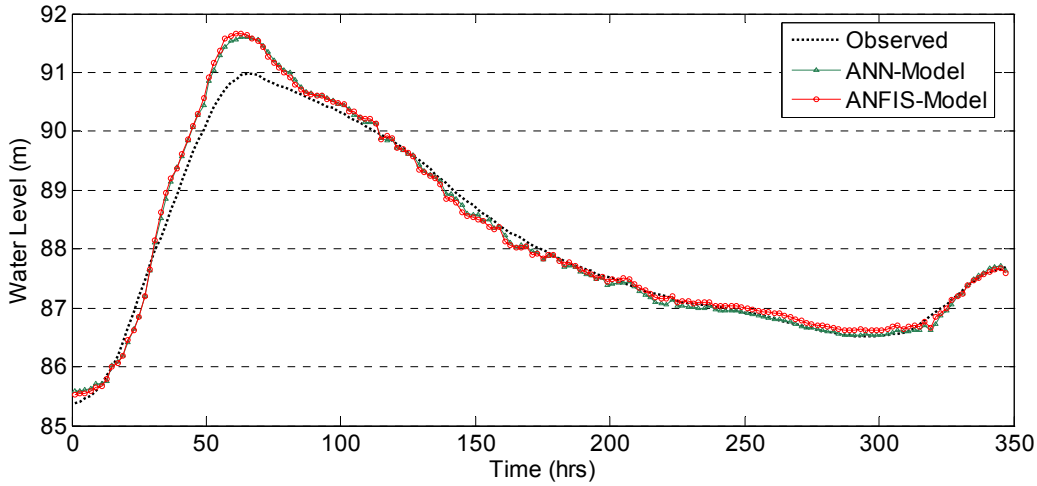

Figure 4.18. Observed, ANN and ANFIS results at the Worms station (1990 validation datasets)

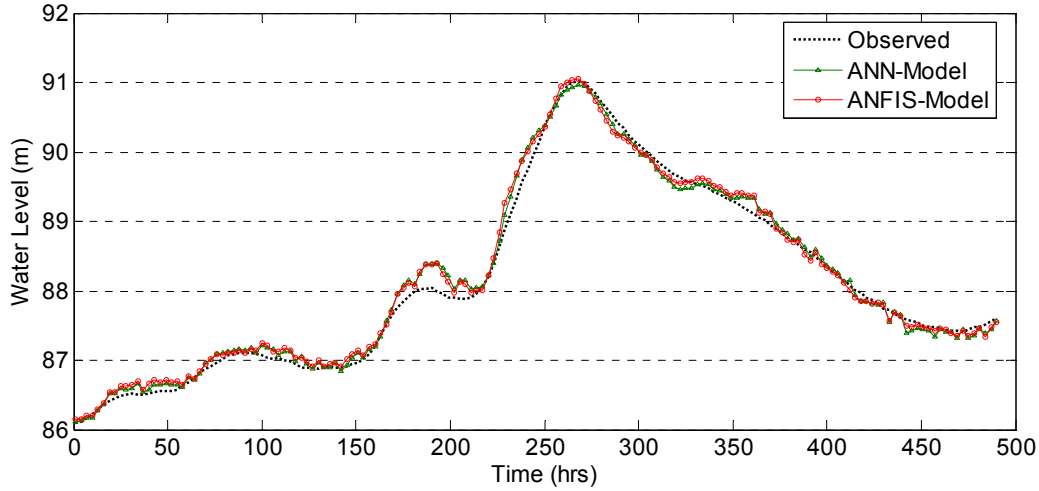

Figure 4.19. Observed, ANN and ANFIS results at the Worms station (1993 test datasets)

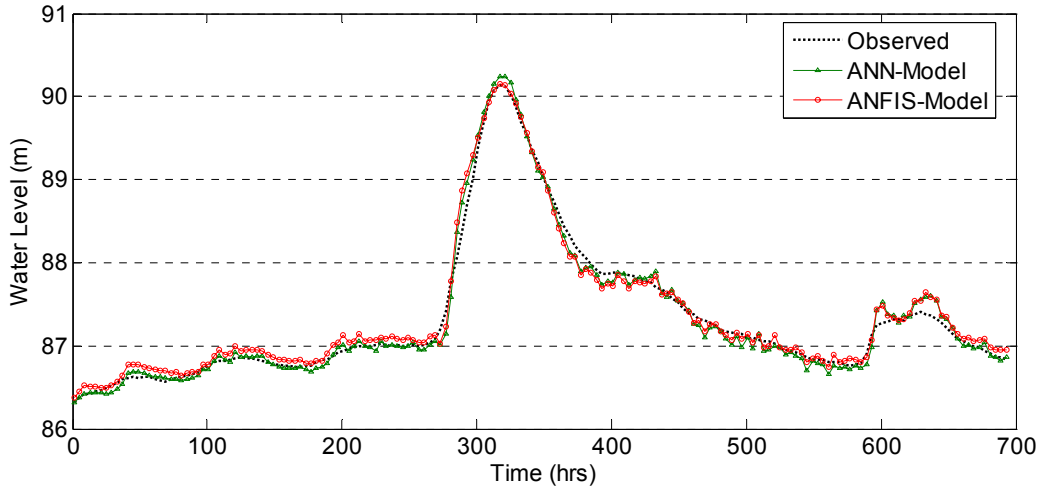

Figure 4.20. Observed, ANN and ANFIS results at the Worms Station (1994 test datasets)

4.6 Data Driven Models Beyond the Range of Training Datasets

Both the data driven models considered in this study performed reasonably well within the range of the training datasets. However, one of the major criticisms against the data driven models is the limited ability of extrapolation beyond the training range. A number of methodologies for improving the generalisation capability of the ANN have been considered. These include different data normalisation range and activation functions as discussed in section 3.2.6.1. Some examples of training the ANNs and ANFIS models for water level data beyond the training range are discussed in the following paragraphs.

The 1988 dataset constitutes the biggest flood event of the four datasets available. The dataset has two peaks: the first peak has a smaller magnitude of 90.55 m and the second peak has the higher magnitude of 91.43 m. For the assessment beyond the training sets, the data containing only the first peak of the 1988 flood event together with the 1994 data (peak = 90.14m) are used as the training set. The 1993 data (peak = 91.01m) is taken as the validation dataset. The 1990 data (peak = 90.98 m) and the dataset containing the higher peak of the 1988 data (peak = 91.43m) are taken as the test sets. The inputs and outputs are normalised in the range of [0.2 – 0.8] for both the ANN and the ANFIS models.

The trainings of both the ANN and the ANFIS in this case are found to be more difficult than when the models are used to predict within the range of the training datasets. This may also be due to lesser number of training patterns used (section 4.2). Hence, a number of experiments are made with different activation functions in the case of the ANN and different membership functions in the case of ANFIS to assess the capability of the data driven models to predict beyond the range of training datasets.

In this case too, the ANNs with the recurrent architecture are chosen. A number of nonlinear activations functions: the sigmoidal function, the hyperbolic tangent function, and a combination of linear and hyperbolic tangent functions are used in the hidden layers of the ANNs. These functions are described in section 3.2.1. The output layer consists of linear activation function. The performance of the ANN models using different activation functions for the validation set (1993) and test sets (1988 second peak and 1990) are summarised in Table 4.6. The results are shown in Figures 4.21, 4.22 and 4.23.

The results show an underestimation of the peak water levels for the 1993 (validation) and the 1988 (test) datasets and an overestimation of the peak for the 1990 (test) datasets. The activation function with higher limiting amplitude led to the higher peaks compared to the activation function with lower limiting amplitude. The overall performance of the model is found to be the best when hyperbolic tangent + linear activation function (weighing factor α = 0.5) in the hidden layers is used.

Table 4.6. Statistical performance of different activation functions for beyond training range

Dataset	Activation function	R^2	RMSE (m)	PE (m)	MAE (m)
Validation (1993)	Sigmoidal	0.9902	0.14	0.25	0.43
	Hyperbolic tangent	0.9921	0.13	0.09	0.41
	Hyperbolic tangent + linear	0.9922	0.13	0.04	0.43
Test (1988)	Sigmoidal	0.9843	0.15	0.22	0.56
	Hyperbolic tangent	0.9851	0.15	0.18	0.48
	Hyperbolic tangent + linear	0.9854	0.15	-0.04	0.55
Test (1990)	Sigmoidal	0.9922	0.17	-0.14	0.75
	Hyperbolic tangent	0.9895	0.19	-0.43	0.74
	Hyperbolic tangent + linear	0.9869	0.25	-0.72	0.90

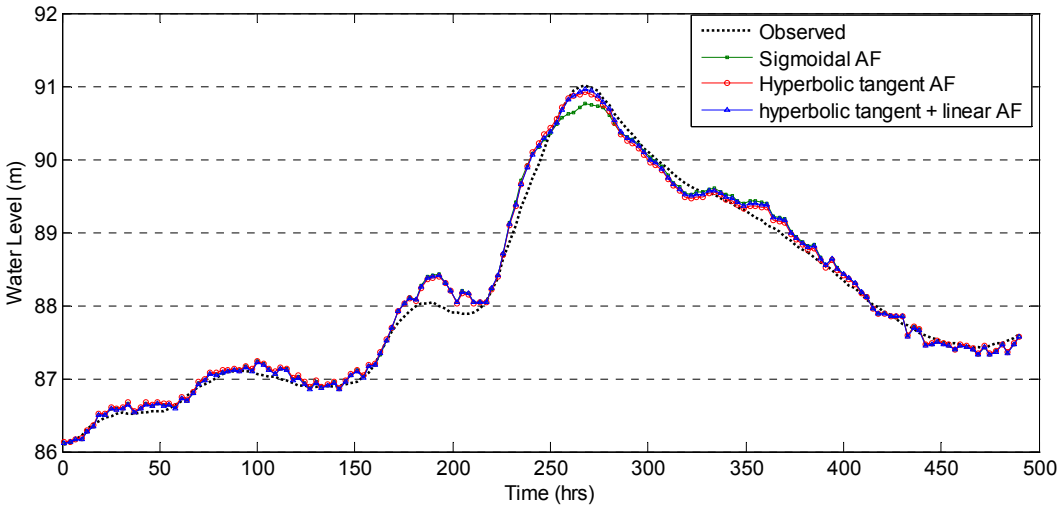

Figure 4.21. Observed and ANNs results with different activation functions at the Worms station (1993 validation datasets)

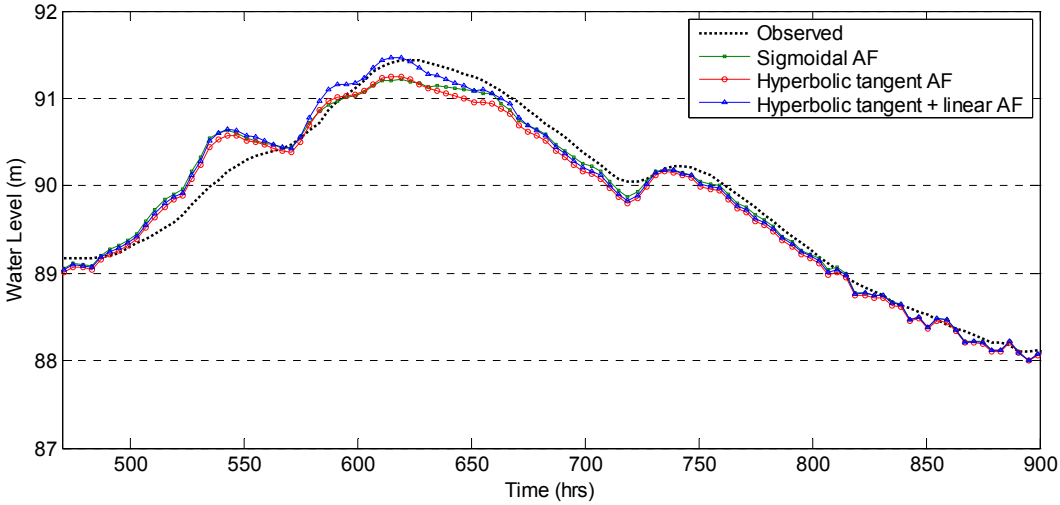

Figure 4.22. Observed and ANNs results with different activation functions at the Worms station (1988 test datasets)

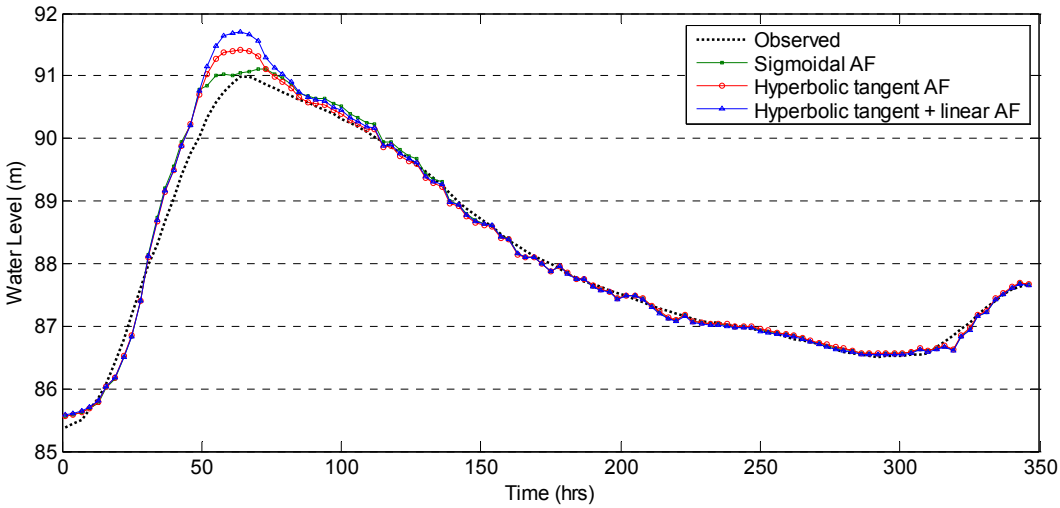

Figure 4.23. Observed and ANNs results with different activation functions at the Worms station (1990 test datasets)

In the similar way a number of different input membership functions are used in the ANFIS for predicting flows beyond the calibrated range. The membership functions include the generalised bell function, the Gaussian function and the triangular function. The performance of ANFIS using different membership functions for the validation (1993) and test (1990 and 1988) datasets are summarised in Table 4.7. The results are compared in Figures 4.24, 4.25 and 4.26. Based on the results, the overall performance of the model is found to be the best when the Gaussian membership function is used.

Table 4.7. Statistical performance of different membership functions for beyond training range

Dataset	Membership function	R^2	RMSE (m)	PE (m)	MAE (m)
Validation (1993)	Gaussian	0.9904	0.14	-0.02	0.47
	Generalised bell	0.9874	0.17	0.05	0.41
	Triangular	0.9880	0.17	-0.11	0.51
Test (1988)	Gaussian	0.9842	0.14	-0.02	0.52
	Generalised bell	0.9754	0.21	0.13	0.68
	Triangular	0.9811	0.17	-0.15	0.60
Test (1990)	Gaussian	0.9851	0.22	-0.70	0.77
	Generalised bell	0.9892	0.19	-0.53	0.62
	Triangular	0.9845	0.30	-0.92	1.05

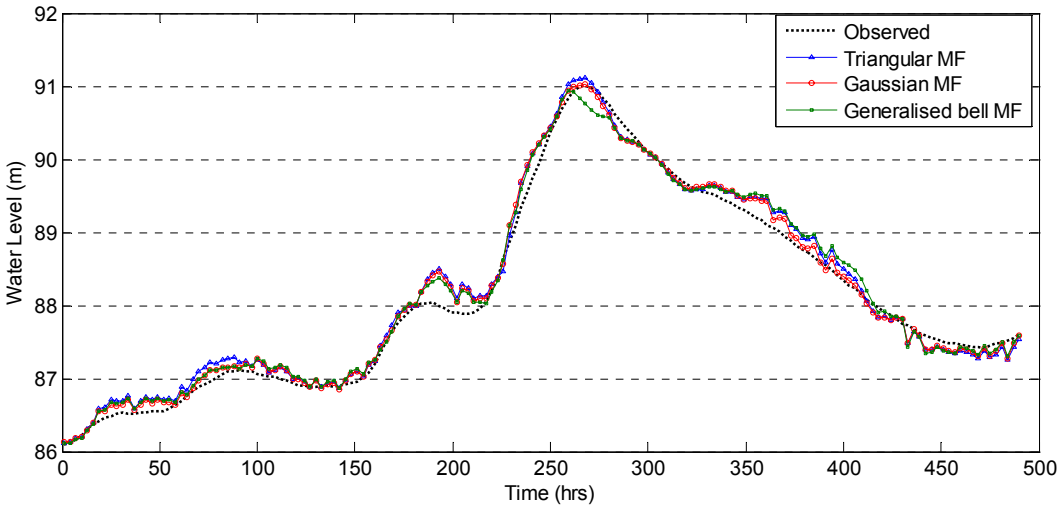

Figure 4.24. Observed and ANFIS results with different membership functions at the Worms station (1993 validation datasets)

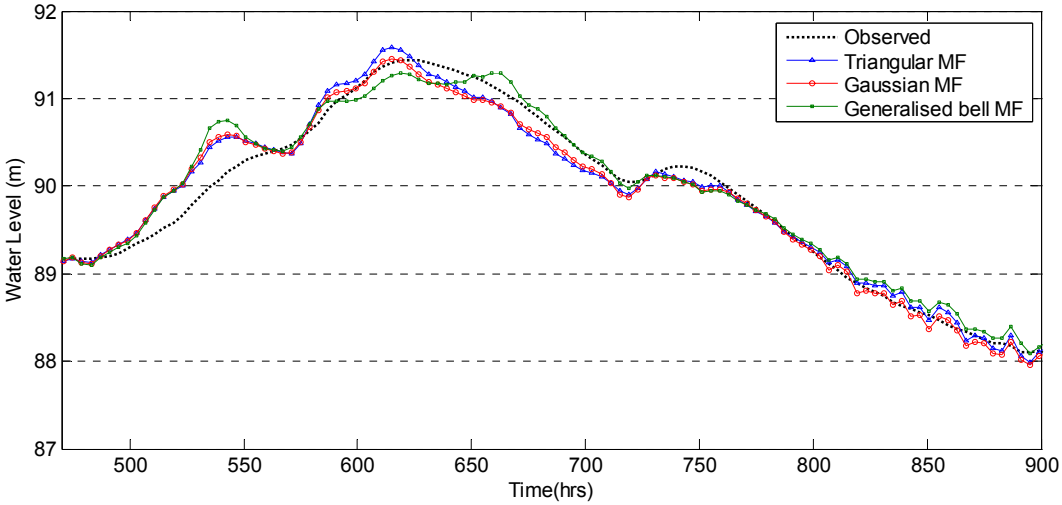

Figure 4.25. Observed and ANFIS results with different membership functions at the Worms station (1988 test datasets)

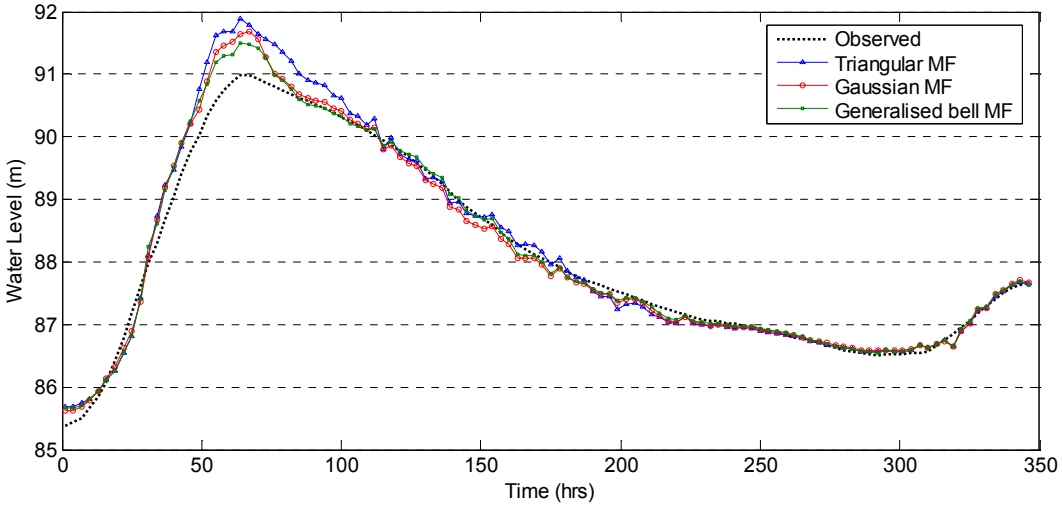

Figure 4.26. Observed and ANFIS results with different membership functions at the Worms station (1990 test datasets)

4.7 Assessment of Models for Extreme Flows

The ability of the hydrodynamic, hydrological and data driven models to predict extreme events is an important criterion in the application of these models for flood forecasting purpose. In order to test this ability, simulations for each the models are made with upstream flows multiplied by a factor of 1.5. As the observations are not available, a reference model is needed for the comparison of results. Of all the models considered, the HN model being based on physical principles offer the best reference for comparison. Hence the MC, ANN and ANFIS model results are compared with that of the HN model.

However, it is to be noted that the HN model parameters (Strickler coefficient) might also change for the extreme events.

Figure 4.27 shows the comparison of the HN and the MC model results with the upstream flows in both the models multiplied by 1.5. The comparison of the models clearly shows that although both the models performed similarly for lower discharges, the MC model underpredicts the peaks water levels compared to the HN model. The underprection in the peak water level is about 50 cm and there is also a considerable difference in the duration of the flood wave peak.

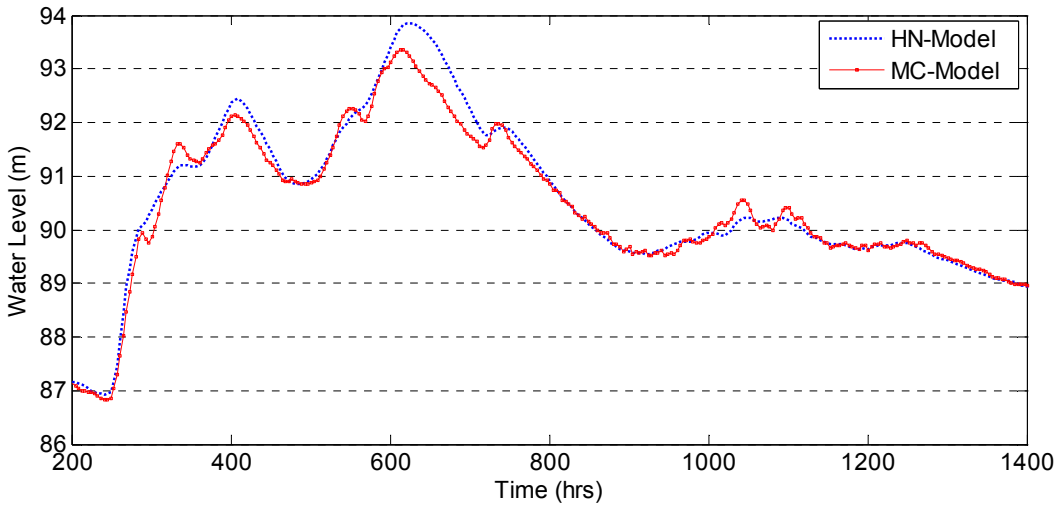

Figure 4.27. Comparison of the HN and MC models results at the Worms station with upstream flows multiplied by 1.5 (1988 data)

Figure 4.28 shows the comparison of the ANN models with the HN model results with upstream flows multiplied by 1.5. The ANN-1 includes the simulation from the ANN model from section 4.5.1, consisting of hyperbolic tangent functions in the hidden layers. The model is trained using 1988 dataset with the maximum peak of 91.43m. The ANN-2 includes the simulation of the best performing ANN model from section 4.6, consisting of a combination of hyperbolic tangent and linear function in the hidden layers. The network is trained with the combination of the smaller peak of the 1988 dataset together with the 1994 datasets. The maximum peak for the training datasets is 90.55 m. The comparison of the results show both the ANN-1 and the ANN-2 underpredicts the second peak. The underpredictions of the peak values are 48 cm and 75 cm for the ANN-1 and the ANN-2 models respectively, which are considerable differences for flood forecasting. In the case of first peak, the ANN-1 predicts the peak quite well and ANN-2 shows underprediction.

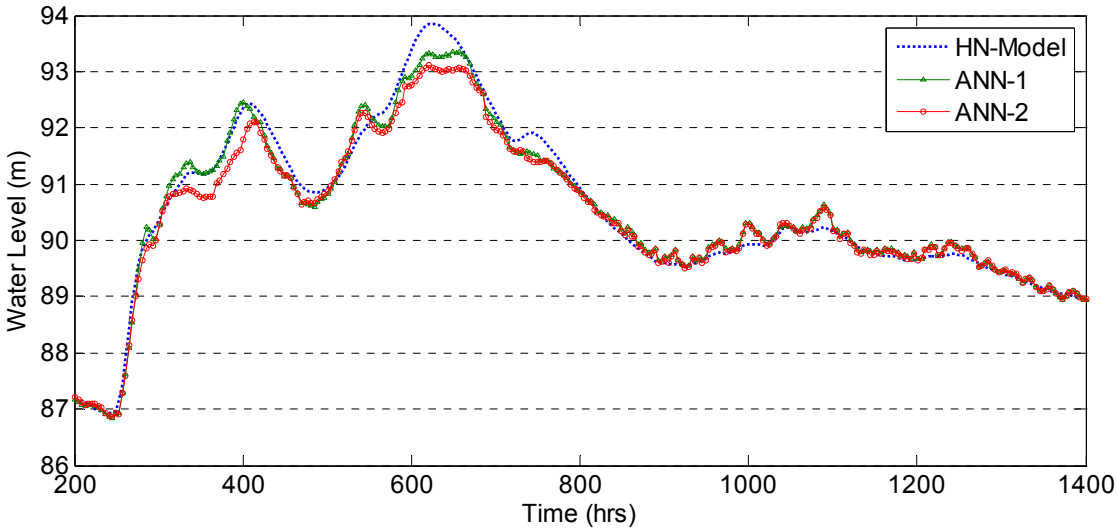

Figure 4.28. Comparison of the HN and ANN models results at the Worms station with upstream flows multiplied by 1.5 (1988 data)

Figure 4.29 shows the comparison of the HN and ANFIS models, with all the upstream flows multiplied by a factor 1.5. The ANFIS-1 consists of the simulation using the ANFIS model from section 4.5.1, which is trained using 1988 dataset with the maximum peak water level of 91.43 m. The network consists of generalised bell input membership function. The ANFIS–2 is the best performing network from section 4.6 with the Gaussian input membership function. The training datasets consists of the smaller peak of 1988 dataset together with the 1994 dataset. The maximum peak water level of the training datasets is 90.55m. The comparison of the model results show that the ANFIS-1 predicts peak reasonably well and the ANFIS-2 shows underprediction. However, there is a considerable difference in the duration of the peak flood wave for both the ANFIS model results.

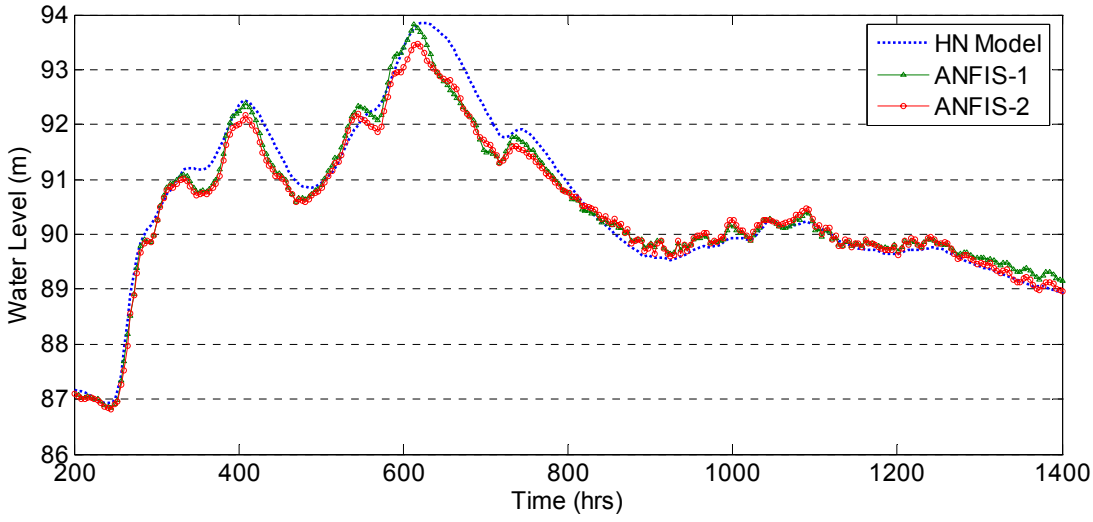

Figure 4.29. Comparison of the HN and ANFIS models results at the Worms station with upstream flows multiplied by 1.5 (1988 data)

The results of the models indicate that there are considerable uncertainties in the prediction of the extreme flood events using the hydrological MC model and the data driven ANN and ANFIS models. There are significant differences in both the magnitude and duration of the peaks. It is interesting here to note that both the ANN and ANFIS trained with the higher range of data as training sets performed better compared to the models with lower range of data as training sets. Hence, the application of the hydrological and data driven models for forecasting extreme events should be viewed with caution. It is also important to define the range of applicability of these models. In this study all the models can be safely expected to give reasonable prediction upto the range of the 1988 peak value (92.5 m).

4.8 Assessment of Model Choices

The hydrodynamic, hydrological and data driven modelling approaches all demonstrated reasonable results for the simulation of water levels at the Worms station using the flows from the upstream location. However, it is also important to consider each of these modelling approaches from the point of view of their strengths and limitations. The important considerations include data requirements, forecasting capabilities, prediction of extreme events and difficulties in model set up. These points are discussed in detail the following paragraphs.

4.8.1 Data Requirement

A 1D hydrodynamic model requires a detailed topographical data from the river bed and floodplains in terms of river cross sections, which may not be available in many locations. The river topography is also constantly changing with time and is affected by factors such as sediment transport from the catchment, processes of river bed scouring and deposition, construction of structures etc. Hence, the topographical data in an HN model need to be updated periodically. This also makes the HN model expensive to develop and operate.

The simplified routing model such as the Muskingum Cunge model requires the description of only a few river cross sections and rating curves. The data driven ANN and ANFIS models do not require any topographical data (cross sections) as the downstream flow parameters can be established directly from input output mapping. From this viewpoint, the data driven and simplified routing models have an advantage over the HN model, especially when only the flow parameters at gauging stations in a river reach are of interest.

The flow data in the river reach is a necessary input to the hydrodynamic, hydrological and data driven models. The upstream flows are necessary as the upstream boundary condition for the HN and MC models and as training inputs to the data driven models.

Both the HN and MC models can be set up without the downstream flow data. The downstream data when available can be used for model calibration. However, a carefully set up HN model with friction loss coefficients based on the site conditions can be expected to give a reasonable simulation of downstream flows, even without calibration. This approach can therefore be adapted to predict flows at intermediate sections in the river reach or in case of an ungauged downstream boundary. The simplified distributed MC model with 'physically based' Strickler coefficients can also be used in ungauged boundary. On the other hand, the downstream data are absolutely necessary as target data for the data driven models. The good quality of target data is also important for data driven models as the models can only be as good as the quality of data.

4.8.2 Prediction Capability

An HN model predicts flows at a downstream location at time t_i based on the flows at the upstream location at the same time t_i. Since the HN model is based on the simultaneous solution of the system of equations for all grid points in a river reach, the model does not make prediction of future events. Usually, a hydrological rainfall runoff model of the upstream catchment is coupled with the HN model to make forecasts.

It is important to note here that the HN model is capable of simulating flow parameters at each grid point in a river reach. The model can be used for a number of engineering problems like dam break simulation, effects of the construction of new structures. The HN model in combination with the geographical information system (GIS) can also be used to depict inundation areas, and for the assessment of flood risks.

The explicit solution of the MC method makes it possible to make a short term prediction based on the lag time from upstream to downstream. The upstream boundary data can be assumed constant for the prediction period. Since the calculation proceeds from time step t_i to t_{i+1} at every subsequent sub-reaches, the changes in the upstream boundary will not be immediately seen at the downstream boundary. This allows the MC model to make the short term prediction of the downstream flow.

In the case of data driven models, the upstream data can be lagged for the model training based on the approximate travel time from upstream to downstream. So it is possible to make predictions directly based on the established lag times. In this study it is possible to make 8 hours predictions based on the travel time from Heidelberg to Worms and 24 hours predictions based on the travel time from the Maxau to Worms station. The forecast horizon at the Worms station can be improved further by integrating with another model to forecast flows at the Heidelberg station (Chapter 5).

Another important aspect of prediction of downstream flow is the influence of minor tributaries. The conservation of mass in physically based models makes it necessary to include the minor tributaries and lateral inflows, which may not be gauged in many

locations and must therefore be estimated. This is true for both the HN and the MC models, which make the models difficult to operate in the case of considerable influence of the ungauged tributaries. This is not very relevant in this given example of prediction of flow at the Worms station, but is an important factor in chapter 5. There is no conservation of mass in the data driven ANN/ANFIS models and a carefully trained data driven model can make good predictions even without the minor tributaries and lateral inflows.

4.8.3 Extrapolation and Prediction of Extreme Events

The prediction of flow beyond the range of calibration is also an important criterion for the flood flows simulation. Being based on the full Saint Venant equations and sound physical hypotheses, the HN model provides a best option for forecasting beyond calibration. It is to be noted that the parameters of the HN model (Strickler coefficient) might also change for extreme events. On the other hand the simplified hydrological models are predictive as long as the inputs stay within the range of calibration. They have only a limited capability of predicting beyond the calibrated range. In the case of data driven models, it is generally accepted that the models are only valid within the range of training (calibration) datasets. The analysis in section 4.6 generally shows underprediction or overprediction of the peak water levels, although the best results of the both ANN and ANFIS are close to the observed values.

The comparison of the HN model with the MC hydrological model and ANN and ANFIS data driven models in section 4.7 show considerable differences in both magnitude and duration of the peak flows for the extreme events. In the case of both the ANN and ANFIS, the models have better performances when the higher range of datasets is used for training purpose. Hence, it is important to exercise caution in using the MC and data driven models in predicting extreme events and the range of applicability of these models should be clearly defined.

Care should also be exercised to properly select the training, validation and test datasets. The use of lower range of data for training purpose and higher range for validation and test purpose is useful in assessing the performance of the data driven models beyond calibration range. The use of the highest of the available data as training sets improve prediction range of the data driven models, which is specially significant if the model is to be used for flood forecasting purpose.

4.8.4 Model Development

An HN model is the most difficult to set up compared to the MC and data driven models considered in this study. The HN model needs to be defined in terms of river cross sections consisting of river channel and floodplains and appropriate values of Strickler coefficients. It is also necessary to include the storage areas and the structures like

bridges and weirs in the model. All these requirements make the HN model not only more data intensive, but also more cumbersome in setting up.

As the simplified MC model requires less data in the form of only a few cross sections and rating curves, the model is easier to set up compared to an HN model. The data driven ANN and the ANFIS models are relatively easy to set up using only the input-output data. However, the data driven models require a good knowledge of the model structures and training algorithms, which are usually not familiar to many hydraulic engineers and hydrologists.

Based upon the above discussion, the HN, MC and data driven models are summarised in Figure 4.30.

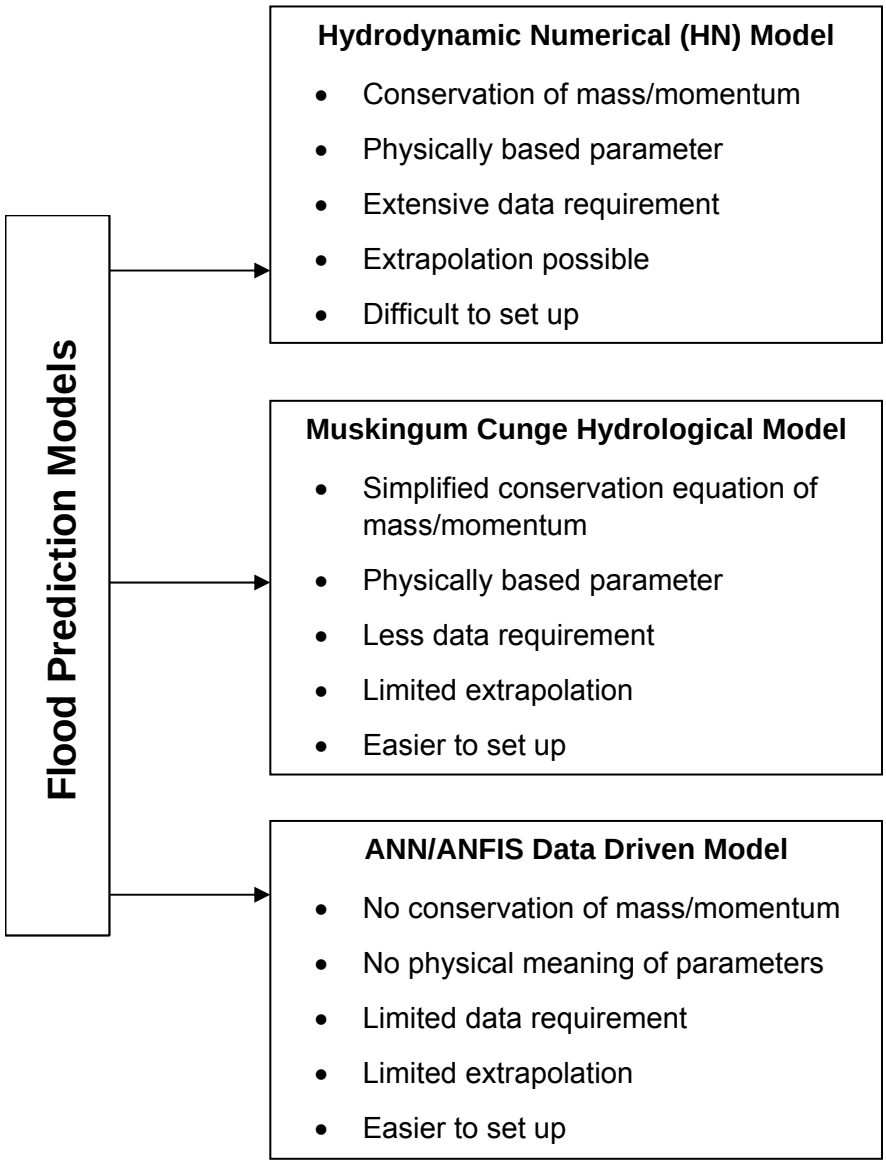

Figure 4.30. Summary of flood prediction models

4.9 Concluding Remarks

The assessment of the hydrodynamic, hydrological and data driven models show that each of the modelling techniques has its own strengths and limitations. The simplified distributed MC model and the data driven ANN/ANFIS models are more efficient compared to the HN model from the point of view of data requirement. Also, the ability of the MC and ANN/ANFIS models to make short term prediction make them suitable for flood forecasting purpose. The ANN and ANFIS models have an advantage over the MC model, as it is not necessary to estimate minor tributaries lateral inflows during flood forecasting.

However, the MC and ANN/ANFIS models have limited capability of prediction beyond the calibration (training) range. In such a situation, the HN model is more reliable. The importance of the HN model also lies in its capability of simulating flow parameters at each grid point in the river reach. The model can be used for a number of engineering problems like the dam break simulation and the effects of structures. The HN model in combination with the GIS can be used to depict inundation areas and for the assessment of risks.

The ability to simulate the dynamics of flood flow timely and accurately is of crucial importance in the flood forecasting operations. Due to the limitations of the hydrodynamic, hydrological and data driven models it might not be sufficient to use a single model. There will be a more reliable solution when the strengths of the models are combined. It is hence argued that it is necessary to set up more than one model for flood forecasting. This is the basis for a parallel complementary modelling approach, where the hydrological and data driven models can be used to make forecasts within the range of calibration and the HN model can be used beyond calibration. The use of more than one model increases the confidence of forecasts as the results can be cross validated. It is important to view the models as complementary rather than competitive so as to combine the strengths and reduce the limitations.

CHAPTER 5

COMBINED HYDRODYNAMIC AND NEURAL NETWORK MODELS

This chapter considers a combined hydrodynamic numerical (HN) and artificial neural network models for river flow forecasting and prediction of inundation extents. The HN model prepared in subsections between the barrages in Neckar River is described. The individual HN models between the barrages from Lauffen to Heidelberg are combined for the prediction of discharge hydrographs at the gauging stations. The performance of the HN model is assessed, which is affected by a number of factors, most notably the imprecision in input data.

The ANN model is also set up for the same river reach to simulate the discharge hydrographs at the gauging stations. The model consists of three independently trained ANNs with the outputs from proceeding block as inputs to succeeding block. The methods of improving ANNs performance for the prediction of flows beyond the range of training datasets are considered using different activation functions.

After the formulation of individual HN and ANN models, the approaches to combine the two models are described. The first approach combines observation data with the HN model simulations at a gauging station where no discharge time series are available for the ANN training. The second approach describes a combined series HN-ANN approach for flood hydrograph simulations at the gauging stations and depiction of the inundation areas at desired locations. The chapter also describes a Muskingum network model, which combines the learning capability of the ANNs with a simple explicit function of the Muskingum model.

5.1 Study Area and Data

The Neckar River is one of the major tributaries of the Rhine River, which flows through the region of Stuttgart, Heidelberg and Mannheim in South-Western Germany. The study area consists of a reach of about 100 km from Lauffen to Heidelberg (Figure 5.1) in navigable section of Neckar River. The catchment areas of the river are 7915 km^2 and 13787 km^2 at the Lauffen and Heidelberg gauging stations respectively [LFU, 2000]. The section of the Neckar River receives a number of tributaries including Kocher, Jagst, Elz, Schwarzbach, Itter and Elsenz. The reach is an impounded river system consisting of a number of barrages, power plants and navigation canals.

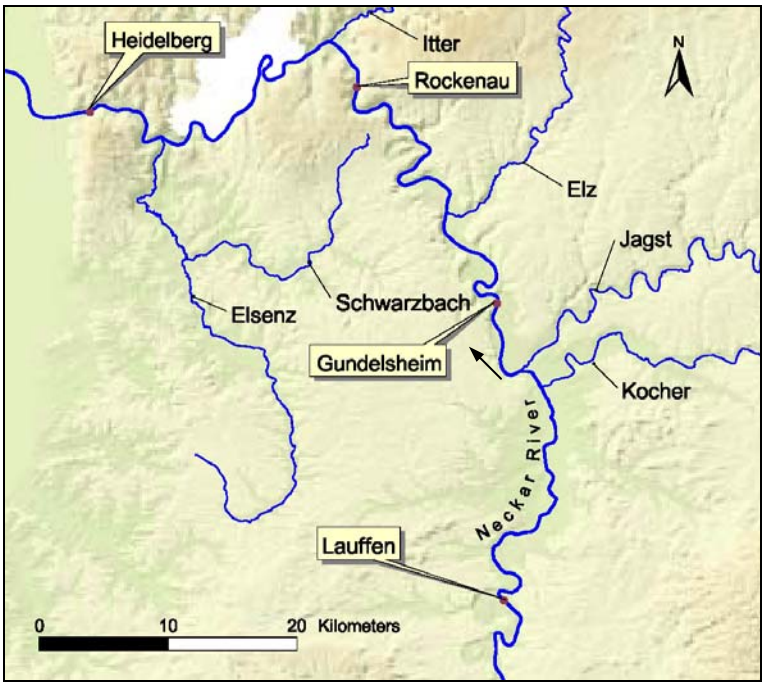

Figure 5.1. Study reach of the Neckar River

The river cross sections consist of river channels and floodplains at 100 m intervals. The cross section data are obtained from the State Office for Land Survey Baden – Württemberg *(Landesvermessungsamt Baden – Württemberg*), Federal Waterways Engineering and Research, Institute (*Bundesanstalt für Wasserbau BAW*), Karlsruhe and Water and Navigation Office (*Wasser und Schifffahrtsamt*), Heidelberg.

The flow time series data of one hour interval from the gauging stations Lauffen (distance from Rhine-Neckar confluence: km 125.10), Rockenau (km 60.70) and Heidelberg (km 26.10) are available for the 1988, 1990 and 1993 flood events. The water level time series and a limited number of flow data points are available from the Gundelsheim (km 93.80) station for the same flood events. Flows from the major tributaries Kocher, Jagst, Elz, Schwarzbach, Itter and Elsenz are also available for the same years. The flow data are obtained from the Water and Navigation Administration (*Wasser und Schifffahrtsdirektion*) South-West, Mainz. The statistical characteristics of the available data from the Lauffen, Rockenau and Gundelsheim stations are summarised in Table 5.1.

Table 5.1. Statistical characteristics of the flow data

Gauging Station	Year	No. of records	Maximum flow (m^3/s)	Minimum flow (m^3/s)	Mean flow (m^3/s)	Standard deviation (m^3/s)
Lauffen	1988	600	1155	162	571	229
	1990	228	1611	148	394	397
	1993	378	1357	121	373	259
Rockenau	1988	600	1930	341	958	399
	1990	228	2225	144	583	576
	1993	378	2680	232	713	579
Heidelberg	1988	600	1945	374	1060	401
	1990	228	2299	224	666	604
	1993	378	2706	275	807	597

5.2 Combined Hydrodynamic and Inundation Models

The combined hydrodynamic and inundation models for the Neckar river are set up for the project "Hydrodynamic Numeric - River Model Neckar" *(Hydrodynamisch-numerisches Flussmodel Neckar*) in the framework of "Integrated Conception Neckar Catchment" (*Integrierende Konzeption Neckar Einzugsgebiet* (IKoNE)) [Oberle, 2004]. The project has been undertaken by the Institute of Water Resources Management, Hydraulic and Rural Engineering (IWK), University of Karlsruhe at the request of the Water Management Administration of Baden Württemberg. In the context of the project, the HN model and the digital terrain model (DTM) are prepared for the river channels and floodplains. Based on the HN model results and the DTM, inundation grids and areas are mapped.

As schematised in Figure 5.2, the study area consists of eleven subsections between the barrages. The HN models are prepared for all individual subsections using the one-dimensional modelling system CARIMA from SOGREAH [1978]. Due to the relatively small distances between the weirs, the HN model of the subsections can be calibrated using steady flow simulations. This involves the selection of realistic Strickler coefficient values based on the site conditions and comparing the steady flow simulations with the observed flood water levels for the relevant flood events. An example of the steady flow calibration of the HN model is shown for Heilbronn sub-reach in Figure 5.3.

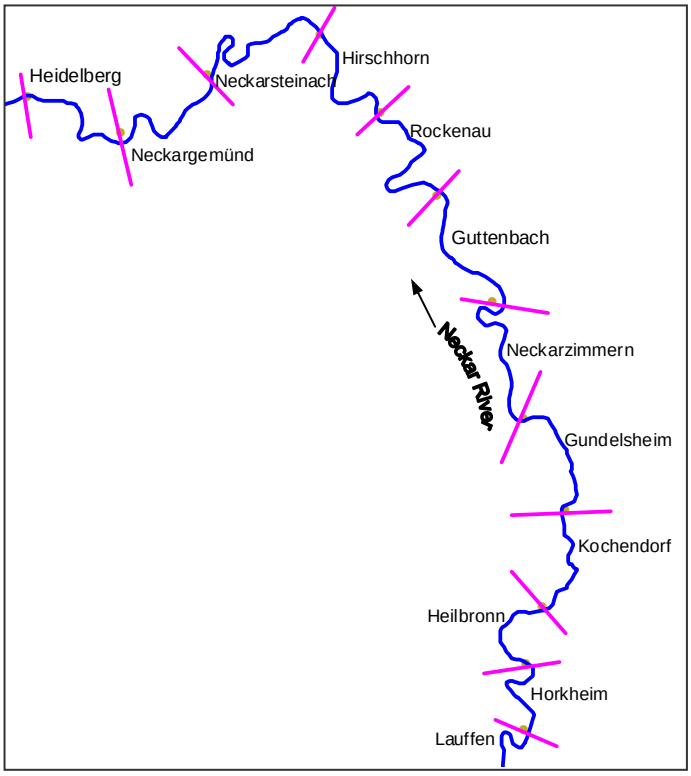

Figure 5.2. Schematisation of sub reaches in the HN model

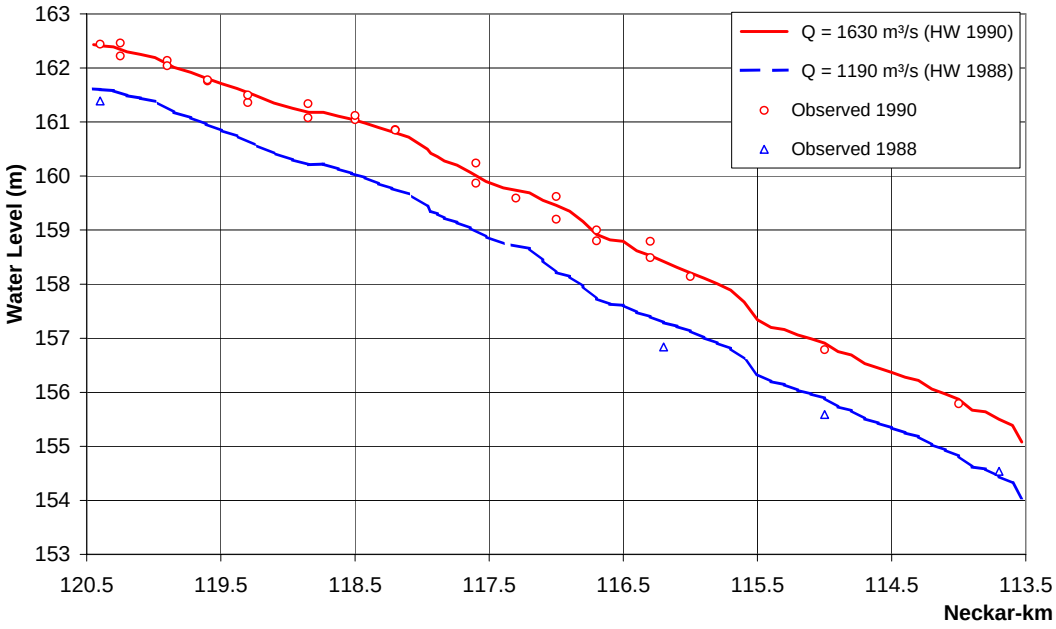

Figure 5.3. Steady flow calibration of the HN model in the Heilbronn sub-reach

The results of the HN models are combined with the DTMs in the GIS environment for the depiction of the inundation areas using tools developed by the IWK [Oberle *et al.*, 2000]. The DTMs of 2.0 m horizontal resolution are prepared in the river channels and

floodplains based on the river cross sections, spot elevations and contour lines. Recently (October, 2004), a DTM based on high resolution Laser induced Detection and Ranging (LiDAR) data of 1.0 m horizontal resolution is available for the study area. Based on the projection of the steady flow profiles into the floodplains in the GIS environment, inundation grids and polygons at the individual subsections can be depicted. The procedure of mapping the inundation extent in the GIS environment are summarised in section 2.4.2. Figure 5.4 shows an example of the DTM for the Heilbronn sub-reach. The difference model (inundation grid) and the inundation areas (blue = inundation, red = potential inundation) for the 1990 flood event are shown in Figures 5.5 and 5.6 respectively.

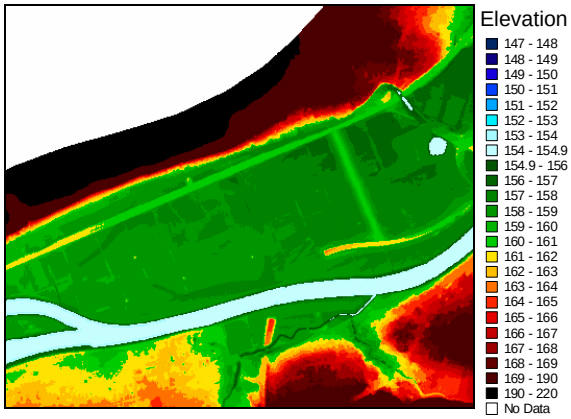

Figure 5.4. Digital terrain model in a section of the Heilbronn sub-reach

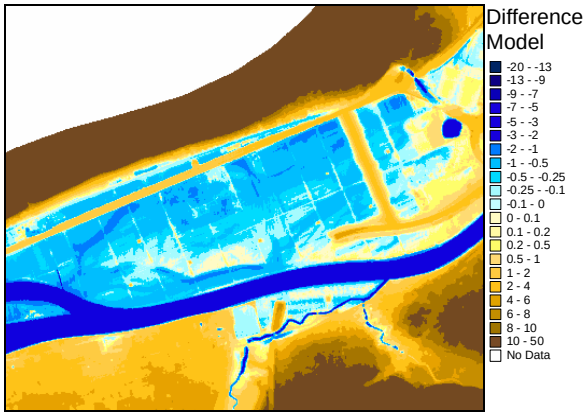

Figure 5.5. Inundation grid in a section of the Heilbronn sub-reach

Figure 5.6. Inundation area overlaid over aerial photograph in a section of the Heilbronn sub-reach (blue = Inundation, red = potential inundation)

5.3 Unsteady Flow Hydrodynamic Model

In order to predict inundation areas in the event of upcoming flood, discharges at all eleven barrages are required. As a first idea, it is considered to use the HN model for

flood routing purpose. The HN models in the entire river reach (Figure 5.2) are combined and unsteady flow simulations are performed. The flow hydrographs from the gauging stations at Lauffen (Neckar) and the tributaries are taken as upstream boundary conditions. As downstream boundary condition, the stage/discharge relationship downstream of the gauging station at Heidelberg is used. Storage cells in the floodplains are also added together with lateral inflows into the river channel at each subsection of the river reach.

Since the model has already been calibrated in a sub-reach by sub-reach basis, no further calibration of the Strickler coefficient is done. The combined HN model is used for the simulation of water level and flows at the gauging stations, Gundelsheim, Rockenau and Heidelberg. The model results are compared with the measured flows at the Rockenau and Heidelberg stations. Since, only a few discharge values are available from the Gundelsheim gauging station, the model results are compared with the water level time series data.

5.3.1 Results and Discussion

The comparison of the HN-simulated results for the Gundelsheim station with the observed water levels and discharges for the 1988 flood events are shown in Figures 5.7 (A) and (B). Similarly, the comparison of the model results for the 1990 and 1993 flood events are shown in Figures 5.8 (A) and (B), and 5.9 (A) and (B) respectively. The results show a good capability of the HN model to reproduce the water level time series for all flood events. The phases are accurately reproduced, although there are some errors in the amplitude. However, a pattern of underestimation of the lower water levels in all three flood events is observed. In the case of discharge time series, there is also a good match between the HN simulated and the limited discharge records for all three flood events.

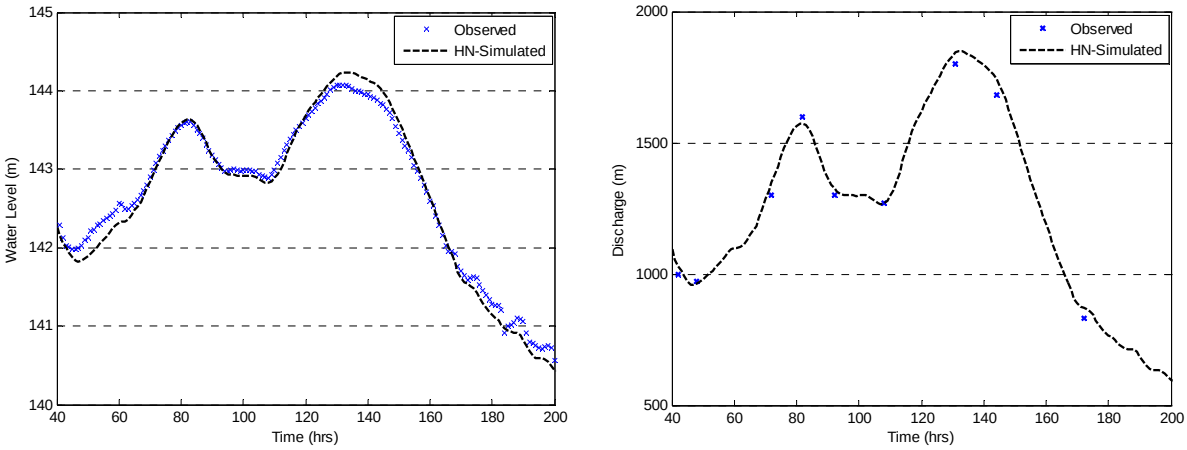

(A) (B)

Figure 5.7. Observed and HN model results at the Gundelsheim station (1988 flood event): (A) water levels, (B) discharges

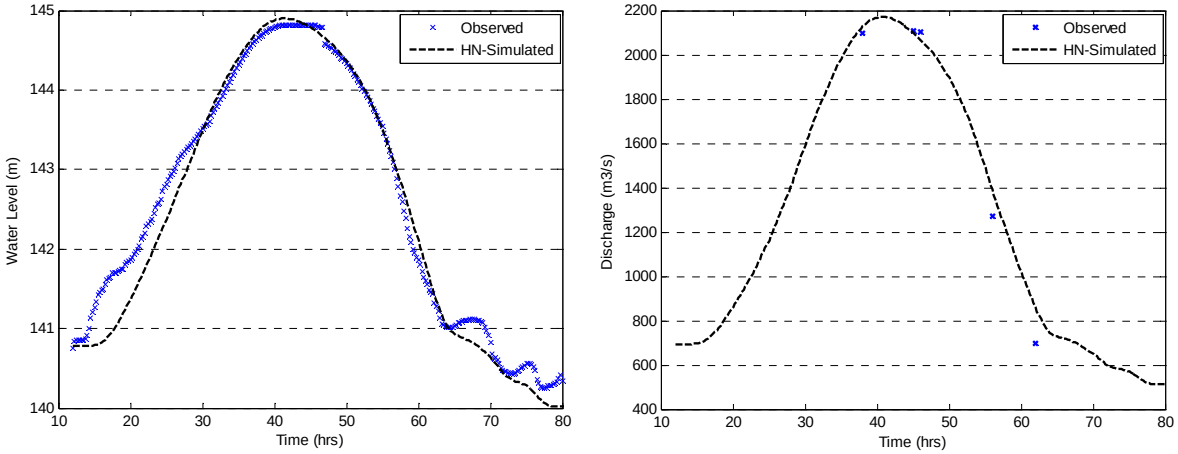

(A) (B)

Figure 5.8. Observed and HN model results at the Gundelsheim station (1990 flood event): (A) water levels, (B) discharges

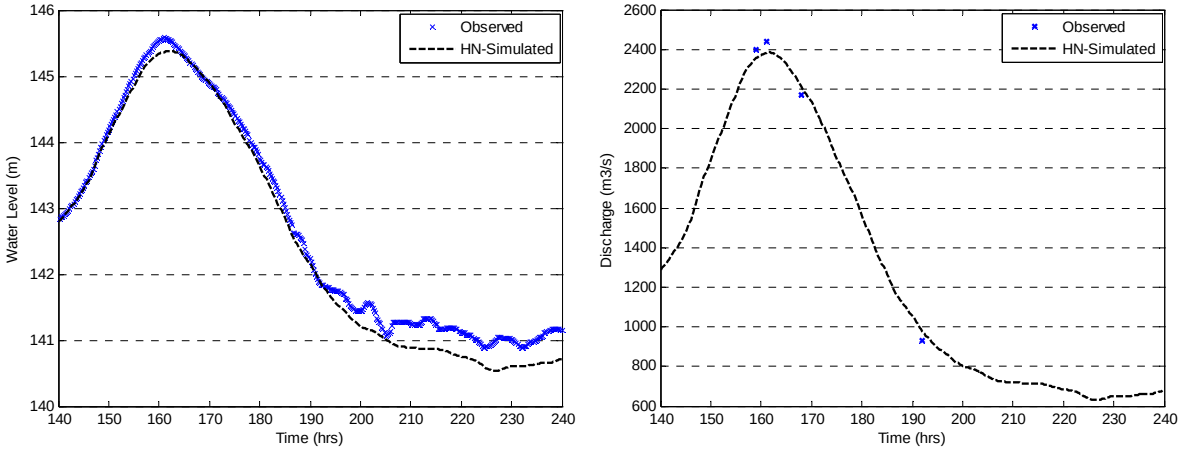

(A) (B)

Figure 5.9. Observed and HN model results at the Gundelsheim station (1993 flood event): (A) water levels, (B) discharges

The HN model is also used to simulate the flood events at Rockenau and Heidelberg. The results of the HN simulated discharges and the observed time series data are compared in Figures 5.10 (A) and (B) (1988 flood event), 5.11 (A) and (B) (1990 flood event) and, 5.12 (A) and (B) (1993 flood event). The comparison of the results shows a progressive deterioration of the quality of results from upstream to downstream. The 1988 discharges are reproduced reasonably well, although there are some phase and amplitude errors in the lower discharges. In the case of 1990 discharge time series, phases are well reproduced for the peaks. But there are apparent shifts in the phase at lower discharges. There are also underpredictions of peaks for both the Rockenau and Heidelberg stations, which can be adjusted to a certain extent by using higher lateral inflows. The results of the 1993 flood simulation depict a considerable underprediction of the peak discharges for both the Rockenau and Heidelberg gauging stations. As the errors are quite considerable, it will be incorrect to adjust the peak values using only the lateral inflows. The issue is dealt in more detail in the section 5.4.

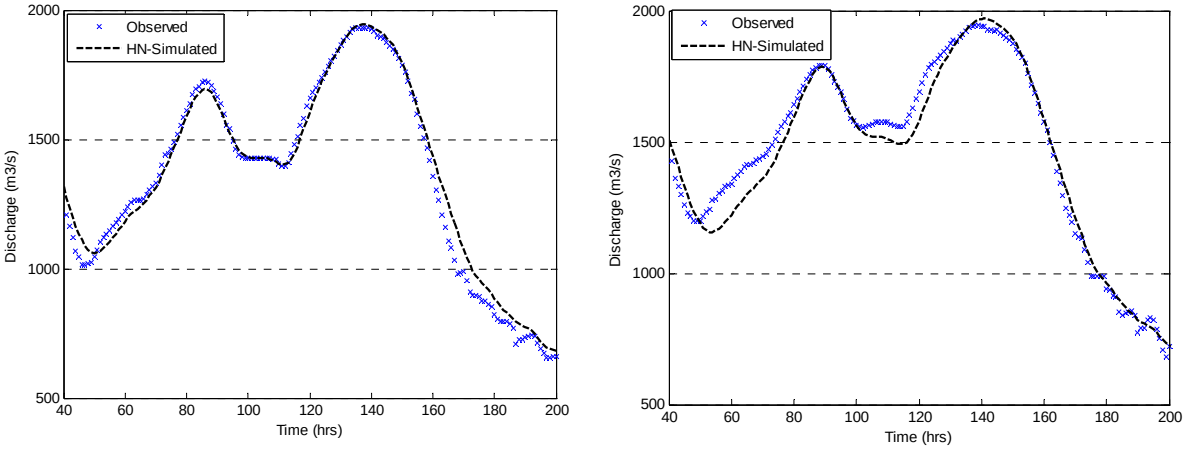

(A) (B)

Figure 5.10. Observed and HN model results for the 1988 flood event: (A) Rockenau station, (B) Heidelberg station

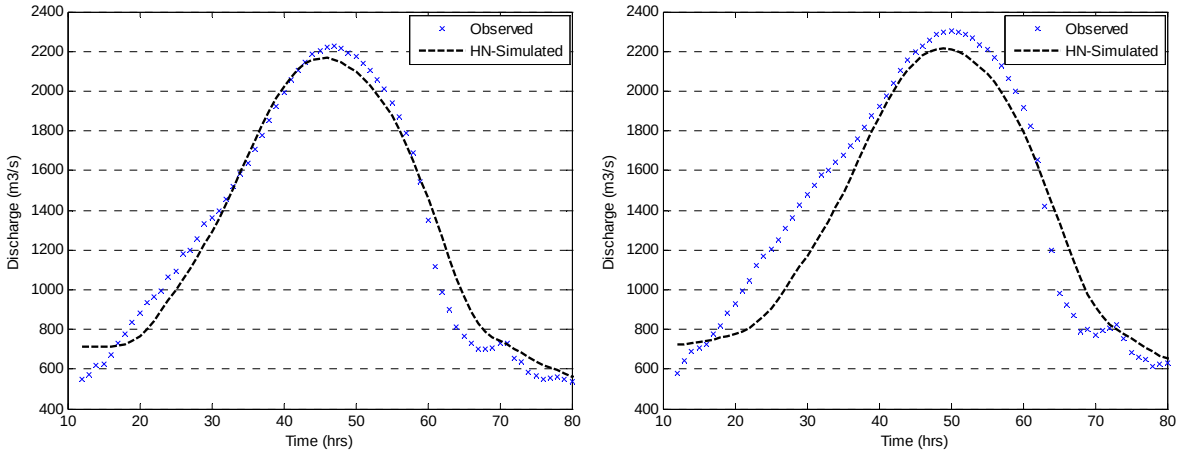

(A) (B)

Figure 5.11. Observed and HN model results for the 1990 flood event: (A) Rockenau station, (B) Heidelberg station

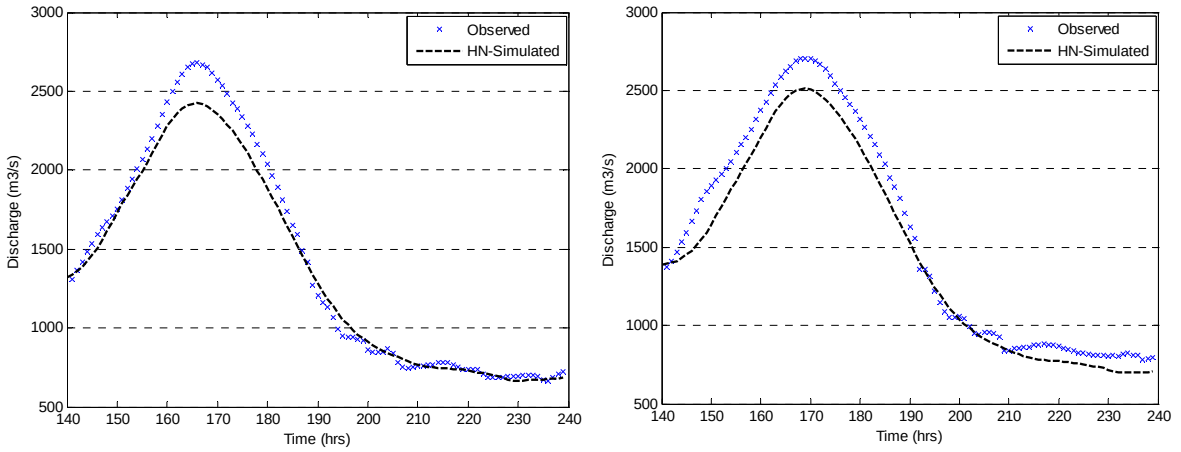

(A) (B)

Figure 5.12. Observed and HN model results for the 1993 flood event: (A) Rockenau station, (B) Heidelberg station

5.4 Uncertainties in the 1993 Discharge

The imprecision in the 1993 flood discharge data has been analysed by Oberle and Theobald [2000]. The analysis found inconsistencies in the peak discharges. The results of the analysis for the peak flow at Rockenau on 21.12.1993 are summarised in Table 5.2. Based on the analysis, it can be seen that the sum of the corresponding upstream discharges from Lauffen, Kocher, Jagst and Elz (2424 m^3/s) is less than the Rockenau value by 256 m^3/s. This is without considering the effects of attenuation and retention in the floodplains.

Table 5.2. Peak discharge analysis for the 1993 flood

Gauging Station	Relevant flow time	Discharge (m^3/s)
Lauffen (Neckar)	15:00	1304
Stein (Kocher)	16:00	585
Untergriesheim (Jagst)	17:00	505
Mosbach (Elz)	20:00	30
Total	-	2424
Rockenau (Neckar)	22:00	2680

For a reasonable match between the observed and the simulated values using the HN model, it is necessary to introduce an additional upstream flow of about 300 m^3/s. It is incorrect to introduce such a high discharge as a lateral inflow in the HN model. Hence, the peak flow at the Rockenau and Heidelberg stations are underestimated as shown in Figures 5.12(A) and 5.12(B).

Such inconsistencies in measured data can adversely affect the performance of physically based HN models, especially for flood forecasting purpose. The conservation of mass in physically based models require lateral inflows and minor tributaries flows to be included in the model. These flows may not be gauged in many locations and hence need to be estimated.

As described in the section 4.8.2, there is no conservation of mass in the data driven models such as the artificial neural networks (ANNs). The ANNs can be trained for the simulation of discharges at the gauging stations. Hence, the ANN model is considered as a complement to the physically based HN model for the simulation of flows at the gauging stations.

5.5 ANN River Flow Prediction Model

This section details the development of a ANN based data driven model for the prediction of flows at the gauging stations, Gundelsheim, Rockenau and Heidelberg. An important initial step in the development of the ANN model is the selection of appropriate input and output datasets. A number of experiments are performed with the division of river reach into different ANN blocks. In the first set of experiments, the ANN is used to predict flows at the gauging station Rockenau, based on the upstream flows from Lauffen (Neckar), and the tributaries Kocher, Jagst and Elz. The network shows a good performance for the training and validation datasets, but not for the test datasets.

As the HN model has performed reasonably well for the section between Lauffen and Gundelsheim, it is decided to integrate the HN simulated results at the Gundelsheim station for the ANN training. The outline of the different approaches for integrating the HN and ANN models has been given by Van den Boogaard and Kruisbrink [1996]. In one of the approaches, the ANN can be used as a model reduction of the HN model, so as to reproduce only a part of HN model results. This approach enables the ANN to simulate missing discharge time series at the Gundelsheim station. In addition, the ANN can be used to predict the future flood events without requiring the HN model run. Accordingly, the corresponding discharge time series at the Gundelsheim station from the HN model is used for the ANN training.

A cross correlation analysis is performed on time series flows to identify a suitable lag time from upstream to downstream points. The cross correlation analyses of the time series water level data from the Lauffen, Gundelsheim and Rockenau stations yields the suitable lag time for Gundelsheim and Rockenau with respect to upstream stations. Similarly, the analysis between the flow data from Rockenau and Heidelberg gives the lag time for the Heidelberg station. The lag times for the tributaries inflows are calculated based on their distances. The lag times for the forecast stations Gundelsheim, Rockenau and Heidelberg with respect to the upstream stations are given in Table 5.3.

Table 5.3. Lag time with respect to forecast stations

Forecast station	Upstream stations	Lag Time (hrs.)
Gundelsheim (Neckar)	Lauffen (Neckar)	4
	Stein (Kocher)	3
	Untergriesheim (Jagst)	2
Rockenau (Neckar)	Gundelsheim (Neckar)	3
	Mosbach (Elz)	2
Heidelberg (Neckar)	Rockenau (Neckar)	2
	Eschelbronn (Schwarzbach)	2
	Eberbach (Itter)	2
	Meckesheim (Elsenz)	2

The forecast horizons at the Gundelsheim, Rockenau and Heidelberg gauging stations with respect to the upstream flows are of 2 hours each. However, the contribution from the tributaries Elz, Schwarzbach, Elsenz and Itter are quite small compared to flows in the Neckar River. Hence, their flows can be assumed to be constant for the duration of forecast to increase forecast horizon. This increases the forecast horizon at the Rockenau and Heidelberg stations to 5 and 7 hours respectively. The forecast horizon can be further increased by integrating external models such as rainfall-runoff models.

5.5.1 Model Implementation

It is observed that the integration of HN model results from Gundelsheim improves the performance of river flow prediction at the Rockenau station. The river reach is therefore divided into three 'sub-reaches' represented by independently trained ANN blocks. The inflows and the desired outflows for each of the ANN blocks are summarised in Table 5.4. The outputs of the best performing networks from preceding blocks are used as inputs to succeeding blocks.

Table 5.4. Network inputs and desired outputs

Network block	River sub-reach	Network input	Desired output
ANN block 1	Lauffen – Gundelsheim	Measured flows from the gauging stations at Lauffen and tributaries Jagst and Kocher	Simulated flows from the HN model at Gundelsheim
ANN block 2	Gundelsheim – Rockenau	Simulated flows from the ANN block 1 at Gundelsheim and measured flow from gauging station at the tributary Enz	Measured flows from the gauging stations at Rockenau
ANN block 3	Rockenau – Heidelberg	Simulated flows from the ANN block 2 at Rockenau and measured flows from gauging stations at the tributaries Schwarzbach, Elsenz, and Itter	Measured flows from the gauging stations at Heidelberg

Due to the better quality of results from the HN model, the 1988 data can be considered as the most reliable data of the available three flood events datasets. Hence, the 1988 data are used as the training sets. The 1990 and 1993 data are used as the validation and test datasets respectively. From the range of data (Table 5.1), the 1993 data consists of highest peak value and the 1988 data consists of lowest peak value. Hence, the ANNs models are formulated so that they are capable of predicting beyond the range of training datasets.

A number of methodologies useful for making prediction beyond calibration range are outlined in section 3.4, Imrie *et al.* [2000] and Shrestha *et al.* [2005]. This includes the scaling of the input and output datasets and use of different activation functions at the hidden layers. Accordingly, the input datasets for the ANN trainings are scaled in the range between 0.2 and 0.8. A number of ANN models are developed, each with one input layer, two hidden layers and one output layer. The numbers of neurons in the networks are kept to a minimum of eight in the first hidden layer, four in the second hidden layer and one in the output layer. There is no significant improvement of the model performance with the increase in number of neurons. Each of the networks consists of linear activation function in the output layer. The weighing factor α for the hyperbolic tangent + linear function is varied between 0.4 and 0.8 during training process.

The networks are trained using the procedures from MATLAB neural network toolbox [Demuth and Beale, 2004]. This involves network designing using text files containing MATLAB code (M-files). The training is done using backpropagation algorithm with Bayesian regularisation of the Levenberg-Marquardt approximation. The early stopping criteria provided by the validation datasets are used to prevent overtraining. The test datasets are used independently for the evaluation of model performance.

5.5.2 Results and Discussion

The statistical performances of the ANN models using different activation function are evaluated in terms of coefficient of determination (R^2) and root mean square error (RMSE). In addition, the peak error (PE) of discharges between observed and calculated flows is considered to assess the capability of the ANNs to predict beyond the range of training datasets. The details of the error measurements are given in Appendix B.

5.5.2.1 Performance of the Rockenau ANN Models

The statistical performance of the ANN models for the validation (1990 flood event) and test (1993 flood event) datasets are summarised in Table 5.5. The ANNs are trained with the upstream flows from Lauffen (Neckar), and the tributaries Kocher, Jagst and Elz. There is an underestimation of the peak flow from all the ANN models using different activation functions at the Rockenau station for the test datasets. The underprediction is higher for the ANNs consisting of activation function with lower limiting amplitude such as sigmoidal and hyperbolic tangent function at the hidden layer. Figures 5.13 (A) and (B) show the partial results of the model for the validation (1990) and the test (1993) datasets.

Table 5.5. Statistical performance of the ANNs with different activation functions at Rockenau station using upstream flows

Datasets	Activation functions	R^2	RMSE (m^3/s)	PE (m^3/s)
Validation (1990)	Sigmoidal	0.9796	89	123
	Hyperbolic tangent	0.9835	84	127
	Hyperbolic tangent + linear	0.9852	82	114
	Linear	0.9816	83	74
Test (1993)	Sigmoidal	0.9740	144	343
	Hyperbolic tangent	0.9733	129	333
	Hyperbolic tangent + linear	0.9729	132	324
	Linear	0.9718	134	246

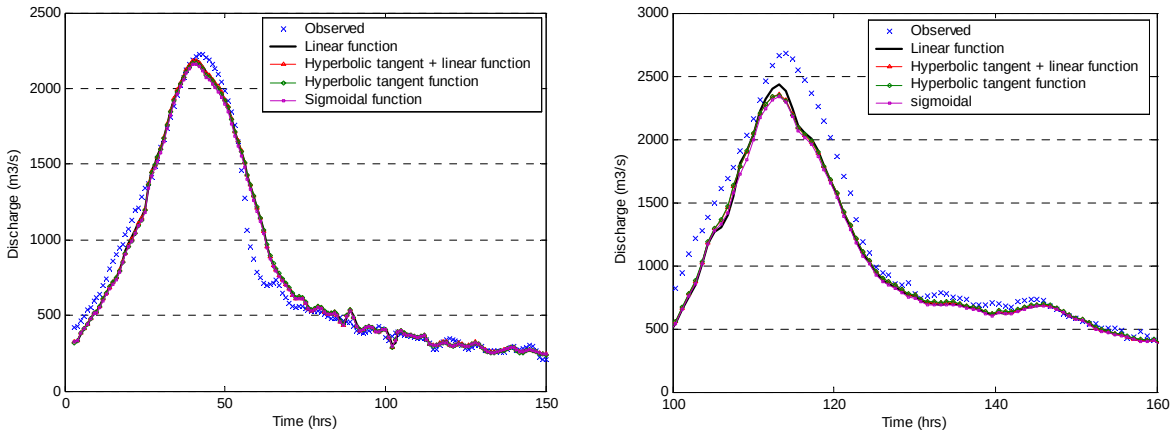

(A) (B)

Figure 5.13. Observed and ANN results with different activation functions at Rockenau using upstream flows (A) 1990 validation data (B) 1993 test data

5.5.2.2 Performance of the Sub-reach Models

The performance of different activation functions for the validation and the test datasets for the stations Gundelsheim, Rockenau and Heidelberg are summarised in Tables 5.6, 5.7, and 5.8. In the ANN block 1 between Lauffen and Gundelsheim, the network can easily approximate the validation and test datasets. There is a tendency of improvement in statistical performance when activation functions with higher limiting amplitudes are used. In the case of the peak values, there is generally an underestimation, with the lowest error for the linear function. The combination of hyperbolic tangent and linear function (α = 0.5) at the first hidden layer gives the best performance in terms of R^2 and RMSE and is hence selected as the best ANN for the Lauffen – Gundelsheim sub-reach. Figures 5.14 (A) and (B) show partial results of the model for the validation (1990) and the test (1993) datasets.

Table 5.6. Statistical performance of the ANNs with different activation functions (Gundelsheim station)

Datasets	Activation functions	R^2	RMSE (m^3/s)	PE (m^3/s)
Validation (1990)	Sigmoidal	0.9912	53	22
	Hyperbolic tangent	0.9920	48	18
	Hyperbolic tangent + linear	0.9926	50	11
	Linear	0.9921	50	-10
Test (1993)	Sigmoidal	0.9936	77	64
	Hyperbolic tangent	0.9932	67	54
	Hyperbolic tangent + linear	0.9932	63	45
	Linear	0.9923	70	43

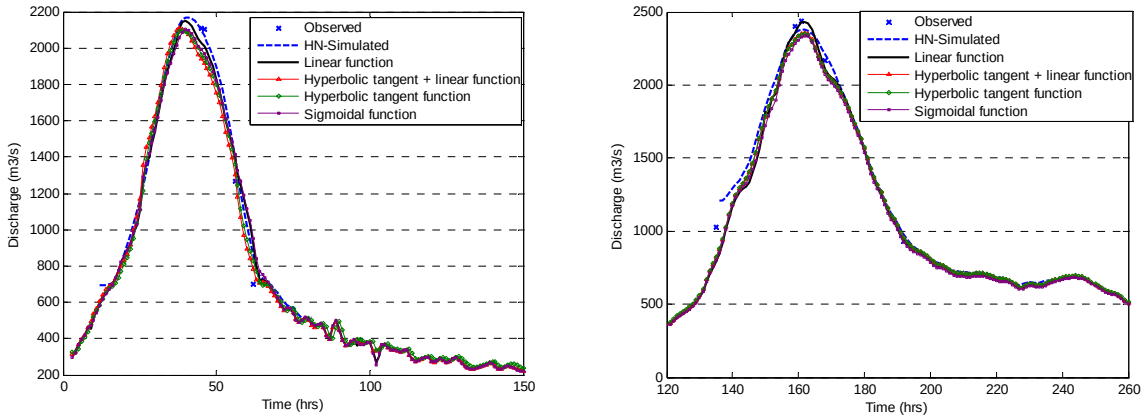

Figure 5.14. Observed, HN and ANN results with different activation functions at the Gundelsheim station (A) 1990 validation data (B) 1993 test data

In the ANN block 2 between Gundelsheim and Rockenau, the performance of the networks is similar to the ANN block 1. The application of activation functions with higher limiting amplitude produce better results in terms of statistical performance criteria R^2 and RMSE. There is an overall trend of underestimation of peaks, even with the linear activation function for the test datasets. With the application of hyperbolic tangent activation functions at the first and second hidden layers, the network is able to predict peak flows with the lowest errors for the both validation and test datasets. The partial results of the model for the validation (1990) and the test (1993) datasets are shown in the Figures 5.15 (A) and (B).

Table 5.7. Statistical performance of the ANNs with different activation functions (Rockenau station)

Datasets	Activation functions	R^2	RMSE (m^3/s)	PE (m^3/s)
Validation (1990)	Sigmoidal	0.9821	79	36
	Hyperbolic tangent	0.9806	84	128
	Hyperbolic tangent + linear	0.9810	81	48
	Hyperbolic tangent in 2 hidden layers	0.9858	73	-17
	Linear	0.9799	86	-43
Test (1993)	Sigmoidal	0.9832	86	184
	Hyperbolic tangent	0.9839	85	166
	Hyperbolic tangent + linear	0.9810	89	147
	Hyperbolic tangent in 2 hidden layers	0.9850	76	100
	Linear	0.9831	96	128

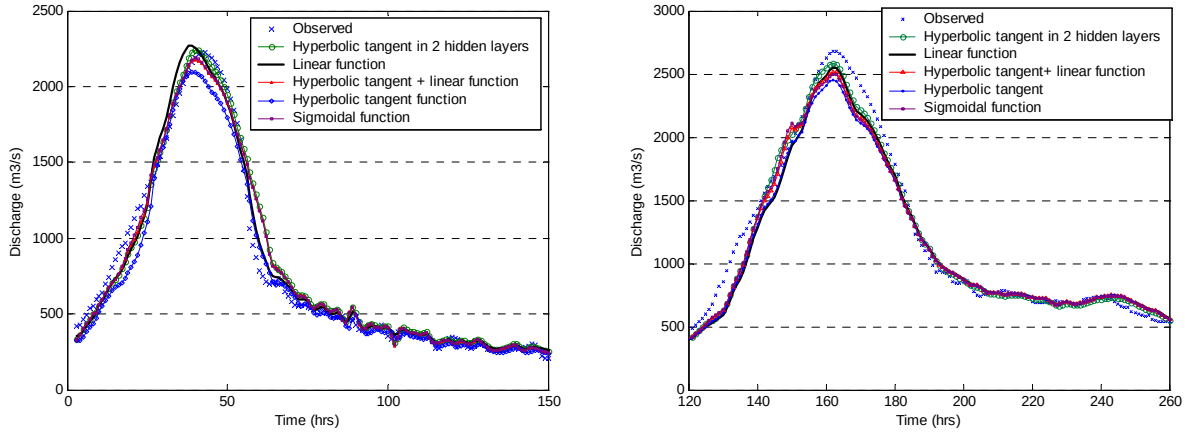

(A) (B)

Figure 5.15. Observed and ANN results with different activation functions at the Rockenau station (A) 1990 validation data (B) 1993 test data

The statistical performances of the model from the Gundelsheim to Rockenau ANN model (Table 5.7) are compared with the Rockenau ANN model, which do not integrate the HN model results from Gundelsheim (Table 5.5). The comparison shows that the statistical performance in terms of R^2, RMSE and the difference in peak flow of the Gundelsheim to Rockenau ANN models are generally superior for all activation functions.

The performance of ANN block 3 between Rockenau and Heidelberg also improves with the application of activation functions with higher limiting amplitude. There is also a general trend of underestimation of peaks. The difference in peak flow prediction is also found to be lower using activation functions with higher limiting amplitude. The hyperbolic

tangent + linear function (α = 0.7) gives the best performance in terms of R^2, RMSE and PE of discharges. The partial results of the model for the validation (1990) and the test (1993) datasets are shown in the Figures 5.16 (A) and (B).

Table 5.8. Statistical performance of the ANNs with different activation functions (Heidelberg station)

Datasets	Activation functions	R^2	RMSE (m^3/s)	PE (m^3/s)
Validation (1990)	Sigmoidal	0.9781	97	102
	Hyperbolic tangent	0.9776	98	67
	Hyperbolic tangent + linear	0.9790	88	36
	Linear	0.9790	92	-28
Test (1993)	Sigmoidal	0.9743	99	153
	Hyperbolic tangent	0.9750	96	130
	Hyperbolic tangent + linear	0.9802	94	49
	Linear	0.9779	98	-61

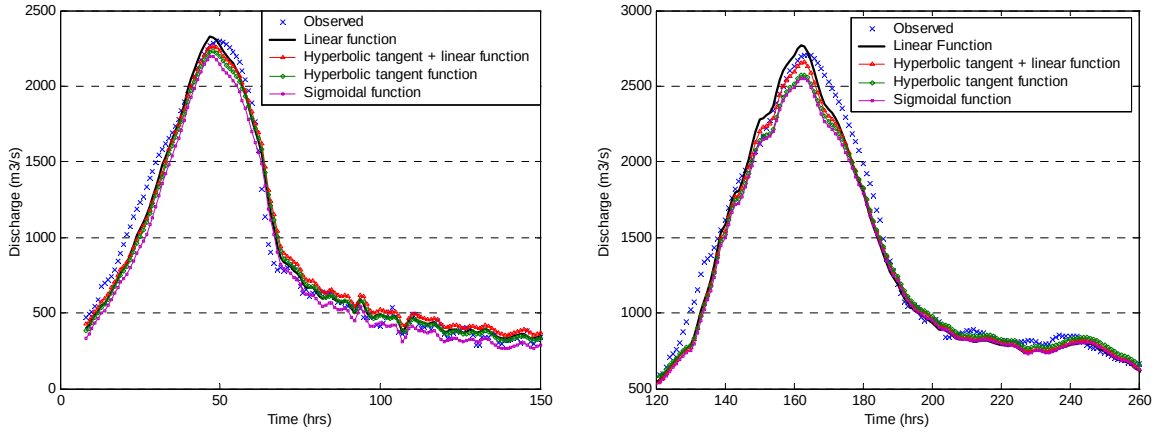

(A) (B)

Figure 5.16. Observed and ANN results with different activation functions at the Heidelberg station (A) 1990 validation data (B) 1993 test data

It is to be noted that the statistical performance of the ANN model for block 1 is not consistent with the blocks 2 and 3 since the results of block 1 is compared with the HN model simulations and the blocks 2 and 3 with the observed data.

5.5.2.3 Combined ANN Simulation Model

The best performing network blocks in each of the sub-reaches are combined in the MATLAB/Simulink environment and an ANN simulation model is developed. This consists of ANNs with the hyperbolic tangent + linear function in first hidden layer in the blocks 1

and 3. The ANN block 2 consists of the hyperbolic tangent function in the first and second hidden layers. The combined ANN simulation model is schematised in Figure 5.17.

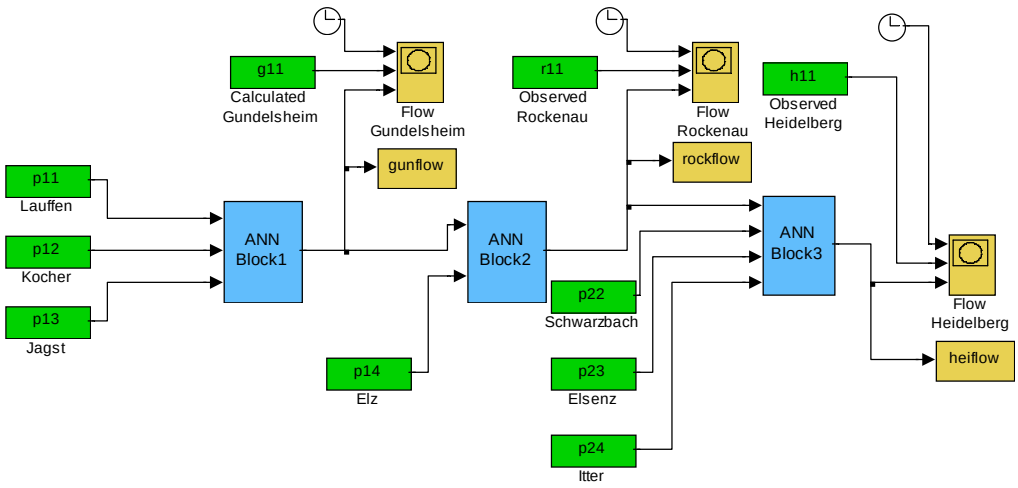

Figure 5.17. ANN simulation model

5.5.2.4 ANN Models for Extreme Flows

In order to test the ability of ANNs to predict extreme events, simulations are made with all the upstream flows multiplied by a factor 1.5. The ANN simulation model contains the best performing ANN blocks as described in section 5.5.2.3. The HN model simulations are also made multiplying the upstream flows by 1.5. The outputs of the HN model and ANN simulated results are compared. However, as described in section 4.6, it is to be noted that HN model parameters (Strickler coefficient) might also change for the extreme events. The Figures 5.18, 5.19 and 5.20 show the comparison of the results at Gundelsheim, Rockenau and Heidelberg respectively with the 1990 and 1993 flows multiplied by 1.5.

The comparison of results of the two models indicates underprediction at all three stations. It is to be noted that the HN model itself underpredicts the flows at Rockenau and Heidelberg for the 1990 and 1993 datasets without multiplications (Figures 5.11 and 5.12). Therefore, overall underestimation can be expected to be higher than that obtained by comparing with the HN model results, especially in case of the 1993 data. The results highlight that the ANNs only have capabilities of predicting flows beyond the calibrated range to a certain range. Beyond the range, the results of the ANNs start to diverge from the actual values. Hence, caution needs to be exercised in the use of ANNs for forecasting extreme events. It is also important to specify forecasting range of the trained ANNs. In this study, reasonable results can be expected from the ANNs upto the 1993 data ranges.

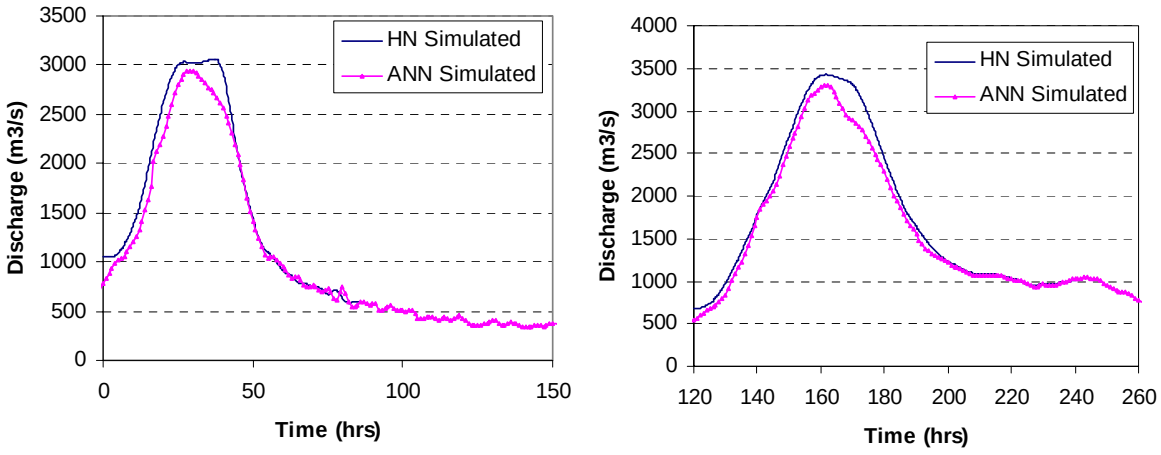

Figure 5.18. HN and ANN results with upstream flows multiplied by 1.5 at the Gundelsheim station (A) 1990 data (B) 1993 data

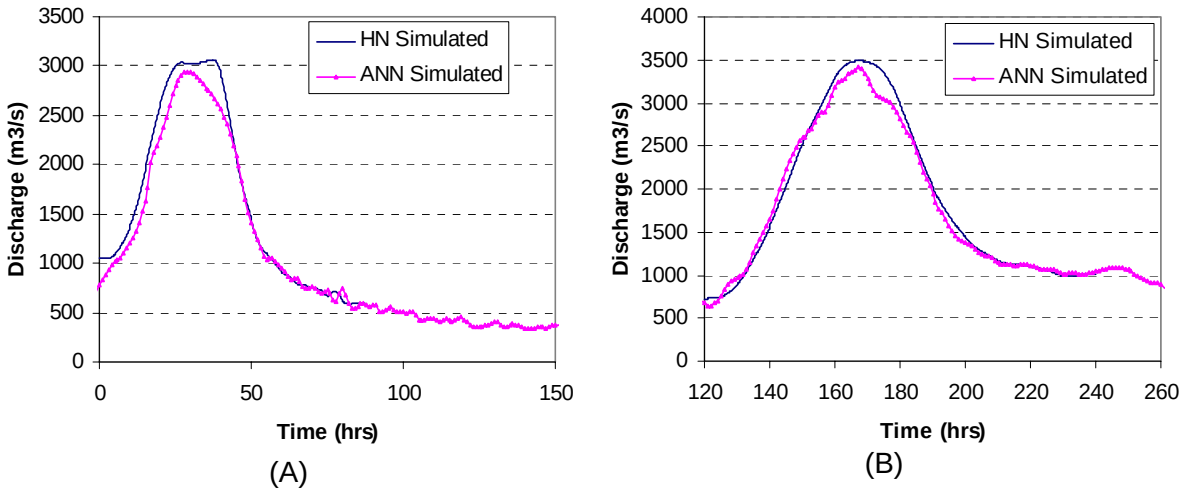

Figure 5.19. HN and ANN results with upstream flows multiplied by 1.5 at the Rockenau station (A) 1990 data (B) 1993 data

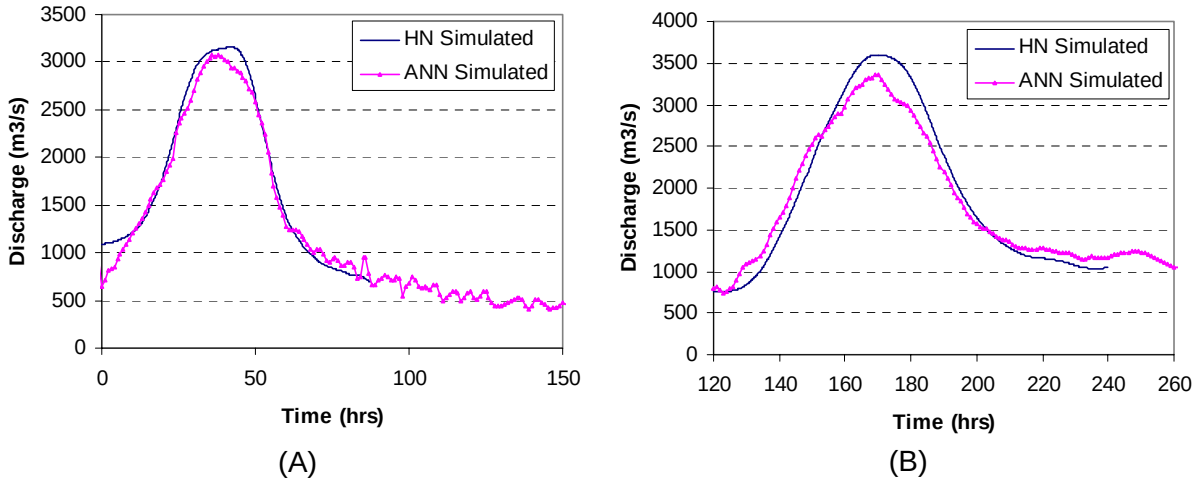

Figure 5.20. HN and ANN results with upstream flows multiplied by 1.5 at the Heidelberg station (A) 1990 data (B) 1993 data

5.6 Combined HN-ANN Model

After the development of independent HN and ANN models, a combined HN-ANN approach can be used [Shrestha *et al.*, 2004]. For the steady flow simulation and the mapping of the inundation extent in the event of an upcoming flood, discharges at each of the subsections between the barrages are necessary. This can be obtained from the unsteady flow HN model. However, as described in section 5.4, the HN model is sensitive to imprecision in the input data. In addition, it is also necessary to estimate minor tributaries and lateral inflows, which makes the HN model difficult to use during flood forecasting. The ANN model on the other hand is less sensitive to uncertainties in data and the model work well without the minor tributaries and lateral inflows. Therefore, the ANN can be used as a preprocessor to generate input discharges of the HN model.

In this approach, the ANN simulation model can be used to forecast flows at Gundelsheim, Rockenau and Heidelberg. Based on the ANN prediction, the discharges at intermediate locations can be interpolated. The discharges at the desired locations can be fed into the HN models at subsections between the barrages and the water levels in the river reaches can be simulated. The results can be used in combination of GIS supported inundation model for the depiction of inundation areas at critical locations. Hence, this approach can also facilitate a quick prediction of inundation extents at critical locations, based on the forecasted discharges at the gauging stations. The combined HN - ANN dynamic flood simulation model is shown in Figure 5.21. As for example, the ANN routing model is used to forecast flows at the Heidelberg gauging station. The peak water levels from the ANN routing model is used to predict inundation extent in the Heidelberg sub-reach. The resulting inundation grid is shown in Figure 5.22.

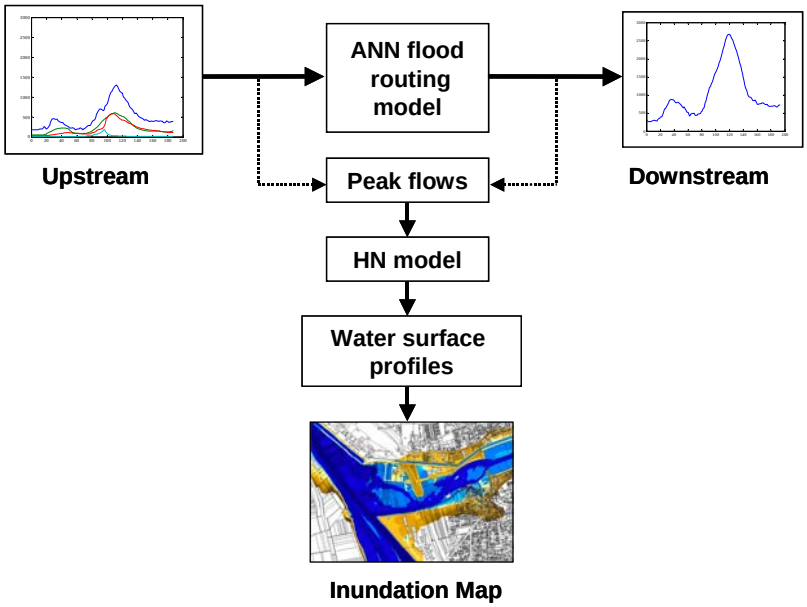

Figure 5.21. Dynamic simulation of inundation areas

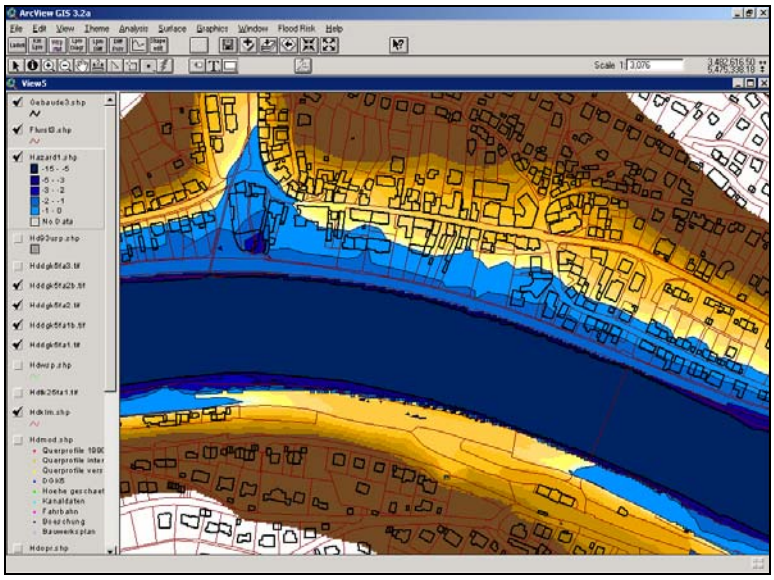

Figure 5.22. Depiction of inundation area in the Heidelberg sub-reach

5.7 Muskingum Network Model

After the development of ANN models for the different sub-reaches of the Neckar River, an approach to combine the learning capability of the ANN with the Muskingum routing model is formulated. The model uses the explicit function of the Muskingum model with the downstream discharges at any time step expressed explicitly in terms of upstream discharges and downstream discharges at previous time step (equation 2.29). The functional parameters can be estimated using optimisation methods such as the Levenberg – Marquardt method.

The model consists of a single layer linear network with only one node, and a single input and single output architecture as shown in Figure 5.23 [Shrestha, 2003]. In this formulation, the discharges at previous time steps can be used as inputs by passing through tapped delay line (TDL) operator. A linear activation function returns the networks output simply as sum of all values passed to it. Hence, the network architecture as shown in Figure 5.23 is the same as the finite difference discretisation in Figure 2.3. The network weights W_{11}, W_{12}, and W_{13} are equivalent to the routing coefficients C_1, C_2 and C_3, and the equation (2.29) takes the form.

$$Q_{out}(n) = W_{11} * Q_{in}(n-1) + W_{12} * Q_{in}(n) + W_{13} * Q_{out}(n-1) \qquad (5.1)$$

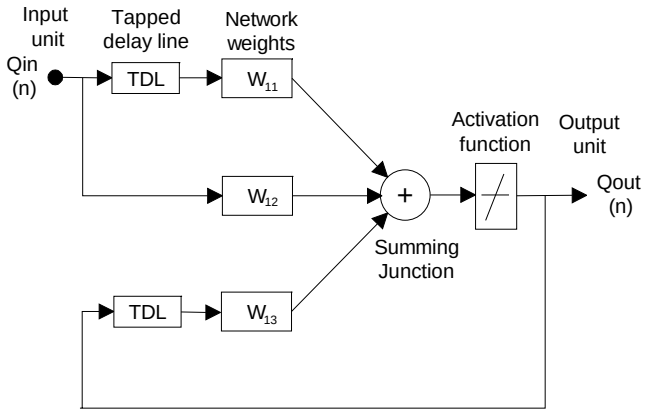

Figure 5.23. Representation of finite difference equation as a linear network model

5.7.1 Model Implementation

The Muskingum network model is applied to the reach between the gauging stations Rockenau and Heidelberg. A number of numerical experiments are carried out to investigate the performance of the network models. The first set of experiments involved the formulation of basic network architecture that replicates the Muskingum method. This consists of a single input, single output linear network (LN) with flow at the upstream boundary as the input and the downstream boundary as the output. In the second case, a bias is introduced to the LN to account for the tributaries and lateral inflows. For the next sets of training, the possibilities of improving the network performance with modification of the network architecture are considered. This involves the formulation of nonlinear network (NLN) with the application of hyperbolic tangent transfer function at the input.

In this case too, the 1988 flood event dataset is used as the training data, and the 1990 and the 1993 event data as validation and test data respectively. The observed flow at Rockenau alone is taken as the model input and that at Heidelberg as the target.

5.7.2 Results and Discussion

The results obtained for the verification of the Muskingum method at the Heidelberg station are summarised in Table 5.9. With a simple LN structure as shown in Figure 5.23, the network is quick to train to the desired output. The analysis of the weights shows the sum of weights as 1.045. The error 0.045 can be attributed to tributaries and lateral inflows, which are not considered. After the distribution of errors and backward calculation, the value of X is obtained at 0.27, well within the desired range between 0 and 0.5. The value of K was obtained at 2.04 hrs, same as 2 hours obtained by the cross correlation analysis. The introduction of bias as expected reduced the error in sum of weights to 0.004. The bias value obtained was equivalent to the discharge of 40 m^3/s.

Table 5.9. Muskingum coefficients calculated from the LN

Network type	Sum of Weights	K	X
LN	1.045	2.04	0.27
LN with bias	1.004	2.06	0.30

The comparison of the performance of the LNs with the NLN are summarised Table 5.10. It is seen that LNs overestimate peak discharges in both validation and test datasets. The application of hyperbolic tangent activation function in the NLN reduces error in peak discharge. The activation function also improves the overall R^2 and RMSE performances for the validation and test datasets. The difference in the peak discharge is also found to be least using the hyperbolic tangent activation function. The Figure 5.24 (A) and (B) show the results obtained with different network structures.

It is to be noted that the statistical performance of the LN and the NLN (Table 5.10) are not consistent with that of the ANN model in the block 3 in section 5.5.2.2 (Table 5.8) as the results from block 2 from the Rockenau station together with the tributaries Schwarzbach, Elsenz, and Itter are taken as inputs. In the LN and the NLN, only the observed flows at Rockenau are taken as inputs.

Table 5.10. Statistical performance of the LN and the NLN results at the Heidelberg station

Datasets	Network type	R^2	RMSE (m^3/s)	PE (m^3/s)
Validation	LN	0.9919	70	-114
(1990)	LN with bias	0.9920	59	-73
	NLN with bias	0.9954	45	11
Test	LN	0.9956	67	-203
(1993)	LN with bias	0.9956	53	-55
	NLN with bias	0.9972	36	36

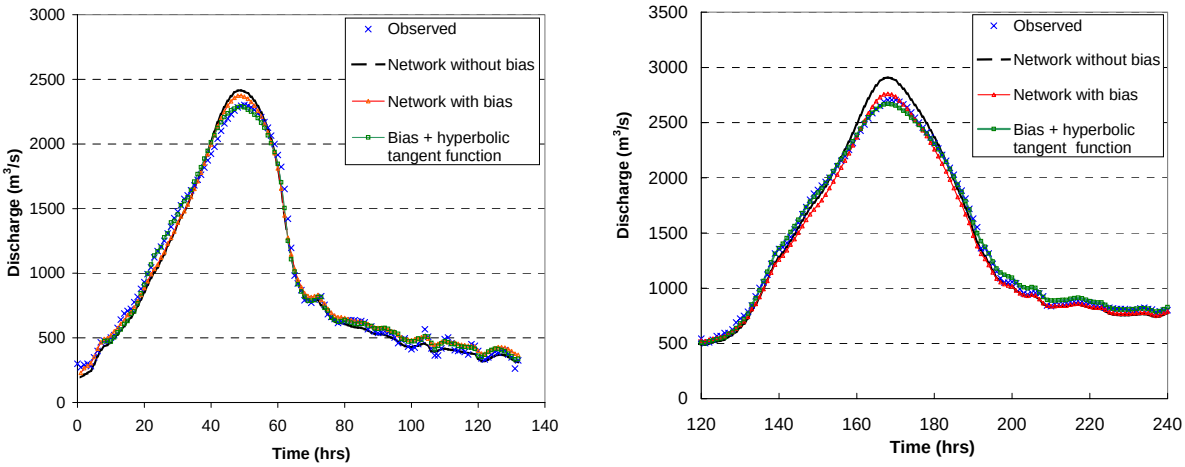

Figure 5.24. Observed and LN and NLN results at the Heidelberg station
(A) 1990 validation data (B) 1993 test data

The results of the model show a good performance of the NLN for the Heidelberg station. However, the network becomes difficult to train when the flows with a larger time lag and multiple tributaries are to be routed as in the case of the Lauffen to Gundelsheim sub-reach. The stability criteria as given by the equation (2.36) – (2.39) also requires the network to be trained in a number of layers, making the process of training more cumbersome. However this procedure is useful for simple reach like Rockenau to Heidelberg, where the nonlinear Muskingum network can be quickly trained.

5.8 Concluding Remarks

This chapter has presented an approach to combine hydrodynamic numerical model with artificial neural networks so that one model can complement the other. The HN model is used to simulate water levels and inundation areas at subsection between the barrages in the river reach. The individual HN models between the barrages are combined for the prediction of discharge hydrographs at the gauging stations. The performance of the HN model is affected by a number of factors, most notably the imprecision in the input data. In addition, for a good match between the observations and the simulated results, it is necessary to estimate the minor tributaries and lateral inflows.

The ANN models can also be trained for the prediction of flow at the gauging stations. Different approaches of combining the ANNs with the HN models are explored. In the first approach, the observation datasets are combined with HN model results for the ANN training in the ‘sub-reaches’. This approach enhances the flexibility of the model combination, so that the results of one can be quickly integrated into the other. It enables the ANN to simulate missing flow time series and forecast the flood events at the

Gundelsheim station without the application of the HN model. This approach also improves the overall model performance in the entire river reach.

In the second approach, the ANN model is used as a pre-processor for the input data of the HN model. As HN models are sensitive to imprecision in the input data, the ANN model can be used to predict flows at the gauging stations in the event of an upcoming flood. Predicted discharges from the ANN can be used as inputs to the HN models at small subsections between the barrages in order to predict the inundation extents. Hence, this series approach combines the potential of both techniques for a quick and accurate prediction of flood hydrographs and simulation of inundation extents.

The effects of different activation functions at the first hidden layer of multilayer perceptron (MLP) neural networks are evaluated for predicting flows beyond the calibrated range. This evaluation is made in terms of test datasets with higher peaks, above the range of training datasets. Four different activation functions, the sigmoidal, hyperbolic tangent, linear, and a combination of hyperbolic tangent and linear functions are investigated in this study. The best performing ANNs at individual sub-reaches are combined, which show a good prediction capability to a certain extent beyond the range of training datasets. The performance of the ANN degrades when the upstream flows are multiplied by a factor 1.5 and the ANN and the HN model results are compared. It is therefore important to exercise caution in the use of ANNs for forecasting extreme flood events.

CHAPTER 6

UNCERTAINTY ANALYSIS OF THE STAGE DISCHARGE RELATIONSHIP

This chapter considers uncertainties in discharges due to the stage discharge relationship. Different sources of uncertainties are outlined and methods of managing analysing and propagating the uncertainties are considered. The uncertainty management method includes nonlinear mapping of the stage discharge relationship using artificial neural network as an alternative to the rating curve. This is demonstrated using the case studies of a highly scattered nonlinear relationship and a looped stage discharge relationship. The uncertainty analysis includes the application of fuzzy regress analysis to define the range of uncertainties of the relationship. The chapter also considers the propagation of uncertainties to river channel and floodplains due to uncertain relationship. This consists of an application of the fuzzy extension principle based alpha level cut in combination with a one-dimensional hydrodynamic numerical model.

6.1 Stage Discharge Relationship

Accurate estimation of discharge in the river is essential for the hydrological and hydraulic analysis of open channel flow. While the water levels (stages) in a river are measured directly and continuously, the flows (discharges) are measured neither directly nor continuously. Most discharge records are derived from a functional relationship between the stage and the discharge $Q(y)$, referred to as the stage discharge curve or the rating curve. The stage discharge relationships constitute a fast and inexpensive means of converting measured stage time series to discharge time series [Schmidt, 2004]. In addition, the stage discharge relationship also constitutes a convenient downstream boundary condition for hydrodynamic numerical models [Cunge *et al.*, 1980].

The relationship between the discharge Q and the corresponding stage h is most often expressed in the forms:

$$Q = A_1 h^{A_2} \tag{6.1a}$$

$$log(Q) = log(A_1) + A_2 * log(h) \tag{6.1b}$$

where A_1 and A_2 are parameters calibrated based on the measured values of the discharge for a range of river stages.

For most gauging stations a single curve relationship between stage and discharge is oversimplification. In general the relationship is in the form of a compound curve with different stages for different flow ranges [Schmidt, 2002]. Depending upon the channel behaviour with respect to stage and flow values at different ranges, two or more curves can be fitted to the data.

6.1.1 Uncertainties in Stage Discharge Relationship

A number of factors affect the accuracy of the stage discharge relationship. The uncertainties associated with the relationship can be broadly classified as the measurement uncertainties, interpolation uncertainties and flow unsteadiness uncertainties. Bárdossy *et al.* [2004] described it in terms of uncertainties due to stage measurement, discharge measurement, discharge curves and dispersion of the flow values.

The uncertainties in the stage measurement are dependent upon the characteristics of the gauging station and water surface elevation. An important source of uncertainty is displacement of measured values from the reference point, caused by processes such as turbulent fluctuations, wind and stationary waves [Bárdossy *et al.*, 2004; Schmidt, 2004].

The limitations of the discharge measurement methods are also a major source of uncertainties. As the discharges are measured indirectly, uncertainties might be introduced due to measurement errors from instrumentation or method of flow measurement. During floods events discharges measurements are never made continuously and can never be considered very accurate [Cunge *et al.*, 1980].

The uncertainties in the discharge curve are dependent upon the number of measurements made. As the discharge values are not measured continuously, it is necessary to make interpolations between the measured values. Hence, there exist large uncertainties in the interpolated region of the data [Bárdossy *et al.*, 2004]. There is usually a lack of measurement of flood discharges and the values are usually derived by extrapolating the existing stage discharge relationship curves. The extrapolation gives rise to uncertainties in flood discharge values.

The dispersion of discharge values with respect to a certain depth of flow is an important source of uncertainties in the stage discharge relationship. The relationship in not a single valued as specified by the most curves but exhibits a looped form as shown in Figure 6.1. The effect also termed as hysteresis indicates that there is no unique relationship between the depth and the discharge values. This is due to the fact that the stage is not just the function of discharge, but also a function of a variable energy slope [Chow *et al.*, 1988]. The slope of the water surface is greater on the rising limb than on the falling limb, thus the flow is accelerating on the rise and decelerating on the fall [USACE, 1993]. Due to this effect the discharge is higher in the rising limb than in the falling limb for a given stage.

Hence, when a single valued relationship is used major uncertainty arises in the derived discharge values.

There may also be considerable uncertainty associated with the temporal variations of a particular river channel condition. Many channel cross sections change considerably throughout the year, especially after a significant flood event. Any change in the channel cross section can have a significant effect on the relationship between stage and discharge. Hence the stage discharge relationship needs to be updated periodically.

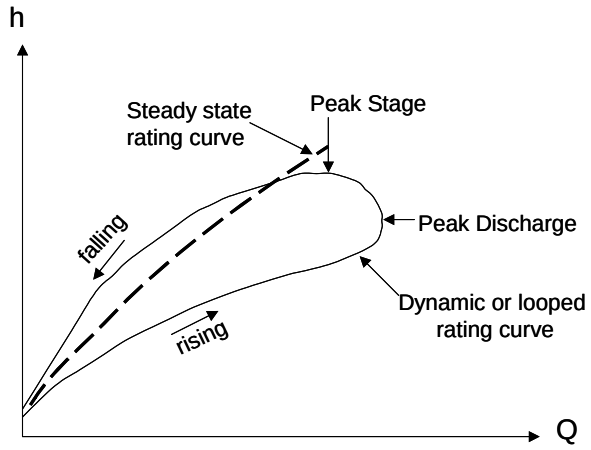

Figure 6.1. Schematic representation of steady and unsteady state rating curves
Adapted from Chow *et al.* [1988]

6.1.2 Methods of Uncertainty Analysis and Management

A number of methods may be used to analyse and manage the uncertainties in the stage discharge relationship. As discussed in section 6.1.1. a major source of uncertainty in the discharge records is the single valued stage discharge relationship. One method of managing this uncertainty is to use a nonlinear mapping method such as artificial neural networks (ANNs) as an alternative to the stage discharge relationship curve. The applications of the ANN in river flow prediction have been demonstrated in chapters 4 and 5. In the recent years several researchers have used ANNs for nonlinear mapping of the stage discharge relationship [Tawfik *et al.*, 1997; Bhattacharya and Solomatine, 2000; Jain and Chalisgaonkar, 2000; Sudheer and Jain, 2003].

With regard to the uncertainty analysis, the probability theory and the fuzzy set theory are the two most widely used methods. The probability theory assumes uncertainty mainly due to randomness while the fuzzy set theory represents the uncertainty due to vagueness and imprecision in a non-probabilistic sense [Maskey, 2004].

Schmidt [2002] used the probability based reliability analysis methods to systematically analyse the uncertainties from different underlying sources of the stage discharge

relationship. The procedure used for the reliability analysis included the combination of mean-value first-order, second-order and point estimation methods. Other widely used probability based uncertainty analysis method used in water resources includes the Monte Carlo simulation, which is based on the probability distribution of the uncertain parameters as random variables [Abebe, 2004; Maskey, 2004].

The inherent uncertainties in the stage discharge relationship can be represented by defining a band of credible upper and lower scenarios of discharges for a given stage as an alternative to a single valued relationship curve. The uncertainty band can be defined in terms of confidence limits using statistical methods. An example of the method can be found in Bárdossy *et al.* (2004), where a combination of the cross validation and the bootstrapping method were used.

The fuzzy regression analysis also provides an alternative tool for the definition of the uncertainty band. Fuzzy regression can be used as an alternative to statistical regression analysis, when the relationship between the variables is imprecise, data are uncertain and sample sizes are insufficient [Bárdossy *et al.*, 1990]. Using this method, the crisp parameters A_1 and A_2 of the equation (6.1) can be replaced by fuzzy numbers, whose spread can be determined using an optimisation algorithm. However, such an application for the stage discharge relationship has not been reported yet. Some of the applications of fuzzy regression analysis include dose response relationship [Bárdossy *et al.*, 1993; Lee *et al.*, 2001], fuzzy linear conceptual rainfall runoff processes [Özelkan and Duckstein, 2000] and organic/nutrient load and river discharge relationship [Chaves and Kojiri, 2003].

The fuzzy sets theory also provides a framework for the propagation of uncertainties. For this purpose, the membership function of the dependent variable (discharge) defined by the fuzzy regression analysis can be used. The uncertainty represented by the fuzzy numbers can be propagated using alpha level cut, which offer a convenient way of resolving fuzzy sets into crisp sets. Recent applications of the fuzzy alpha level cut methods include parameter uncertainty of water transport in layered soil profile [Schulz and Huwe, 1999] and precipitation uncertainty of a deterministic rainfall-runoff model [Maskey, 2004].

This chapter considers the methods of uncertainty analysis and management in the stage discharge relationship. An artificial neural network based nonlinear mapping method is developed to handle the uncertainties. The fuzzy regression analysis is used to define the uncertainty band of discharges in the stage discharge relationship. A resulting membership function of discharges is used with the extension principle based alpha cut method to analyse the propagation of uncertainties in river channels and floodplains.

6.2 Uncertainty Management of Stage Discharge Relationship Using ANNs

This study includes two applications of the ANNs for the nonlinear mapping of the stage discharge relationship. The applications are undertaken using the measured and simulated time series data, as an alternative to a single valued stage discharge relationship curve. The first case study consists of mapping a highly scattered nonlinear relationship between stage and discharge values using the observed flow and stage time series data. The second case study deals with the reproduction of looped rating curves using simulated flow and water level time series data from a hydrodynamic numerical model.

6.2.1 Modelling Nonlinear Stage Discharge Relationship

The stage and flow time series data from the Lauffen gauging station (Figure 5.1) in the Neckar River were obtained from Water and Navigation Administration, South-West Mainz. The rating curve in the Lauffen gauging station is considered unreliable and the obtained discharge time series was actually based on discharges from the gauging stations at Bessigheim and the tributary Enz, both located at a distance of about 12 km upstream. The discharges in Bessigheim and Enz are based up rating curve derivations. Hence the obtained discharge values in the Lauffen gauging station is affected by uncertainties due to (i) rating curve conversion in the upstream stations, (ii) derivation based on the upstream stations. When the stage and discharge time series data are plotted against one another a highly scattered relationship is depicted (Fig. 6.2).

The process of establishing discharges at the Lauffen gauging station based on the upstream flows can be replaced by a nonlinear mapping method. From the measured stages and derived discharge values of historical flood events, a nonlinear mapping problem can be formulated with stage as the input variable and discharge as the output variable. In this example, the ANN is used as nonlinear mapping tool for the derivation of the discharge time series based on the stage time series. The results of the ANN method are compared with the conventional rating curve method.

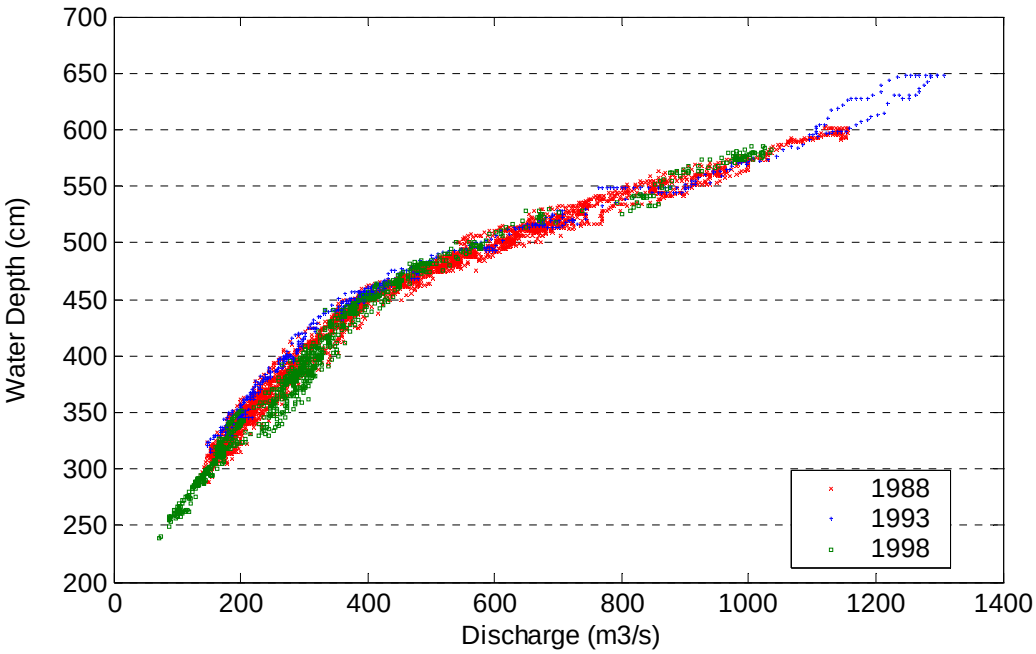

Figure 6.2. Stage discharge relationship at the Lauffen gauging station

6.2.1.1 Model Implementation

The two ANN architectures consisting of a multilayer perceptron (MLP) and a radial basis function network (RBFN) are used in this study. The available data consists of 1988, 1993 and 1998 stage and discharge time series. The 1993 dataset consists of the highest range of data. However, it is subject to uncertainties as discussed in section 5.4. Hence, the 1988 datasets are used for the training purpose, and the 1998 and 1993 datasets are used for validation and test purposes respectively. As the model involves extrapolation beyond the range of training datasets, the inputs and output datasets are normalised between 0.2 and 0.8. The ANNs are trained with the stage time series *h* and its rate of change *dh/dt* as inputs and the discharge time series *Q* as a target as shown in Figure 6.3.

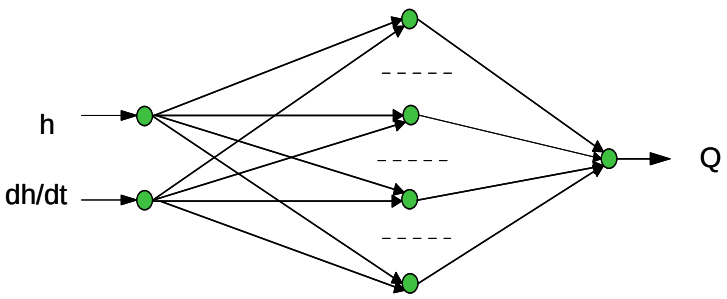

Figure 6.3. Structure of the ANN nonlinear mapping model

The four layer MLP neural network is used with 2 neurons in the input layer, 10 neurons in the first hidden layer, 8 neurons in the second hidden layer and 1 neuron in the output layer. The MLP consists of hyperbolic tangent activation function in the hidden layers and linear activation function in the output layer. The RBFN has a two layer network architecture consisting of Gaussian activation functions in the hidden layer and a linear activation function in the output layer. The number of neurons in the hidden layer of the RBFN is 28 neurons as determined iteratively during the training process. Both the ANN models are developed using the procedures of the MATLAB Neural Network Toolbox [Demuth and Beale, 2004].

There is no rating curve available for the Lauffen gauging station. For the comparison of the results with the ANN models, linear regression of the available stage discharge data is carried out. The relationship derived from the regression analysis consists of a two stage compound rating curve for low flow and high flows with the boundary point h_{bound} at 450 cm. The relationship is of the form of equation (6.1a):

$$Q_i = 2.1553x10^{-5} h_i^{2.7527} \quad \text{for } h_i < h_{bound} \tag{6.2a}$$

$$Q_i = 1.4850x10^{-6} h_i^{3.1910} \quad \text{for } h_i > h_{bound} \tag{6.2b}$$

6.2.1.2 Results and Discussion

The results of the ANN models are analysed using the statistical criteria of coefficient of determination (R^2) and the root mean square error (RMSE). Similarly, the peak error (PE) and the maximum absolute error (MAE) in discharge are also considered. Details of the error measurements are outlined in Appendix B. Additional criteria for the error measurement include the discharge errors for three different ranges. Based on the analysis, it can be seen that the performance of both the ANN models are better compared to the conventional rating curve method. The discharge errors obtained by the ANN models are less than that from the rating curve. The comparison of the statistical performance of the ANNs in terms of R^2 and RMSE show that MLP is superior to the RBFN network for both the validation and test datasets. The MLP also has the lower difference in the peak flow in the validation and test datasets. The discharge hydrographs derived from MLP ANNs and the rating curves are compared with the observations for the validation and test datasets in Figures 6.4 and 6.5 respectively. The results of the model clearly show that ANN nonlinear mapping is superior to the rating curve relationship.

Table 6.1. Statistical performance of the ANN model and the rating curve

Data	Model type	R^2	RMSE (m^3/s)	PE (m^3/s)	MAE (m^3/s)	Discharge error range (%)		
						< 20 m^3/s	20-50 m^3/s	>50 m^3/s
1998	MLP	0.9891	24	-19	87	67.4	27.3	5.2
(validation)	RBFN	0.9874	25	-21	81	59.0	35.7	5.3
	Rating curve	0.9864	26	29	77	58.9	34.4	6.7
1993	MLP	0.9922	33	-68	145	43.0	50.0	7.0
(test)	RBFN	0.9899	35	-85	150	42.9	49.1	8.0
	Rating curve	0.9851	49	-88	153	22.2	50.4	27.4

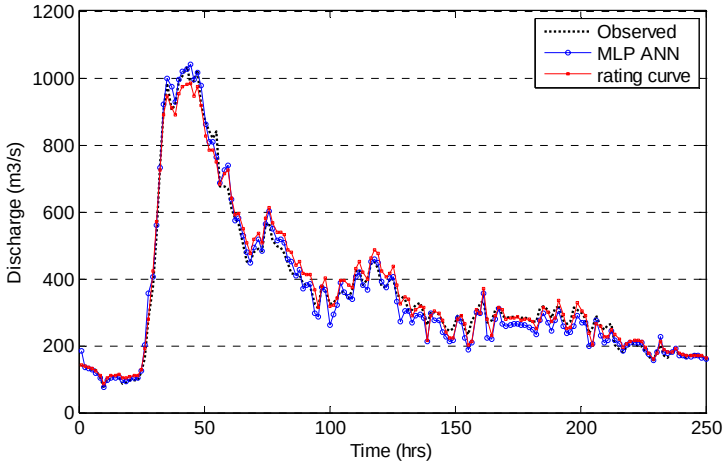

Figure 6.4. Observed, MLP ANN simulated and rating curve derived hydrographs for validation datasets (1998)

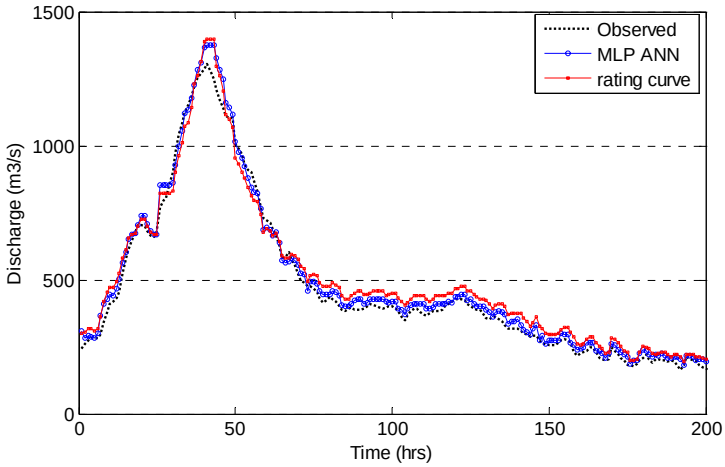

Figure 6.5. Observed, MLP ANN simulated and rating curve derived hydrographs for test datasets (1993)

6.2.2 Modelling Looped Rating Curve

The application consists of reproduction of the hydrodynamic numerical (HN) model simulated looped stage discharge relationship using the ANNs. For this purpose, the HN model simulated hydrographs at the Worms gauging station in the Rhine River are used. The HN model is described in detail in chapter 4 section 4.3.

Both the measured stage and discharge hydrographs are available from the gauging station. The discharge hydrograph is derived from a single valued stage discharge relationship curve as seen in Figure 4.4. However, the relationship may show a looped effect due to the unsteady nature of the flood wave propagation. Hence, discharge hydrographs derived from the single valued stage discharge relationship are subject to uncertainties. An HN model based on full Saint Venant equations is capable of simulating the looped effect. This is evident from the relationship between the simulated stage and discharge hydrographs as shown in the Figure 6.6.

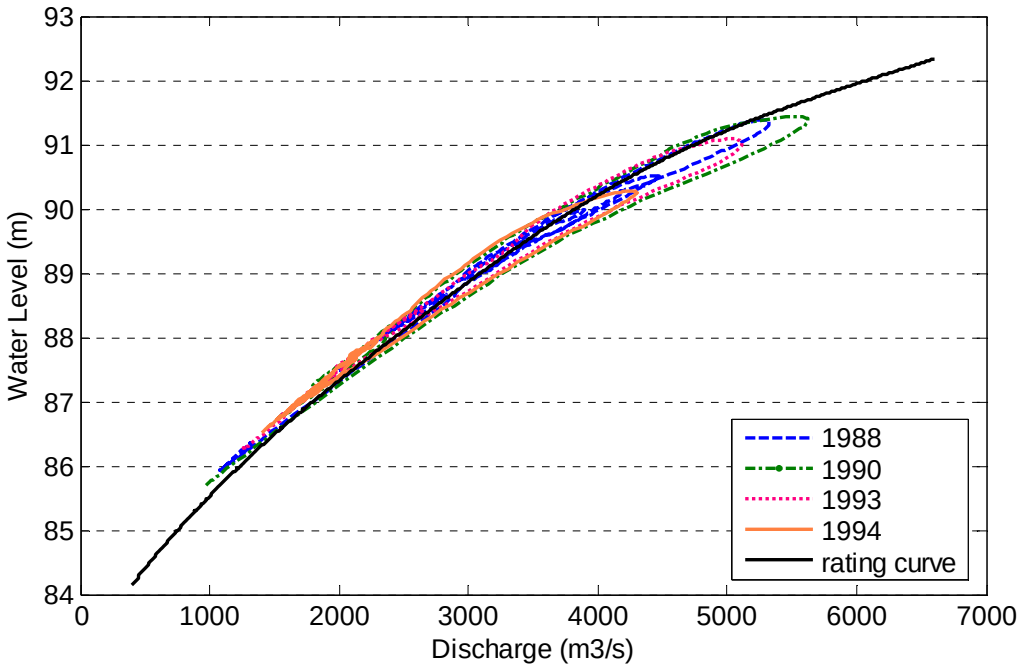

Figure 6.6. HN model simulated stage discharge relationship compared to the rating curve at the Worms gauging station

6.2.2.1 Model Implementation

A number of ANN models are trained for the nonlinear mapping of the looped relationship. The architectures of the ANNs used in this example include the MLP and the RBFN. The four HN model simulated datasets from 1988, 1990, 1993 and 1994 flood events are available. The 1988 data is used as the training set, which consists of the highest range of available data. This is done deliberately to improve the prediction range of the model as described in section 3.2.6.1. The HN model simulated data from 1990 is used for

validation, and 1993 and 1994 as test datasets. The input and output datasets are normalised between –1 and 1. In this case too, the ANN inputs consist of the water level time series *h* and its rate of change *dh/dt* and the targets consist of the discharge time series *Q* as shown in Figure 6.3.

The structure of the MLP consists of 10 neurons in the hidden layer, and 1 neuron in the output layer. The MLP consists of hyperbolic tangent activation functions in the hidden layers and linear activation function in the output layer. The RBFN has a two layer architecture consisting of Gaussian activation functions in the hidden layer and a linear activation function in the output layer. The hidden layer of the RBFN consists of 14 neurons, which is determined iteratively during the training process, by adding one neuron after every training step.

6.2.2.2 Results and Discussion

The performance of the ANN models are analysed using the criteria R^2, RMSE, PE and MAE in discharges. In addition, the discharge errors for three different ranges are considered. The results of the analysis for the MLP and RBFN are summarised in Table 6.2. Based on the performance of the model, it can be seen that the performance of the MLP are slightly better than the RBFN for both the validation (1990) and the test (1993 and 1994) datasets. The discharge errors for the most of the data is less than 50 m^3/s, which is a good result considering the total discharge lie in the range from 1000 to 5000 m^3/s. The results of the MLP networks are compared with the targets values and the single valued rating curve in Figures 6.7 for the validation dataset and Figures 6.8 and 6.9 for the test datasets. The model results clearly show a very good reproduction capability of the ANN for simulating a looped rating relationship.

Table 6.2. Statistical performance of the ANN model results

Data	Network type	R^2	RMSE (m^3/s)	PE (m^3/s)	MAE (m^3/s)	Discharge error range (%)		
						<20 m^3/s	20–50 m^3/s	>50 m^3/s
1990	MLP	0.9995	29	-6	61	67.9	29.3	2.8
(validation)	RBFN	0.9994	35	10	64	57.4	35.9	6.7
1993	MLP	0.9997	18	29	46	79.0	19.8	1.2
(test)	RBFN	0.9995	22	17	49	60.4	38.0	1.6
1994	MLP	0.9993	20	30	47	87.0	10.6	2.4
(test)	RBFN	0.9988	23	56	68	63.7	32.5	3.8

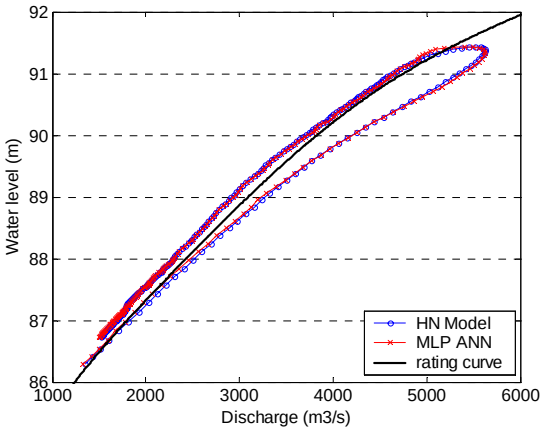

Figure 6.7. Reproduction of looped rating curve for validation datasets (1990)

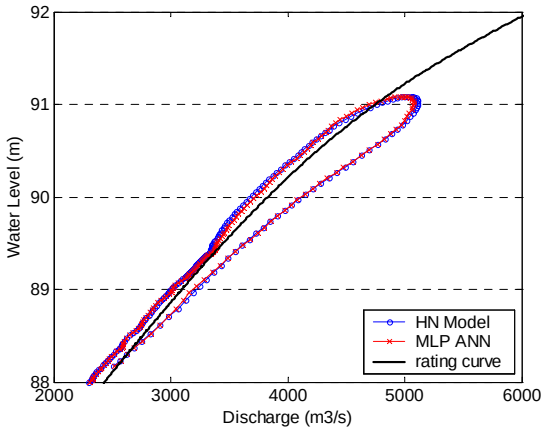

Figure 6.8. Reproduction of looped rating curve for test datasets (1993)

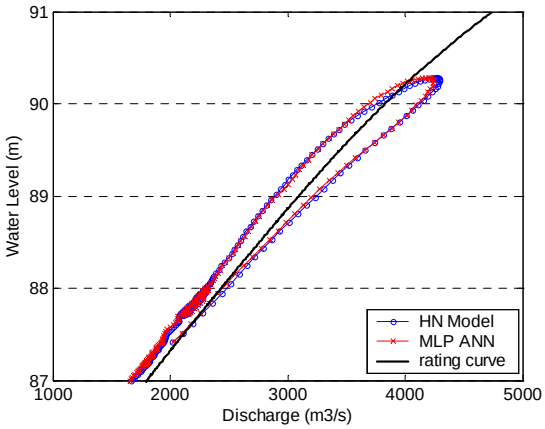

Figure 6.9. Reproduction of looped rating curve for test datasets (1994)

6.3 Uncertainty Analysis Using Fuzzy Regression

Statistical regression is a widely used method to develop a relationship between dependent and independent variables of a dataset. However, as described in section 6.1.1, there is no unique one to one relationship between the dependent variable (discharge, *Q*) and independent variable (stage, *h*), in the stage discharge relationship Hence, the stage and discharge do not have a unique one to one relationship. The fuzzy regression analysis can deal with such a problem by expressing the uncertain parameters in terms of fuzzy numbers. Bárdossy *et al.* [1993] described the method in terms of (i) L-R (left-right) representation of fuzzy number; and (ii) the extension principle. These components are described in detail in chapter 3.

For the fuzzy regression analysis of stage discharge relationship, the stages can be assumed as crisp and discharge as fuzzy numbers, with the crisp parameters A_1 and A_2 of the equations (6.1a) or (6.1b) expressed in terms of fuzzy numbers. The analysis can be undertaken using both the power relationship (equation 1a) and the logarithmic

relationship (equation 1b). The former relationship leads to a nonlinear fuzzy regression model and the latter to a linear fuzzy regression model. Both the fuzzy regression models are used in this study for the assessment of the stage discharge relationship of the Lauffen gauging station in the Neckar River.

6.3.1 Fuzzy Nonlinear Regression Model

The nonlinear fuzzy regression model is based upon the power relationship (equation 1a), with a compound curve for low and high flows meeting at the boundary point h_{bound}. Considering the parameters A_1 and A_2 as fuzzy numbers the equation (6.1a) can be rewritten as:

$$Q_i = A_1^* h_i^{A_2^*} \qquad \text{for } h_i < h_{bound} \tag{6.3a}$$

$$Q_i = A_3^* h_i^{A_4^*} \qquad \text{for } h_i > h_{bound} \tag{6.3b}$$

$$A_1^* h_i^{A_2^*} = A_3^* h_i^{A_4^*} \qquad \text{for } h_i = h_{bound} \tag{6.3c}$$

Where, $A_j^* = \left(m_j, \alpha_j, \beta_j\right)_{LR}$ is defined by L-R fuzzy functions with the boundary (0,1), with m_j, α_j, and β_j representing the central value and the left and right spreads respectively. The membership functions corresponding to the L and R parameters can be taken as continuously linearly decreasing as shown in Figure 6.10 and defined by the equation (6.4):

$$L(z) = R(z) = 1 - z \tag{6.4}$$

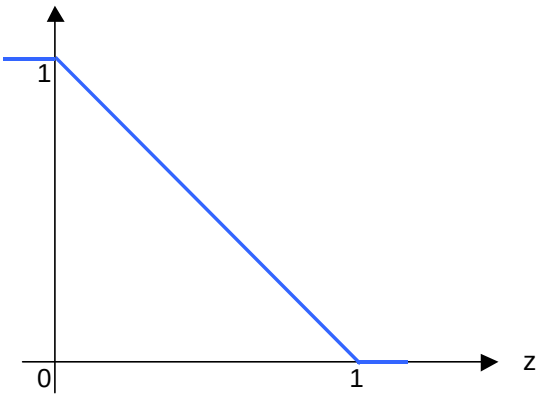

Figure 6.10. Linear representation of L-R fuzzy functions

The left and right spreads of the membership functions can be extended to incorporate the out of sample points using a credibility factor. By specifying the credibility at a certain level H, the fuzziness of the spreads can be controlled. In particular, as the H level increases,

the spreads α_j and β_j also increase. The L-R fuzzy condition for the credibility level H, can be written as [Bárdossy, 1990]:

$$m_j - \alpha_j L_j^{-1}(H) \le A_j^* \le m_j + \beta_j R_j^{-1}(H) \tag{6.5}$$

The spread of the membership function also depends upon the reference point in the data region corresponding to which fuzzy regression analysis is performed. The reference point should be selected in the region where the regression is supposed to be crispest, which may be the average or maximum of the variables, or in any way fitting the context of the problem (Bárdossy *et al.*, 1990). In the case of nonlinear regression, the reference point can be considered by dividing the stages h_i by the reference point h_{ref}. Hence, the mathematical formulation of the fuzzy nonlinear regression equation for the low and high flow can be obtained by combining the equations (6.3) and (6.5):

$$\left.\begin{aligned} \left(m_1 - \alpha_1\left(L_1^{-1}(H)\right)\right)\left(\frac{h_i}{h_{ref}}\right)^{m_2-\alpha_2\left(L_2^{-1}(H)\right)} &\le Q_i \\ \left(m_1 + \beta_1\left(R_1^{-1}(H)\right)\right)\left(\frac{h_i}{h_{ref}}\right)^{m_2+\beta_2\left(R_2^{-1}(H)\right)} &\ge Q_i \end{aligned}\right\} \quad \text{for } h_i < h_{bound} \tag{6.6a}$$

$$\left.\begin{aligned} \left(m_3 - \alpha_3\left(L_3^{-1}(H)\right)\right)\left(\frac{h_i}{h_{ref}}\right)^{m_4-\alpha_4\left(L_4^{-1}(H)\right)} &\le Q_i \\ \left(m_3 + \beta_3\left(R_3^{-1}(H)\right)\right)\left(\frac{h_i}{h_{ref}}\right)^{m_4+\beta_4\left(R_4^{-1}(H)\right)} &\ge Q_i \end{aligned}\right\} \quad \text{for } h_i > h_{bound} \tag{6.6b}$$

$$\left.\begin{aligned} m_1\left(\frac{h_i}{h_{ref}}\right)^{m_2} &= m_3\left(\frac{h_i}{h_{ref}}\right)^{m_4} \\ \left(m_1 - \alpha_1\left(L_1^{-1}(H)\right)\right)\left(\frac{h_i}{h_{ref}}\right)^{m_2-\alpha_2\left(L_2^{-1}(H)\right)} &= \left(m_3 - \alpha_3\left(L_3^{-1}(H)\right)\right)\left(\frac{h_i}{h_{ref}}\right)^{m_4-\alpha_4\left(L_4^{-1}(H)\right)} \\ \left(m_1 + \alpha_1\left(R_1^{-1}(H)\right)\right)\left(\frac{h_i}{h_{ref}}\right)^{m_2+\alpha_2\left(R_2^{-1}(H)\right)} &= \left(m_3 + \alpha_3\left(R_3^{-1}(H)\right)\right)\left(\frac{h_i}{h_{ref}}\right)^{m_4+\alpha_4\left(R_4^{-1}(H)\right)} \end{aligned}\right\} \quad \text{for } h_i = h_{bound} \tag{6.6c}$$

6.3.2 Fuzzy Linear Regression Model

The formulation of the fuzzy linear regression model is also based on the compound curve stage-discharge relationship for the linear equation (6.1b). The linear equation (6.1b) in combination with the equation (6.5) leads to the following system of equations for low and high flows.

$$\left.\begin{aligned}\left(m_1-\alpha_1\left(L_1^{-1}(H)\right)\right)+\left(m_2-\alpha_2\left(L_2^{-1}(H)\right)\right)\left(log\left(\frac{h_i}{h_{ref}}\right)\right)\le log(Q_i)\\ \left(m_1+\beta_1\left(R_1^{-1}(H)\right)\right)+\left(m_2+\beta_2\left(R_2^{-1}(H)\right)\right)\left(log\left(\frac{h_i}{h_{ref}}\right)\right)\ge log(Q_i)\end{aligned}\right\} \text{ for } h_i < h_{bound} \quad (6.7a)$$

$$\left.\begin{aligned}\left(m_3-\alpha_3\left(L_3^{-1}(H)\right)\right)+\left(m_4-\alpha_4\left(L_4^{-1}(H)\right)\right)\left(log\left(\frac{h_i}{h_{ref}}\right)\right)\le log(Q_i)\\ \left(m_3+\beta_3\left(R_3^{-1}(H)\right)\right)+\left(m_4+\beta_4\left(R_4^{-1}(H)\right)\right)\left(log\left(\frac{h_i}{h_{ref}}\right)\right)\ge log(Q_i)\end{aligned}\right\} \text{ for } h_i > h_{bound} \quad (6.7b)$$

$$\left.\begin{aligned}m_1+m_2\left(log\left(\frac{h_i}{h_{ref}}\right)\right)=m_3+m_4\left(log\left(\frac{h_i}{h_{ref}}\right)\right)\\ \left(m_1-\alpha_1\left(L_1^{-1}(H)\right)\right)+\left(m_2-\alpha_2\left(L_2^{-1}(H)\right)\right)\left(log\left(\frac{h_i}{h_{ref}}\right)\right)=\\ \left(m_3-\alpha_3\left(L_3^{-1}(H)\right)\right)+\left(m_4-\alpha_4\left(L_4^{-1}(H)\right)\right)\left(log\left(\frac{h_i}{h_{ref}}\right)\right)\\ \left(m_1+\beta_1\left(R_1^{-1}(H)\right)\right)+\left(m_2+\beta_2\left(R_2^{-1}(H)\right)\right)\left(log\left(\frac{h_i}{h_{ref}}\right)\right)=\\ \left(m_3+\beta_3\left(R_3^{-1}(H)\right)\right)+\left(m_4+\beta_4\left(R_4^{-1}(H)\right)\right)\left(log\left(\frac{h_i}{h_{ref}}\right)\right)\end{aligned}\right\} \text{ for } h_i = h_{bound} \quad (6.7c)$$

6.3.3 Fuzzy Regression Model Fitting

The goodness of fit of both the linear and the nonlinear fuzzy regression models can be measured in terms of the vagueness criteria of the uncertain parameters. The maximum parameter vagueness V is one such criterion, given by the spread of the membership functions α_j and β_j:

$$V = max\left(\alpha_j, \beta_j\right) \quad (6.8)$$

For simplicity, a symmetrical membership function is chosen for the left and right sides such that, $\alpha_j = \beta_j$. This reduces the maximum vagueness of the model to four parameters α_1, α_2, α_3, and α_4, two each for the low and the high flows, which need to be minimised. Hence both the linear and the nonlinear formulations lead to a multiobjective optimisation problem with constraints. In the case of fuzzy nonlinear model, the equations (6.6a, 6.6b and 6.6c) and (6.8) provide the constraints and the objective functions. Similarly, for the

fuzzy linear model the equations (6.7a, 6.7b and 6.7c) and (6.8) provide the constraints and the objective functions respectively.

The time series stage and discharge hydrographs (Figure 6.2) is used for the fuzzy regression analyses. The 1988 and 1993 data are used for the analyses purpose and 1998 data for the verification purpose. A credibility level H of 0.5 is selected for the analyses. A stage value of h_{bound} = 450 cm is chosen as the boundary between the low flow and high flow. The reference point is also specified as h_{ref} = 450 cm, which is approximately the average of the stages. The optimisations are performed using the sequential quadratic programming method based on the procedures of the MATLAB optimization toolbox [The MathWorks Inc., 2004b].

6.3.4 Results and Discussion

The results of both nonlinear and the linear fuzzy regression analyses produced envelopes for the regression data of 1988 and 1993 as shown in Figures 6.11 and 6.12. For the validation data of 1998, some low flow points are outside the 0.5(L) and 0.5(R) envelopes but well inside 0.0(L) and 0.0(R) level envelopes. The 1998 high flow data are all inside the 0.5 level envelopes and the level can be considered as a suitable representation of uncertainties for high flows.

The membership functions of discharges from nonlinear and linear regression corresponding to the stages of 450 and 648 cm are illustrated in Figs. 6.13(A) and 6.13(B). Table 6.3 shows the comparison of the discharges obtained from the nonlinear and linear fuzzy regression analyses at membership levels 1, 0.5(L) and 0.5(R). As expected, the results of the nonlinear and the linear fuzzy regression models are slightly different. The linear fuzzy regression model uses the transformed vagueness criteria, which is ultimately minimised (Bárdossy *et al.*, 1993). This leads to higher uncertainty in the case of the linear model compared to the correct untransformed nonlinear model.

The differences in discharges due to the uncertainties are found to be considerable in both the analyses. It can also be seen that the spread of the membership function of discharges increases with the stages. Therefore, the uncertainties in discharges beyond the observed stage of 648 cm will be even greater. The reference point for the analyses is taken as the average value of the stages. If the reference point is taken at the minimum of observed stages, the spread at the higher discharges can be expected to be even higher.

Table 6.3. Comparison of the nonlinear and linear fuzzy regression models

Stage h_i (cm)	Discharges from nonlinear regression model (m^3/s)			Discharges from linear regression model (m^3/s)		
	$\mu = 1$	$\mu = 0.5$ (R) (upper)	$\mu = 0.5$ (L) (lower)	$\mu = 1$	$\mu = 0.5$ (R) (upper)	$\mu = 0.5$ (L) (lower)
250	86	106	71	84	106	67
350	221	269	182	215	269	173
450	445	539	370	435	539	351
550	831	938	730	813	941	703
648	1383	1475	1273	1356	1485	1239

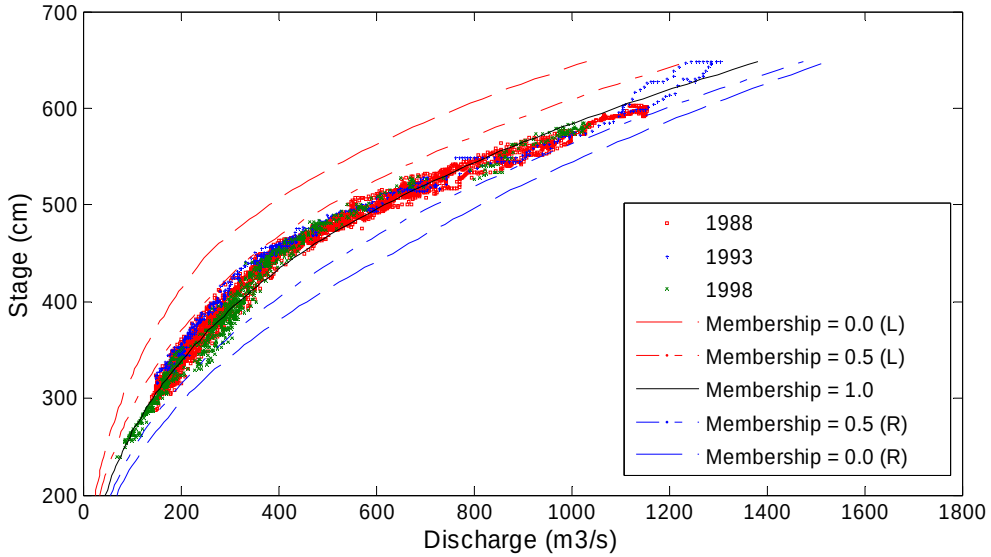

Figure 6.11. Fuzzy regression curves with scattered data for nonlinear model

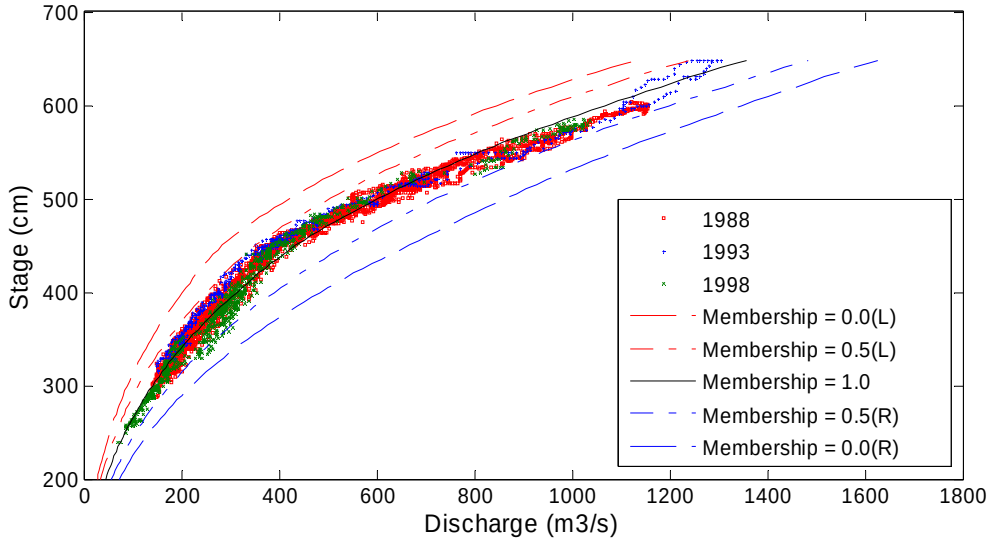

Figure 6.12. Fuzzy regression curves with scattered data for linear model

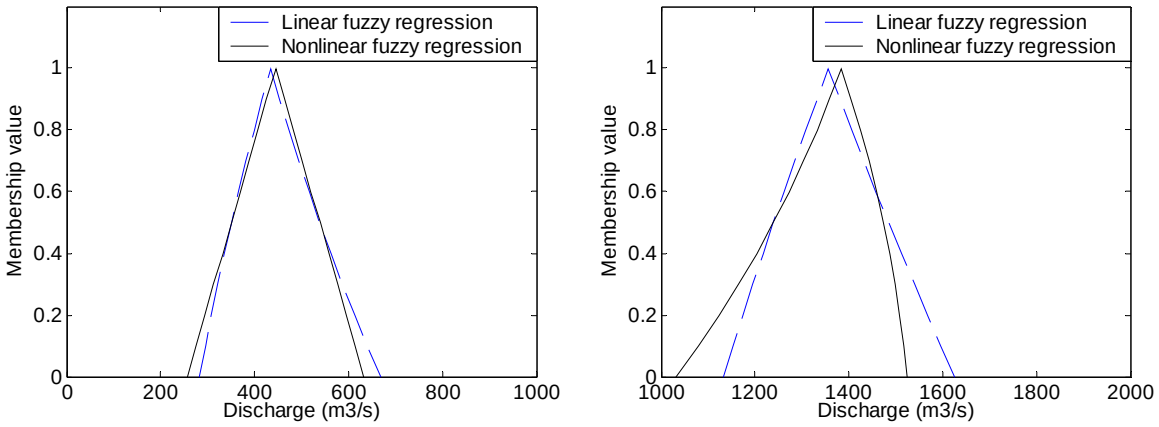

Figure 6.13. Membership functions of nonlinear and linear regression models corresponding to stages of (A) 450 cm, (B) 648 cm

6.4 Uncertainty Analysis in Water Level Simulation

The discharge hydrographs constitute a convenient upstream boundary condition in the unsteady flow simulation of the hydrodynamic numerical (HN) models. Similarly, upstream discharge values are required for the steady flow simulations of the water surface profiles. Hence, the uncertainties in discharge values will lead to uncertainties in the HN model simulations. The uncertainties can be taken into account by representing the discharge values as fuzzy numbers characterised by their membership functions.

In the present study, the nonlinear membership functions of the discharge values defined by the fuzzy nonlinear regression analysis corresponding to stage 648 cm (Figure 6.13(B)) is taken for the propagation of uncertainties in an HN model. The alpha level cut method based on the extension principle is used for this analysis. The application involves the following steps:

i. The use of interval arithmetic for horizontal cutting of the membership function of discharges at a finite number of α - levels between 0 and 1.

ii. The steady flow water surface profiles computations using the HN model for the lower and upper bound discharges from the α – level cuts.

iii. Derivation of the membership function of the water levels using the HN model simulations at each of the α – levels.

An example of the α – level cut for the membership function corresponding to stage 648 cm is shown in Figure 6.14. Since the analysis involves steady flow simulations, the water levels along the river reach increase or decrease strictly monotonically with the increase or decrease in discharges. Hence, for an α – level cut, the discharges corresponding to

lower and upper bounds also give the corresponding lower and upper bound water levels in the river reach.

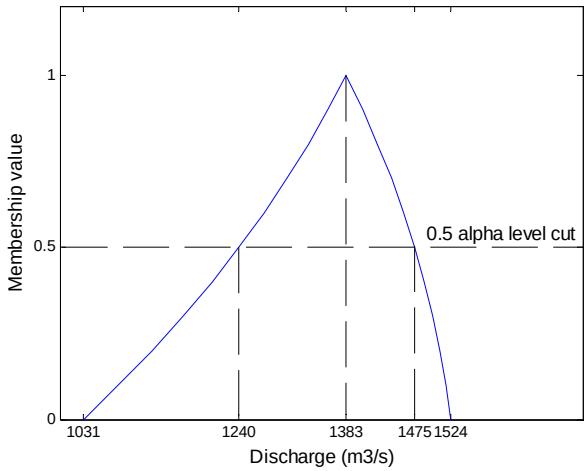

Figure 6.14. Alpha cut at 0.5 level of the membership function obtained by nonlinear regression analysis corresponding to the stage of 648 cm

6.4.1 Model Implementation

The above methodology is applied to assess the propagation of uncertainties in a river channel due to the uncertainties in discharge. The one-dimensional HN model described in detail in chapter 5 is used to make the steady flow simulations. The river section consists of the Horkheim subreach from the Weir Lauffen to the Weir Horkheim at the immediate downstream of the Lauffen gauging station (Figure 5.2), where uncertainties in the stage discharge relationship are analysed. The river section is extended further downstream to the Heilbronn subreach so that downstream boundary condition does not influence the water levels at the Horkheim subreach.

The α - level cuts are applied at eleven different levels, at an interval of 0.1 between the membership levels (0.0 – 1.0). The discharge values corresponding to the α - levels are used as upstream boundary conditions of the HN model. The water levels obtained from the HN model are used to derive their membership functions. The resulting water levels are also used in combination with geographical information systems (GIS) for the depiction of uncertainties in the inundation areas. Other sources of uncertainties such as model and parameter uncertainties of the HN model are not considered in this study.

6.4.2 Results and Discussion

The Figure 6.15 shows the uncertainties in water surface profiles in the Horkheim subreach due to uncertainties in the discharges values. The water surface profiles relate to discharges corresponding to an upstream stage of 648 cm at the Lauffen gauging station for the membership levels 0.5(L), 1.0 and O.5(R). The uncertainty analysis leads to

nonlinear membership function of the water levels throughout the river subreach. An example of the resulting water level membership function at the Weir Horkheim in the downstream section is shown in Figure 6.16. From the illustrations, it is clear that uncertainties in the water levels is about 0.5 m between the 0.5 upper and the 0.5 lower membership levels, which is a significant value in flood water levels.

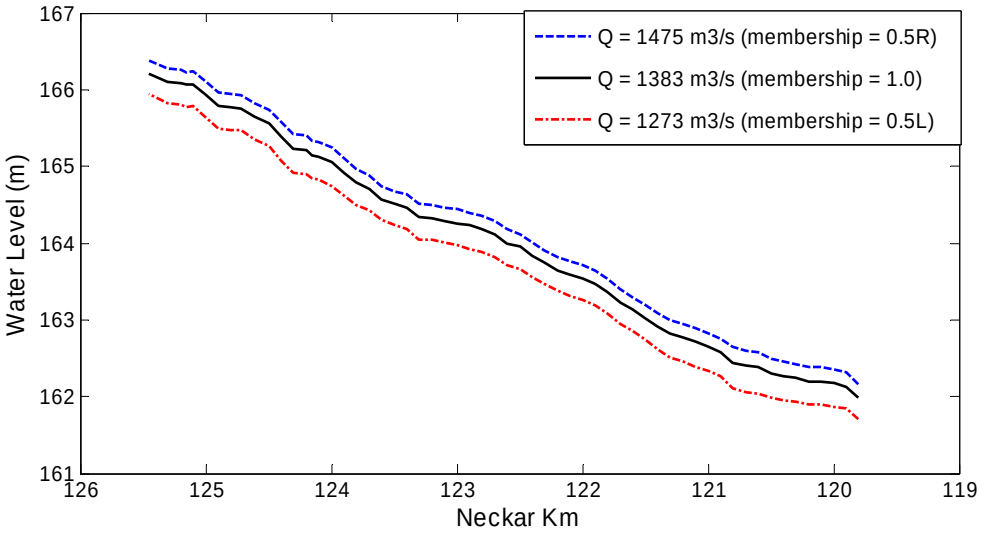

Figure 6.15. Uncertainties in water surface profiles in the Horkheim subreach (Neckar River) corresponding to uncertain upstream discharges

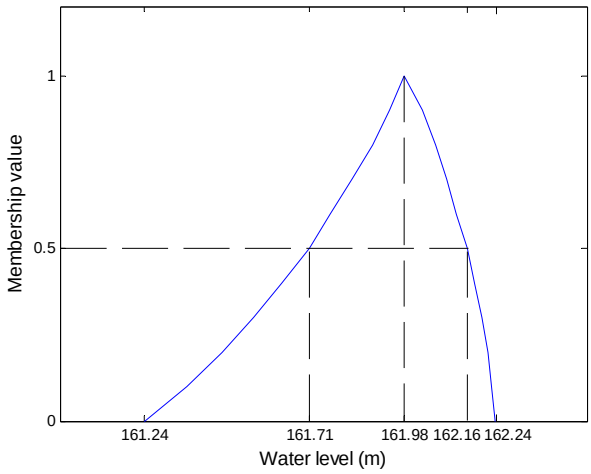

Figure 6.16. Water level membership function at the Weir Horkheim corresponding to uncertain upstream discharges

The resulting water surface profiles in the Neckar River subreach at Horkheim are used in combination with the GIS for depiction of uncertainties in floodplain modelling. The digital terrain model consists of a high resolution Laser induced Detection and Ranging (LiDAR) measurements of 1.0 m horizontal resolution. The water surface profiles of the membership levels 0.5(R), 1.0 and 0.5(L) corresponding to the upstream stage of 648 cm

at the Lauffen gauging station are used to analyse the uncertainties in the floodplain. Figures 6.17(A), 6.17(B) and 6.17(C) depict the difference models of the inundation grids (water surface grid – terrain grid) for a section of the Horkheim subreach. The uncertainties in the inundation areas due to the uncertainties in discharge values for the same section is shown in Figure 6.18. The figures clearly depict a large variation in the inundation depths and areas due to the uncertainties in discharge values.

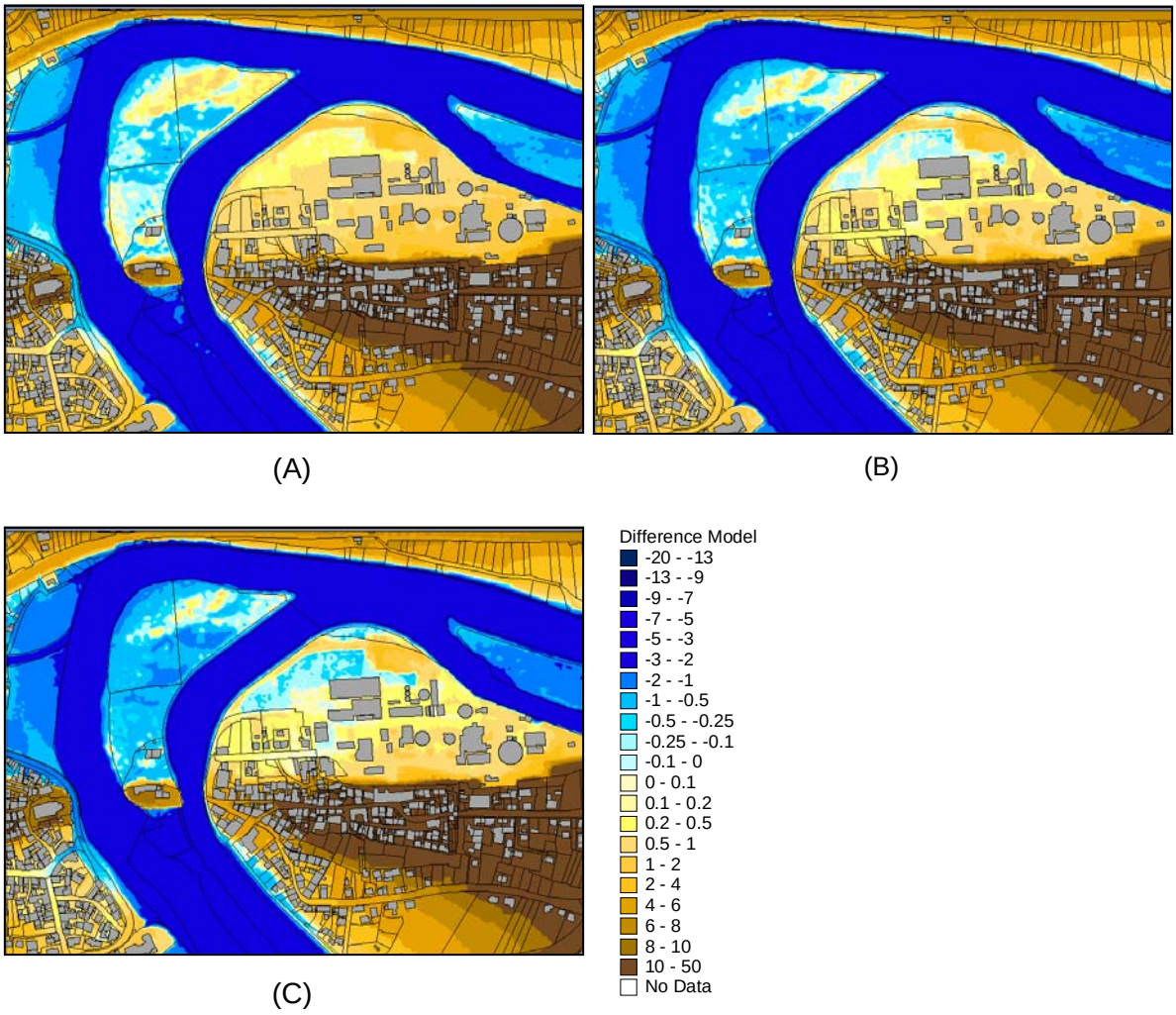

Figure 6.17. Difference model for difference membership levels (A) 0.5L (B) 1.0 (C) 0.5R

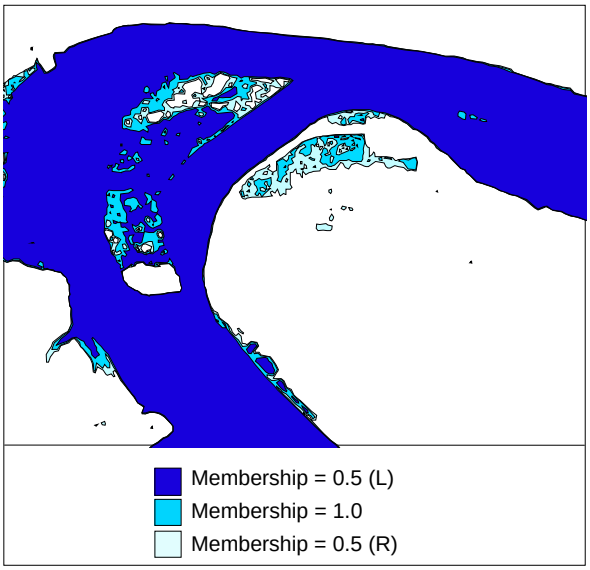

Figure 6.18. Inundation areas for difference membership levels

6.5 Concluding Remarks

This chapter has presented different approaches for managing and analysing the uncertainties in the stage discharge relationship. In the first part of this chapter, artificial neural networks are used to manage the uncertainties of the relationship by directly mapping the discharge values from the stage values as an alternative to the relationship curve. The ANNs are used to reproduce the highly scattered nonlinear relationship and mapping looped rating curves. Based on the results of this study, it can be seen that the ANN based nonlinear mapping technique provides a superior alternative to the single valued relationship curve. When the measured discharges are available, this method can be extended to map the nonlinear relationship between the measured stage and discharge values.

In the second part of this chapter, uncertainty analysis of the stage discharge relationship curve using the fuzzy extension principle based methods is explored. The uncertainties in the relationship are analysed using fuzzy regression methods, which define the lower and upper uncertainty bounds of the relationship. The important factors for the regression include the selection of the credibility level and the reference point. The nonlinear fuzzy regression analysis generally produce a lower spread of dependent variable (discharge) compared to the linear fuzzy regression analysis as the latter uses a transformed relationship, which is ultimately minimised. The resulting membership function of discharge is used for the propagation of uncertainties, using fuzzy alpha level cut in combination with a hydrodynamic model. When relationship between the dependent and independent variables are monotonic, the fuzzy alpha level cut offers a fast and effective methodology for propagating the uncertainties. The results of the study show that the uncertainties in the stage discharge relationship can have a considerable effect in the

estimation of discharge values. The propagation of uncertainties can cause large errors and seriously undermine the performance of the systems such as hydrodynamic models. Hence, it is argued that the uncertainty analysis should be an integral part of flood risk assessment studies.

The methods of uncertainty management, analysis and propagation of uncertainties due to stage discharge relationship also leads to the possibility of complementary modelling. For example, the ANN nonlinear mapping method can be used in a series with the flood routing model so that model boundary data can be generated from the stage time series. The second application of the analysis and propagation of uncertainties using the fuzzy regression and fuzzy alpha cut methods is also an example of series complementary approach.

CHAPTER 7

CONCLUSIONS AND PERSPECTIVES

7.1 Conclusions

This thesis has been inspired by different modelling approaches for river flood prediction that originate from hydraulics, hydrology and artificial intelligence. For the scientific community to benefit more from these tools, it is important to bring them to a common platform and analyse their capabilities. It is also necessary to explore methods of analysing uncertainties in river flood forecasting systems so as to facilitate better decision making process. Driven by these objectives a number of studies have been undertaken using the cases of the Rhine and the Neckar Rivers.

The research presented in this thesis indicates that carefully set up hydrodynamic numerical (HN), hydrological, and data driven models such as artificial neural networks (ANNs) and neuro-fuzzy systems are all capable of producing good results. The application of the HN model in chapters 4, 5 and 6 demonstrate the versatility of these tools in the context of river flood forecasting and prediction of inundation extent. The application of the ANN in chapters 4, 5 and 6, and neuro-fuzzy and Muskingum Cunge (MC) hydrological models in chapter 4 demonstrate that these models provide effective and efficient tools, especially when used within the range of training datasets. Besides forecasting, the data driven ANN and fuzzy systems can be used to support uncertainty analysis applications. The application in chapter 6 shows the usefulness of these tools for the management, analysis and propagation of uncertainties.

7.1.1 Model Strengths and Limitations

This thesis has extensively assessed the strengths and limitations of hydrodynamic, hydrological and data driven modelling approaches in the context of river flood prediction. The capabilities of the HN model, Muskingum-Cunge (MC) hydrological model, and ANN and neuro-fuzzy data driven models are assessed with a case study from the Rhine River reach in chapter 4. Similarly, the thesis considers the capabilities of the HN and ANN models with a case study from the Neckar River reach in chapter 5. The philosophy behind each of these models is entirely different, although the end result might be the same. Important considerations in the context of strength and limitations of the models include, data requirements and forecasting capabilities.

There are major differences with regard to the data requirement and modelling capabilities of these tools. The HN model requires detailed topographical data in the river channel and floodplains. The hydrological and data driven models in contrast require little or no topographical data. With regard modelling capabilities, the HN model is capable of making predictions at every cross section while the hydrological and data driven models are only capable of making predictions at the model output boundaries.

Forecast horizon is another important criterion to be considered. In this regard, an HN model predicts flows at a downstream location at a time step based on the flows at the upstream location at the same time step. In contrast, the hydrological and data driven models, can extend the forecast horizon based on the travel time of the flood wave from upstream to downstream. Based on the travel time, it is possible to make short term flood forecasts, using only upstream flows as inputs.

The tributaries and lateral inflows can affect the performance of river flood prediction models. Being based on the conservation equations, the HN and hydrological models require the consideration of all relevant inputs to the system including minor tributaries and lateral inflows. These inflows may not be gauged in many locations, and quite often it is necessary to make estimations. On the other hand, the data driven models are based on the universal approximation of the input and output variables and do not follow conservation principles. Due to this reason, data driven models can be used to predict downstream flows even without the minor tributaries and lateral inflows.

The prediction of flow beyond the range of calibration is an important criterion of the flood forecasting systems. Being based on the sound physical principles, the HN model provides the best option to simulate the unrecorded events beyond calibration. On the other hand, the simplified hydrological models are predictive as long as the inputs stay within the range of calibration. The same is true for the data driven models, too. The analysis in this thesis has shown that it is also possible to extend the forecasting range of the data driven models to a certain extent beyond calibration. In particular, the possible methods for the ANNs include the normalisation of data in a range such as [0.2 – 0.8], the use of activation function with higher limiting amplitude and the use of the highest range of available data for training.

Further analyses of capabilities of the MC, ANN and ANFIS models in predicting extreme events in the Rhine River reach are undertaken by comparing independently with the HN model. For this analysis, the upstream flow data are multiplied by a factor of 1.5. The results however, show considerable differences in both magnitude and duration of the peaks. The assessment of the performances of the ANN and HN models for the Neckar River with flow data multiplied by a factor of 1.5 also yielded similar results. Hence, the application of these models for predicting extreme events can lead to a considerable uncertainty. For this reason, the range of applicability of these models should be clearly specified.

An important strength of the data driven models to be considered is that they provide fast and relatively easy means of model development for highly complex nonlinear dynamic systems. They provide flexibility that makes it possible to use for the stand alone application and in combination with the other modelling tools. The only requirement is the selection of appropriate independent and dependent variables for model development.

7.1.2 Complementary Modelling

The assessment of the hydrodynamic, hydrological and data driven models show that each of the modelling techniques has its own strengths and limitations. The differences in modelling philosophies and their inherent capabilities raise the potentials of complementary modelling instead of using them in competitive ways.

Due to the underlying limitations of each of these models, it may not be sufficient to use a single model for flood forecasting purpose. There will be a more reliable solution when the strengths of the models are combined. This fact underlines the need to set up more than one model, which is the basis of the parallel complementary approach. For instance, the hydrological and data driven models can be used to make forecasts within the calibration range, where these models offer ease of use. The HN model is the best model available for forecasting beyond the calibration, as there are uncertainties in the hydrological and data driven approaches. The use of more than one model also increases the confidence of forecasts as results can be cross validated and different scenarios can be tested.

A series approach can also be used for the complementary physically based and data driven modelling, where the results of one model may be used as input to another model. In this context, a number of approaches for combining the ANNs with the HN models are explored. First, the observation datasets are combined with the HN model results for training the ANNs. This constitutes the HN model reduction, with the encapsulation of a part of the HN model into the ANN. The ANNs are trained to forecast flows at a gauging station, where only a few discharge data are available using the upstream flows as inputs and the HN model results as targets. The trained ANNs can later be used for making forecasts at the gauging station without requiring the HN model run.

In the second approach, the ANN model is used as a pre-processor of the input data for the HN model. As the HN model requires the estimation of lateral inflows and tributaries, it is not very suitable for real time applications. In such a situation the ANN can be used as a flood routing model for the prediction of discharge hydrographs at the gauging stations. The flood peaks from the predicted hydrographs can be used as inputs to the HN models for the simulation of water levels at critical sections. In combination with a digital terrain model (DTM), this approach facilitates quick prediction of inundation extents based on the forecasted discharges at the gauging stations.

7.1.3 Uncertainty Management and Analysis

Uncertainty analysis is another area of application where the data driven models can complement the hydrodynamic models. One of the major sources of uncertainties in the river flood prediction models is due to discharges derived from the stage discharge relationship curves. A number of methods are explored for managing, analysing and propagating uncertainties. The method for the uncertainty management includes the ANN nonlinear mapping of the relationship. The ANNs are used to reproduce the looped rating curves from the Worms gauging station in the Rhine River. Similarly, the ANNs are used for mapping the highly scattered nonlinear relationship from the Lauffen gauging station in the Neckar River. Both of the applications show that the ANN based nonlinear mapping method provides a superior alternative to the single value relationship curve.

The nonlinear mapping method of the stage discharge relationship also leads to a possibility of complementary modelling. For instance, in a series complementary approach the ANN nonlinear mapping method can be used as a pre-processor and post-processor of data to a flood routing model. Accordingly, the method can be used to transform water level hydrographs into discharge hydrographs, which give the boundary conditions for the flood routing model.

In order to analyse and propagate uncertainties due to the stage discharge relationship, methods based on the fuzzy extension principle: fuzzy regression analysis and fuzzy alpha cut are used. For this purpose the stage discharge data from the Lauffen gauging station is used. The fuzzy regression analysis is used to define the upper and lower uncertainty bounds of the relationship, which produces membership functions of discharges corresponding to any measured water levels. The alpha cuts of the discharge membership function together with the HN model are used to analyse the propagation of uncertainties in water levels and inundation areas. This also constitutes a series complementary approach between the fuzzy extension principle based methods and the HN model.

Based on the results of analysis and propagation of uncertainties, it can be seen that the uncertainties in discharges can lead to significant uncertainties in water levels and inundation areas. Hence, by using method of quantification and propagation of these uncertainties it will be possible to make better flood risk management decisions.

7.2 Perspectives for Future Research

A number of potential areas of future research with regard to river flood prediction and related uncertainty analysis are identified. They are outlined below.

7.2.1 Combined Data Driven and Multidimensional Models

The research carried out in this thesis concentrated on the complementary application of data driven models and 1D HN models. There are also possibilities to use the complementary models with the two-dimensional and three-dimensional models. For example, the application of data driven models as a pre-processor to the multidimensional models can be another area of application. Such an application may include the simulation of boundary conditions of the multidimensional models using data driven models. In another complementary modelling approach the data driven models such as the ANNs can be used for model reduction of the multidimensional models. The 2D and 3D models require a lot of computing power and time for simulation and are not suitable for real time application. The data driven model can be trained to reproduce a part of the results of these models, which can be used for real time applications.

7.2.2 Integrated Data Driven and Physically Based Models

One of the limitations of the data driven models like the ANNs is their lack of relationship with physical processes. For the ANNs to gain wider acceptability it is important that they have some explanation capability after training has been completed [ASCE, 2000b]. In this regard, one potential area of application is linking the parameters of the hydrodynamic and hydrological models with the weights and biases of the neural networks. An application using the simple Muskingum method has been demonstrated in chapter 5. The next step will be to implement a similar approach in a more complex and extended application of hydrological and hydrodynamic modelling.

7.2.3 Uncertainty Analysis in River Flood Forecasting Systems

This thesis explored the methods of management and analysis of uncertainties using ANNs and fuzzy numbers. The application of probability based methods of uncertainty analysis is popular in many fields. These methods may also be employed in river flood modelling problems. In addition, some variables in river flood modelling may be better represented by a probability distribution and others may be better represented by fuzzy numbers. The application of a hybrid approach for an uncertainty analysis which combines probability based methods with fuzzy based methods [Example: Guyonnet *et al*., 2003; Maskey, 2004] can also be a potential area of application in river flood prediction.

This thesis concentrated on the methods of analysis, management and propagation of uncertainties due to the stage discharge relationship. The propagation of uncertainty has been undertaken in combination with a 1D hydrodynamic model, which can also be extended for application in combination with multidimensional models. The uncertainty due to model parameters such as the Strickler coefficient in hydrodynamic models can

also be a subject of further research, especially in the region where data for model calibration is scarce.

The uncertainty analysis methods can also be extended to the applications covering data driven models. The data driven models are also affected by both data and model uncertainties. For instance, a data driven flood routing model is affected by data uncertainties in the input and target data. In addition, model uncertainties may arise when these models are used beyond calibrated range. Therefore, uncertainty in data driven model can be a subject of further investigation.

7.2.4 Combined Flood Risk and Uncertainty Assessment

Flood risk assessment consists of components of hazard and vulnerability, both subject to uncertainties. For instance, it is a common practice to assess flood hazards in terms of associated exceedance probability of a flood event. The vulnerability assessment might involve setting tolerance levels of different land use types to parameters such as water depth and velocities. Further assessment for damages may involve making estimations of parameters such as likely flood losses. Specifying these assessment parameters, especially in relation to extreme events, may be affected by significant uncertainties. Hence, the uncertainty analysis should be considered as an integral component of flood risk assessment.

APPENDIX A

NEURAL NETWORK TRAINING ALGORITHMS

A.1 Backpropagation Algorithm

The most common type of algorithm used for training the MLPs networks is called error backpropagation algorithm. Basically, backpropagation consists of two passes; a forward pass and a backward pass through different layers of the network as shown in Figure. A.1. The forward pass is applied to transmit the function signal of the network layer by layer. The backward pass is used to transmit the error signal and the synaptic weights are adjusted based on an error correction rule. The network training procedure can be summarised in the following steps:

i. **Initialisation**: All the synaptic weights and biases are set to suitable values, usually random numbers.

ii. **Presentation of training example**: The network is presented with input and output vectors as training examples.

iii. **Forward computation**: After the application of input vectors, the functional signals of the network are computed proceeding forward through the network, layer by layer.

iv. **Backward computation**: Computation of the local gradients of the network by proceeding backwards layer by layer. The synaptic weights are also adjusted layer by layer using an error correction rule.

v. **Iteration**: The training proceeds with a new epoch of computations of steps (iii) and (iv) until the cost function is at a minimum or an acceptably minimum value.

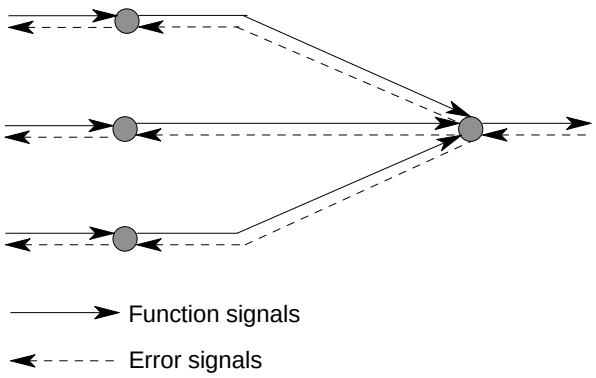

Figure A.1. Signal flows in backpropagation networks
Source: Haykin [1994]

A.1.1 Network Errors

The general approach for the backpropagation training is based on the adjustment of weights that minimise the network error. The error signal is taken at the output layer of the network, as it is the only "visible" layer for which errors can be calculated. Considering the neuron j, the instantaneous error e_j at the output of a neuron d_j with desired value y_j and at iteration n is defined as:

$$e_j(n) = d_j(n) - y_j(n) \tag{A.1}$$

The instantaneous sum of the squared errors at the output of the network is thus written as:

$$E(n) = \frac{1}{2}\sum_{j \in C} e_j^2(n) \tag{A.2}$$

where C includes all neurons at the output of the network. The average summed square error is obtained by summing $E(n)$ over the entire training set N and normalising with respect to set size n, as given by:

$$E_{av} = \frac{1}{N}\sum_{n=1}^{N} E(n) \tag{A.3}$$

The instantaneous sum of the squared errors $E(n)$ and therefore the average summed square error is the function of all free parameters (synaptic weights and biases) of the network. During the network training, E_{av} represents the cost function as the measure of training set network performance. The objective of the network training is to minimise the cost function E_{av} such that the actual response of the network approaches the target response.

The networks can be trained with two different training styles. In the incremental training, the weights of the network are updated each time an input is presented. In this case, the instantaneous sum of the squared errors $E(n)$ is used as the cost function. In batch training, weights are updated only after all the inputs are presented and the average summed square error E_{av} is used as the cost function.

A.1.2 Adjustment of Weights

The standard backpropagation error correction rule is based on the gradient descent algorithm. The simplest implementation of the gradient descent method updates the weights in the direction of negative gradient. One iteration of this algorithm can be written as:

$$w_{ji}(n+1) = w_{ji}(n) + \Delta w_{ji}(n) \tag{A.4}$$

Where $w_{ji}(n+1)$ is the vector of updated weights at iteration (*n +1*) with respect to weights $w_{ji}(n)$ and weight increment $\Delta w_{ji}(n)$, at iteration *n*, between the neurons *j* and *i.* In the batch training mode the network weight increment is defined by the delta rule:

$$\Delta w_{ji}(n) = -\eta \frac{\partial E(n)}{\partial w_{ji}(n)} \tag{A.5}$$

where η is the learning rate constant. The use of a minus sign in Equation (A.5) accounts for gradient descent in weight space. Considering a network with linear activation functions, the instantaneous error gradient term $\frac{\partial E(n)}{\partial w_{ji}(n)}$ is given by:

$$\frac{\partial E(n)}{\partial w_{ji}(n)} = \frac{\partial E(n)}{\partial u_j(n)} * \frac{\partial u_j(n)}{\partial w_{ji}(n)} \tag{A.6}$$

The output activation $u_{j(n)}$ appearing at neuron *j* is given by the sum of input signal $x_i(n)$ weighted by synaptic weights $w_{ji}(n)$:

$$u_j(n) = \sum w_{ji}(n) x_i(n) \tag{A.7}$$

Differentiating Equation (A.7), $\frac{\partial u_j(n)}{\partial w_{ji}(n)} = x_j$ for the output layer, associative derivative $\frac{\partial E(n)}{\partial u_j(n)}$ is defined as the local gradient $\delta_j(n)$. Substituting the values in Equation (A.5), the weight increment $\Delta w_{ji}(n)$ between the neurons *j* and *i* can be expressed as the product of learning rate constant η, local gradient $\delta_j(n)$ and input signal $x_i(n)$:

$$\Delta w_{ji}(n) = \eta \delta_j(n) x_i(n) \tag{A.8}$$

Hence, in case of output layer, the local gradient $\delta_j(n)$ can be expressed as:

$$\delta_j(n) = \frac{\partial E(n)}{\partial u_k} = -\{d_j(n) - y_j(n)\} \frac{\partial y_k}{\partial u_k} \tag{A.9}$$

In case of hidden layers, the local gradient $\delta_j(n)$ is given by product of the derivative $\frac{\partial y(n)}{\partial u_j(n)}$ and the weighted sum of δ's is computed for the neurons in the next hidden or output layer connected to the neuron *j*.

$$\delta_j(n) = \sum \delta_j w_j \frac{\partial y_i}{\partial u_i} \tag{A.10}$$

A.2 Faster Training

The standard backpropagation algorithm when applied to a multilayer network is often too slow for most practical applications [Hagen *et al.*, 1995]. This has to do with the performance surface (like mean square error) of the multilayer networks, which may consist of many local minimum points. Variations on the backpropagation like the Newton and Levenberg-Marquardt algorithm offer faster and efficient training methods.

A.2.1 Newton's Method

The Newton's method is based on the second order search method for a minimum. It updates the weights between iteration steps n and n+1 using the following relationship:

$$w^{(n+1)} = w^n - H^{-1}g \tag{A.11}$$

where the vector $H^{-1}g$ consists of variants of Hessian matrix H and gradient vector g, which is given by:

$$g = \frac{\partial E}{\partial w} \tag{A.12}$$

$$H = \frac{\partial^2 E}{\partial w^2} \tag{A.13}$$

The gradient and Hessian Matrix may be represented in the matrix forms as:

$$g = \begin{bmatrix} \frac{\partial E}{\partial w_1} \\ \frac{\partial E}{\partial w_2} \\ .... \\ \frac{\partial E}{\partial w_N} \end{bmatrix} \qquad H = \begin{bmatrix} \frac{\partial^2 E}{\partial w_1^2} & \frac{\partial^2 E}{\partial w_2 \partial w_1} & .... & \frac{\partial^2 E}{\partial w_N \partial w_1} \\ \frac{\partial^2 E}{\partial w_1 \partial w_2} & \frac{\partial^2 E}{\partial w_2^2} & .... & \frac{\partial^2 E}{\partial w_N \partial w_1} \\ .... & .... & .... & .... \\ \frac{\partial^2 E}{\partial w_1 \partial w_N} & \frac{\partial^2 E}{\partial w_2 \partial w_N} & .... & \frac{\partial^2 E}{\partial w_N^2} \end{bmatrix}$$

where N is the number of weights

The application of the Newton's method in training multilayer perceptron is hindered by the need to compute the Hessian matrix, which is a second order derivative. This would be computationally very demanding if done at each stage of an iteration algorithm. This would also require the Hessian matrix to be inverted at each stage, which will make computational procedure very expensive.

Alternative approaches based on modification of the Newton method have been suggested to make it a practical optimisation rule. A quasi-Newton algorithm belongs to this class of method and updates the approximate Hessian matrix at each stage of iteration. This involves generating a sequence of matrices, which represent increasingly

accurate approximation to the inverse Hessian matrix H^{-1}. The updating is based on the first order derivative of the error function.

From the Newton's method (Equation A.11), the weight vectors at iterations *n* and *n*+1 can be related by following approximate condition:

$$w^{(n+1)} \text{-} w^{(n)} - H^{-1}\left(g^{(n+1)} \text{-} g^{(n)}\right) \tag{A.14}$$

This is also known as the quasi-Newton condition function. The approximate inverse Hessian matrix is updated at each iteration n so as to satisfy the condition.

A.2.2 Levenberg-Marquardt Method

The Levenberg-Marquardt algorithm is specially designed for minimising the error function at each layer. From Equation (A.2) the sum of square error may be rewritten as

$$E(n) = \frac{1}{2}\sum_{j \in C} e_j^{\,2}(n) \tag{A.15}$$

Then, the gradient vector may be expressed as

$$g = \frac{\partial E}{\partial w} = \sum_{j \in C} \frac{\partial e_j}{\partial w} e_j = J^T e_j \tag{A.16}$$

where *J* is the Jacobian vector. The Hessian matrix can also be approximated by Jacobians as:

$$H = \frac{\partial^2 E}{\partial w^2} = J^T J \tag{A.17}$$

The Jacobian matrix *J* may be defined as differentials of the output errors with respect to network weights.

$$J = \begin{bmatrix} \frac{\partial e_{11}}{\partial w_1} & \frac{\partial e_{11}}{\partial w_2} & .... & \frac{\partial e_{11}}{\partial w_N} \\ \frac{\partial e_{21}}{\partial w_1} & \frac{\partial e_{21}}{\partial w_2} & .... & \frac{\partial e_{21}}{\partial w_N} \\ .... & .... & .... & .... \\ \frac{\partial e_{M1}}{\partial w_1} & \frac{\partial e_{M1}}{\partial w_2} & .... & \frac{\partial e_{M1}}{\partial w_N} \end{bmatrix} \qquad e = \begin{bmatrix} e_{11} \\ e_{21} \\ .... \\ e_{M1} \end{bmatrix}$$

where *N* is number of weights and *M* is number of outputs

A.3 Improving Generalisation

Normally the sum of the square errors of the training sets is chosen as the cost function given by the equations (A.1), (A.2) and (A.3). Sometimes, it is possible to improve generalisation using modified performance (cost) function. This technique is called regularisation, which encourages smoother network mapping by adding a penalty to the error function [Bishop, 1999]. A method of regularization by adding a penalty term that consists of the mean sum of squares of weights and biases from Demuth and Beale [2004]. This is given by

$$F = \gamma E_{av} + (1-\gamma) W_{av} \tag{A.18}$$

where E_{av} is the mean sum of squares of network errors, W_{av} consists of mean sum of squares of the network weights and biases and γ is the performance ratio.

The optimum value of the performance function can be determined in an automated way in the framework of Bayesian regularisation. In this framework, the weights and biases are assumed to be random variables with specified distribution. The regularisation parameters are related to the unknown distribution, which can be determined using statistical techniques. The Bayesian regularisation in combination with the Levenberg-Marquardt training has been used extensively in this work.

APPENDIX B

ERROR MEASUREMENT

Table B.1 shows the statistics of the error comparison used in this study. The error measurement process consists of analysis of errors between observed and calculated values. The overall performance of trained networks can be judged with respect to criteria such as the coefficient of determination (R^2). The R^2 is defined as the ratio of the sum of squares of the regression to the total sum of squares. The coefficient is independent of the scale of data used and useful in assessing the goodness of fit of the model. The root mean square error (RMSE) evaluates the error independent of sample size and can give useful insights to amplitude errors. Two additional criteria, the peak error (PE) and maximum error (ME) are also considered in this thesis.

Table B.1. Error measurement formula

Error measurement	Name	Formula
Coefficient of determination	R^2	$\frac{\sum_{i=1}^{n}(y_{cal}-y_{av})^2}{\sum_{i=1}^{n}(y_{obs}-y_{av})^2}$
Root mean square errors	RMSE	$\sqrt{\frac{1}{n}\sum_{i=1}^{n}(y_{obs}-y_{cal})^2}$
Peak error	PE	$y_{obs}(max)-y_{cal}(max)$
Maximum absolute error	MAE	$max\lvert y_{obs}-y_{cal}\rvert$

where n is the number of observations, y_{obs} and y_{cal} are the observed and calculated values respectively, and y_{av} is the mean of the observed values. y_{obs} (max) and y_{cal} (max) are the maximum of observed and calculated values.

REFERENCES

Abbott, M.B. [1991]. *Hydroinformatics, Information Technology and the Aquatic Enviroment*, Avebury Technical, Aldershot, UK.

Abbott, M.B. [1992]. *Computational Hydraulics, Elements of the Theory of Free Surface Flows*, Ashgate Publishing Limited, England.

Abbott, M.B., Babovic, V.M. and Cunge, J.A. [2001]. Towards the hydraulics of the hydroinformatics era, *Journal of Hydraulic Research,* 39(4), p. 339-349.

Abebe, A.J. [2004]. *Information Theory and Artificial Intelligence to Manage Uncertainty in Hydrodynamic and Hydrological Models,* Doctoral Dissertation, UNESCO-IHE Institute for Water Education, Taylor & Francis Group plc, London.

Abebe, A.J. and Price, R.K. [2000]. Application of neural networks to complement physically based hydrodynamic models, Proc*., 4th International Conference on Hydroinformatics*, Iowa City, CD-ROM.

Abebe, A.J., Guinot, V. and Solomatine, D.P. [2000]. Fuzzy alpha-cut vs. Monte Carlo techniques in assessing uncertainty in model parameters, Proc., *Hydroinformatics 2000,* CD-ROM.

APFM [2004]. *Integrated Flood Management Concept Paper*, Associated Programme on Flood Management (APFM), World Meteorological Organization & Global Water Partnership, Online documentation: http://www.apfm.info/pdf/concept_paper_e.pdf

Aronica, G., Hankin, B. and Beven, K. [1998]. Uncertainty and equifinality in calibrating distributed roughness coefficients in a flood propagation model with limited data, *Advances in Water Research*, 22(4), p 349-365.

Aronica, G., Tucciarelli, T. and Nasello, C. [1998]. 2D multilevel model for flood wave propagation in flood-affected areas, *Journal of Water Resources Planning and Management*, ASCE, 124(4), p. 210-217.

ASCE [2000a]. Artificial neural networks in hydrology I: preliminary concepts, ASCE Task Committee on Application of Artificial Neural Networks in Hydrology, *Journal of Hydrologic Engineering*, ASCE, 5 (2), p. 115-123.

ASCE [2000b]. Artificial neural networks in hydrology II: hydrologic applications, ASCE Task Committee on Application of Artificial Neural Networks in Hydrology, *Journal of Hydrologic Engineering*, ASCE, 5 (2), p. 124-137.

Babovic, V., Canizares, R., Jensen, H.R. and Klinting, A. [2000]. Neural networks as routine for error updating of numerical models, *Journal of Hydraulic Engineering*, ASCE, 127(3), p. 181-193.

Bárdossy, A. [1990]. Notes on fuzzy regression, *Fuzzy Sets and Systems*, 37, p. 65-75.

Bárdossy, A. [1996]. The use of fuzzy rules for the description of elements of the hydrological cycle, *Ecological Modelling*, 85 (1), p. 59-66.

Bárdossy, A. [2000]. Fuzzy rule based flood forecasting, Proc., *European Conference on Advances in Flood Research*, Potsdam, p. 510-519.

Bárdossy, A. and Disse, M. [1993]. Fuzzy rule based models for infiltration, *Water Resources Research,* 29(2), p 373-382.

Bárdossy, A. and Duckstein, L. [1995]. *Fuzzy Rule Based Modelling with Application to Geophysical, Biological and Engineering Systems*, CRC Press Inc., Boca Raton, Florida.

Bárdossy, A., Bogardi, I. and Duckstein, L. [1990]. Fuzzy regression in hydrology, *Water Resources Research,* 26(7), p 1497-1508.

Bárdossy, A., Bogardi, I. and Duckstein, L. [1993]. Fuzzy nonlinear regression analysis of dose-response curve, *European Journal of Operational Research*, 66, p. 36-51.

Bárdossy, A., Hölderle, M. and Markovic, D. [2004]. *Arbeitanleitung Pegel und Datendienst Baden-Württemberg - Unsicherheit von Durchflusswerten*, Institut für Wasserbau, Universität Stuttgart, Stuttgart & Landesanstalt für Umweltschutz Baden-Württemberg, Karlsruhe.

Bates, P.D. and de Roo, A.P.J. [2000]. A simple raster-based model for flood inundation simulation, *Journal of Hydrology*, 236, p. 54-77.

Bates, P.D., Anderson, M.G., Price, D.A., Hardy, R.J. and Smith, C.N. [1996]. Analysis and development of hydraulic models for floodplain flows, in *Floodplain Processes*, M.G. Anderson, D.E. Walling and P.D. Bates (eds.), John Wiley & Sons Ltd., Chichester, U. K., p 215-254.

Bazartseren, B., Hildebrandt, G. and Holz, K.-P. [2003]. Short-term water level prediction using neural networks and neuro-fuzzy approach, *Neurocomputing*, 55(3-4), p. 439-450.

Beffa, C. and Connell, R.J. [2001]. Two-dimensional flood plain flow I: model description, *Journal of Hydrologic Engineering*, ASCE, 6(5) p. 397-405.

Berz, G. [2000]. Flood disasters: lessons from the past – worries for the future*,* Proc*., Institution of Civil Engineers, Water and Maritime Engineering*, 142(1), p 3-8.

Bhattacharya, B. and Solomatine, D.P. [2000]. Application of artificial neural network in stage-discharge relationship, Proc., *4th International Conference on Hydroinformatics*, Iowa City, CD-ROM.

Bishop, C.M. [1999]. *Neural Networks for Pattern Recognition*, Oxford University Press, Oxford.

Chaves, P. and Kojiri, T. [2003]. Multi-objective storage reservoir operation under uncertainty, *Annuals of Disaster Prevention Research Institute*, Kyoto University, Kyoto, 46(b), p. 899-918.

Chow, V.T. [1959]. *Open Channel Hydraulics*, McGraw Hill Inc., Singapore.

Chow, V.T., Maidment, D.R. and Mays, L.W. [1988]. *Applied Hydrology*, McGraw Hill Inc., Singapore.

Connell, R.J., Painter, D.J. and Beffa, C. [2001]. Two-dimensional flood plain flow II: model validation, *Journal of Hydrologic Engineering*, ASCE, 6(5), p. 406-415.

Cunge, J.A. [1969]. On the subject of a flood propagation computation method (Muskingum method), *Journal of Hydraulic Research*, 7 (2), p. 205-230.

Cunge, J.A. [1998]. From hydraulics to hydroinformatics, Keynote lecture, Proc., *3rd International Conference on Hydroscience and Engineering*, Cottbus.

Cunge, J.A., Holly, F.M., and Verway, A. [1980]. *Practical Aspects of Computational River Hydraulics*, Pitman, London.

Dawson, C.W., Harpham C., Wilby, R.B. and Chen, Y. [2002]. Evaluation of artificial neural network techniques for flow forecasting in River Yangtze, China, *Hydrology and Earth System Sciences*, 6(4), p. 619-626.

De Roo, A.P.J., Bartholmes, J., Bongioannini-Cerlini, P., Todini, E., Bates, P.D., Horrit, M., Hunter, N., Beven, K., Pappenberger, F., Heise, E., Rivin, G., Hils, M., Hollingsworth, A., Holst, B., Kwadijk, J., Reggiani, P., Van Dijk, M., Sattler, K. and Sprokkereef, E. [2003]. Development of a European flood forecasting system, *International Journal of River Basin Management*, 1(1), p. 49-59.

Demuth, H. and Beale, M. [2004]. *Neural Network Toolbox User's Guide*, The MathWorks Inc., Online documentation: http://www.mathworks.com/access/helpdesk/help/toolbox/nnet/

Dhondia, F. and Stelling, G.S. [2002]. Application of one dimensional - two dimensional integrated hydraulic model for flood simulation and damage assessment, Proc., *Hydroinformatics 2002*, Cardiff, p 265-276.

Dibike, Y.B. [2002]. *Model Induction from Data: Towards the Next Generation of Computational Engines in Hydraulics and Hydrology,* Doctoral Dissertation, UNESCO-IHE Institute for Water Education, Swets and Zeitlinger B.V., Lisse, The Netherlands

Dibike, Y.B. and Abbott, M.B. [1999]. Application of artificial neural networks to the simulation of a two dimensional flow, *Journal of Hydraulic Research*, 37(4), p. 435-446.

Dibike, Y.B., Solomatine, D. and Abbott, M.B. [1999]. On the encapsulation of numerical-hydraulic models in artificial neural network, *Journal of Hydraulic Research*, 37(2), p. 147-161.

Dubois, D. and Prade, H. [1980]. *Fuzzy Sets and Systems: Theory and Applications*, Mathematics in Science and Engineering, 144, Academic Press Inc, New York.

Fread, D.L. [1992]. Flood routing, in *Handbook of Hydrology*, D. Maidment (ed.), McGraw-Hill, New York, p. 10.1-10.36.

Fread, D.L. and Lewis, J.M. [1993]. Selection of Δx and Δt computational steps for four-point implicit finite non-linear dynamic routing models, Proc*., National Hydraulic Engineering Conference,* ASCE*,* San Francisco.

Fread, D.L and Lewis, J.M. [1998]. *NWS FLDWAV Model*, Hydrologic Research Laboratory, Office of Hydrology, National Weather Service (NWS), Maryland.

Gautam, D.K. [2000]. *Neural Network and Fuzzy Logic Based System Identification in Hydroinformatics*, Doctoral Dissertation, Brandenburg Technical University at Cottbus, Cottbus.

Gendreau, N. and Gillard, O. [1998] Structural and non-structural implementations – Choice's arguments provided by inondabilité method, Proc., First Workshop, *Ribamod River Basin Modelling, Management and Flood Mitigation Concerted, Action*, R. Casale, G.B. Pedroli and P. Samuels (eds.), European Commission, Brussels, p. 241-250.

Gilard, O. [1996]. Flood risk management: risk cartography for objective negotiations, Proc*., 3rd IHP/IAHS George Kovacs colloquium*, UNESCO, Paris.

Gupta, H.V., Hsu, K. and Sorooshian, S. [2000]. Effective and efficient modelling for streamflow forecasting, In: *Artificial neural networks in hydrology*, R. S. Govindaraju and A. Ramachandra Rao (eds.), Kluwer Academic Publishers, Dordrecht, The Netherlands, p. 7-22.

Guyonnet, D., Bourgine, B., Dubois, D., Fargier, H., Côme, B. and Chilès, J.-P. [2003]. Hybrid approach for addressing uncertainty in risk assessments, *Journal of Environmental Engineering*, ASCE, 129(1), p. 68-78.

Haykin, S. [1994]. *Neural Networks a Comprehensive Foundation*, 1st Edition, Macmillan College Publishing Company, Inc., New York.

Henderson, F.M. [1966]. *Open Channel Flow*, The Macmillan Company, New York.

Horritt, M.S. and Bates, P.D. [2002]. Evaluation of 1D and 2D numerical models for predicting river flood inundation, *Journal of Hydrology*, 268, p. 87-99.

Imrie, C.E., Durucan, S. and Korre, A. [2000]. River flow prediction using artificial neural network: generalisation beyond calibration range, *Journal of Hydrology*, 233, p. 138-153.

ISDR [2004]. *Guidelines for Reducing Flood Losses*, A contribution to International Strategy for Disaster Reduction (ISDR), United Nations, Online documentation: http://www.unisdr.org

Jain, S.K. and Chalisgaonkar, D. [2000]. Setting up stage-discharge relations using ANN, *Journal of Hydrologic Engineering*, ASCE, 5(4), p. 428-433.

Jang, J.-S.R. [1993]. ANFIS: Adaptive network based fuzzy inference system, *IEEE Transactions on Systems, Man and Cybernetics*, 23(3), p. 665-685.

Jang, J.-S.R. and Sun C.-T. [1995]. Neuro-fuzzy modeling and control, *The Proceedings of the IEEE*, 83(3), p 378-406.

Kohonen, T. [1995]. *Self-Organizing Maps*, Springer, Berlin.

Lee, Y.W., Chung, S.Y., Bogardi, I., Dahab, M.F., and Oh, S.E. [2001]. Dose-response assessment by a fuzzy linear-regression method, *Water Science and Technology*, 43(2), p. 133–140.

Lekkas, D.F., Imrie, C.E. and Lees, M.J. [2001]. Improved nonlinear transfer function and neural network methods for flow routing for real-time flood forecasting, *Journal of Hydroinformatics*, 3, p. 153-164.

LFU [2000]. *Deutsches Gewässerkundliches Jahrbuch*, Rheingebiet, Teil 1, Landesanstalt für Umweltschutz (LFU), Baden-Württemberg, Karlsruhe.

Liong, S.-Y., Lim, W.-H., and Paudyal, G. [2000]. River stage forecasting in Bangladesh: neural network approach, *Journal of Computing in Civil Engineering*, ASCE, 4(1), p. 1-8.

Maskey, S. [2001]. Uncertainty analysis in flood forecasting and warning system using expert judgement and fuzzy set theory, *Safety & Reliability*, Zio, E., Demichela, M. and Piccinini, N. (eds.), p. 1787-1794.

Maskey, S. [2004]. *Modelling Uncertainty in Flood Forecasting Systems,* Doctoral Dissertation, UNESCO-IHE Institute for Water Education, Taylor & Francis Group plc, London.

McCulloch, W.S. and Pitts, W. [1943]. A logical calculus of the ideas immanent in nervous activity, *Bulletin of Mathematical Biophysics*, 5, 115-137, Reprinted in: *The Philosophy of Artificial Intelligence*, M. A. Boden (ed.), Oxford University Press, Oxford, 1990.

Minh Thu, P.T. [2002]. *A Hydrodynamic-Numeric Model of the Rhine River*, Dissertation, Institut für Wasserwirtschaft und Kulturtechnik, Universität Karlsruhe, Karlsruhe.

Minns, A.W. [1996]. *Extended rainfall-runoff modelling using artificial neural networks*, Proc., Hydroinformatics '96, A. Müller (ed.), Balkema, Rotterdam, 207-213.

Mishra, S.K. and Singh, V.P. [2002]. Role of dimensionless numbers in wave analysis, *Hydrological Processes*, 17(3), p. 651- 669.

Nestmann, F. [1998]. Hydraulics basics, Proc., *Coordinated Operation of a Cascade Hydropower Plants*, International Hydropower Association & Institute of Water Resources Management, Hydraulic and Rural Engineering, University of Karlsruhe, Karlsruhe.

Nestmann, F. and Emmermann, R. [2003]. Technologies for the operational flood protection, Proc., *acqua alta München 2003*, Int. Kongress für Hochwasserschutz und Katastrophenmanagement, Klima und Flussbau, p. 99-101.

Oberle, P. [2004]. *Integrales Hochwassersimulationssystem Neckar, Verfahren – Werkzeuge - Anwendungen*, Dissertation, Institut für Wasserwirtschaft und Kulturtechnik, Universität Karlsruhe, Karlsruhe.

Oberle, P. and Theobald, S. [2000]. *Hydrodynamisch-numerisches Flussmodel Neckar. Bericht zum Instationären Gesamtmodell der Staustufenkette*, Abschlussbericht in Auftrag des Landes Baden Württemberg.

Oberle, P., Theobald, S. Evdakov. O. and Nestmann, F. [2002]. GIS-supported flood modelling, by the example of River Neckar, Proc*., International Symposium on Flood Defence*, University of Kassel, Kassel.

Özelkan, E.C. and Duckstein, L. [2000]. Multiobjective fuzzy regression: a general framework, *Computer and Operations Research*, 27, p. 635-652.

Plate, E.J. [1998]. Probabilistic design of flood protection structures, Proc., First Workshop, *Ribamod River Basin Modelling, Management and Flood Mitigation Concerted, Action*, R. Casale, G.B. Pedroli and P. Samuels (eds.), European Commission, Brussels, p. 43-56.

Ponce, V.M. [1994]. *Engineering Hydrology, Principles and Practice*, Prentice Hall, New Jersey.

Price, R.K. [1985]. Flood routing, in *Developments in Hydraulic Engineering,* P. Novak (ed.), Elsevier Applied Science Publishers, London, p. 129-174.

Samuels, P.G., Bramley, M.E., and Evans, E.P. [2002]. Reducing uncertainty in conveyance estimation, Proc., *River Flow 2002 - International Conference on Fluvial Hydraulics*, D. Bousmar and Y. Zech, (eds.) Swets & Zeitlinger, Lisse, The Netherlands, CD-ROM.

Schalkoff, R.J. [1997]. *Artificial Neural Networks*, McGraw – Hill Companies Inc., New York,

Schmidt, A.R. [2002]. *Analysis of Stage-Discharge Relations for Open-Channel Flows and Their Associated Uncertainties*, Ph. D. Thesis, Department of Civil and Environmental Engineering, University of Illinois at Urbana-Champaign.

Schmidt, A.R. [2004]. Application of point-estimation method to calculate uncertainties in discharges from stage-discharge ratings, Proc., *EWRI World Water and Environmental Resources Congress*, G. Sehlke, D. F. Hayes, and D.K. Stevens (eds.), Salt Lake City, CD-ROM.

Schulz, K. and Huwe, B. [1999]. Uncertainty and sensitivity analysis of water transport modeling in a layered soil profile using fuzzy set theory, *Journal of Hydroinformatics*, 1(2), p. 127-138.

Shamseldin, A.Y., Nasr, A.E. and O'Connor, K.M. [2002]. Comparison of different forms of the multi-layer feed-forward neural network method used for river flow forecasting, *Hydrology and Earth System Sciences*, 6(4), p 671–684.

Shrestha, R.R. [2000]. *Application of Geographic Information System and Numerical Modelling Tools for Floodplain Analysis and Flood Risk Assessment of Babai River in Nepal*, M. Sc. thesis (unpublished), Resources Engineering, University of Karlsruhe, Karlsruhe.

Shrestha, R.R. [2003]. Flood routing using artificial neural networks, Proc., *XXX IAHR Congress*, Thessaloniki, CD-ROM.

Shrestha, R.R., Theobald, S., and. Nestmann, F. [2002]. Flood risk modelling of Babai River in Nepal, Proc., *International Conference on Flood Estimation*, M. Spreafico and W. Weingartner (eds.), CHR Report II-17, Berne, p. 679-686.

Shrestha, R. R., Theobald, S., and. Nestmann, F. [2004]. Combined hydrodynamic–neural network model for flood flow simulation, Proc., *Sixth International Conference of Hydroinformatics*, Singapore, Liong, Phoon and Babovic (eds.), World Scientific Publishing Company, CD-ROM.

Shrestha, R.R., Theobald, S. and Nestmann, F. [2005]. Simulation of flood flow in a river system using artificial neural networks, *Hydrology and Earth System Sciences*, Special Issue on Advances in Flood Forecasting in Europe (In press).

Simonovic, S.P. [1998]. *Decision Support System for Flood Management in the Red River Basin*, International Joint Commission Red River Task Force, Slobodan P. Simonovic Consulting Engineers Ltd., Winnipeg, Canada.

Sivakumar, B., Jayawardena, A.W. and Fernando, T.M.K.G. [2002]. River flow forecasting: use of phase-space reconstruction and artificial neural networks approaches, *Journal of Hydrology*, 265, p. 225-245.

Smith, K. and Ward, R. [1998]. *Floods: Physical Processes and Human Impacts*, John Wiley and Sons, Chichester, England.

SOGREAH [1978]. *Modelling Unsteady Flow in River and Flood Plains Networks Using the CARIMA System*, SOGREAH, Grenoble.

Solas, J.D., Markus, M. and Tokar, A.S. [2000]. Streamflow forecasting based on artificial neural networks, In: *Artificial neural networks in hydrology*, R. S. Govindaraju and A. Ramachandra Rao (eds.), Kluwer Academic Publishers, Dordrecht, The Netherlands, p. 23-52.

Stüber, M., Gemmar, P. and Greving, M. [2000]. Machine supported development of fuzzy – flood forecast systems, Proc., *European Conference on Advances in Flood Research*, Potsdam, p. 520-531.

Sudheer, K.P. and Jain, S.K. [2003]. Radial basis function neural network for modeling rating curves, *Journal of Hydrologic Engineering*, ASCE, 8(3), p. 161-164.

Tate, E.C., Maidment, D.R., Olivera, F., and Anderson, D.J. [2002]. Creating a terrain model for floodplain mapping, *Journal of Hydrologic Engineering*, ASCE, 7(2), p. 100-108.

Tawfik, M., Ibrahim, A. and Fahmy, H. [1997]. Hysteresis sensitive neural network for modeling rating curves. *Journal of Computing in Civil Engineering*, ASCE, 11(3), p. 206–211.

The MathWorks Inc. [2004a]. *Fuzzy Logic Toolbox for Use with MATLAB*, The Mathworks Inc., Online documentation: http://www.mathworks.com/access/helpdesk/help/toolbox/fuzzy/

The MathWorks Inc. [2004b]. *Optimization Toolbox for use with MATLAB*, The Mathworks Inc., Online documentation: http://www.mathworks.com/access/helpdesk/help/toolbox/optim

Theobald, S. [1999]. *Numerische Simulation von Staustufenketten mit automatisiertem Betrieb*, Dissertation, Institut für Wasserwirtschaft und Kulturtechnik, Universität Karlsruhe, Karlsruhe.

Thirumalaiah, K. and Deo, M.C. [1998]. River stage forecasting using artificial neural networks, *Journal of Hydrological Engineering,* ASCE, 3 (1), p. 26-31.

Tsoukalas, L.H. and Uhrig, R.E. [1997]. *Fuzzy and Neural Approaches in Engineering*, John Wiley and Sons, Inc., New York.

Tucciarelli, T. and Termini, D. [2000]. Finite-element modelling of floodplain flow, *Journal of Hydraulic Engineering*, ASCE, 126(6) p. 416-424.

USACE [1993]. *Engineering and Design, River Hydraulics,* Engineer Manual 1110-2-1416, US Army Corps of Engineers (USACE), Washington DC.

USACE [1994]. *Engineering and Design, Flood-Runoff Analysis,* Engineer Manual 1110-2-1417, US Army Corps of Engineers (USACE), Washington DC.

USACE [1997]. *One Dimensional Unsteady Flow Through Open Channels,* UNET User's Manual, US Army Corps of Engineers (USACE), Hydrological Engineering Center, Davis, California.

USACE [2002]. *HEC-GeoRAS An Extension for Support of HEC-RAS Using ArcView,* User's Manual, US Army Corps of Engineers (USACE), Hydrological Engineering Center, Davis, California.

Van den Boogaard, H.F.P. and Kruisbrink, A.C.H. [1996]. Hybrid modelling by integrating neural networks and numerical models, Proc., *Hydroinformatics 96*, A. Müller (ed.), Balkema Rotterdam, p 471-477,

White, W.R. [2000]. *Water in Rivers: Flooding,* A contribution to the World Water Vision, International Association of Hydraulic Engineering and Research (IAHR) & Wallingford, UK, Online documentation: http://www.worldwatercouncil.org/Vision/Documents/RodneyWhitePaper.PDF

Willems, P., Vaes, G., Popa, D., Timbe, L. and Berlamont, J. [2002]. Quasi 2D river flood modelling, Proc., *River Flow 2002*, D. Bousmar and Y. Zech (eds.), Swets & Zeitlinger, Lisse, The Netherlands, CD-ROM.

Wolkenhauer, O. [2001]. *Data Engineering, Fuzzy Mathematics in Systems Theory and Data Analysis*, John Wiley and Sons, Inc., New York.

Wright, N. and Dastorani, M. [2003]. Combined hydrodynamic/neural network modelling of river flow, Proc., *XXX IAHR Congress*, Thessoloniki, CD-ROM.

Yang, T.-C., Yu, P.-S,. Kuo, C.-M., and Wang, Y.-C. [2004]. Application of fuzzy multiobjective function on storm-event rainfall-runoff model calibration, *Journal of Hydrologic Engineering*, ASCE, 9(5), p. 440-445.

Zadeh, L.A. [1965]. Fuzzy sets, *Information and Control*, Vol. 8, p 338-353. Reprinted in: *Fuzzy sets and applications*: selected papers by L.A. Zadeh, R.R. Yager, S Ovchinnikov, R.M. Tong, H.T. Nguyen (eds.) John Wiley and Sons, Inc., New York, 1987.

LIST OF SYMBOLS

Hydrodynamic and Hydrological Models

Symbol	Meaning	Unit
A	Active cross sectional area of flow	[m^2]
A	Rating curve parameter	
B	Top width of flow	[m]
c	Wave celerity	[m/s]
C	Chezy coefficient	[$m^{1/2}$/s]
C	Routing coefficient	
D	Hydraulic depth	[m]
D	Cell Reynolds number	
Fr	Froude Number	
f	Function variable	
g	Gravitational acceleration	[m/s^2]
h	Depth of flow /water level	[m]
j	Space index	
K	Conveyance of the channel section	[m^3/s]
K	Storage time coefficient	[s]
k_{st}	Strickler coefficient	[$m^{1/3}$/s]
L	Characteristics length	[m]
n	Manning resistance coefficient	[$s/m^{1/3}$]
n	Time index	
N	Grid point	
Q	Discharge	[m^3/s]
R	Hydraulic radius	[m]
Re	Reynolds number	
S	Storage in the routing reach	[m^2]
S_0	Bed slope	
S_f	Friction slope	
t	Time coordinate	[s]
T_r	Minimum time of rise of hydrograph of upstream hydrograph	[s]
v	Mean flow velocity in the channel	[m/s]
X	Dimensionless weighing factor, ($0 \le X \le 0.5$)	
x	Space coordinate	[m]
y	Water surface elevation	[m]
Δt	Time increment	[s]
Δx	Space increment	[m]
θ	Time weighing factor	
ψ	Space weighing factor	
ν	Kinematic viscosity	[m^2/s]

Artificial Neural Networks

Symbol	Meaning
d	Output of a neuron
e	Instantaneous error
$E(n)$	Instantaneous sum of the squared errors
E_{av}	Average summed square error
g	Gradient vector
H	Hessian matrix
j	Neuron index
J	Jacobian vector
k	Modifying factor
u	Output from summing junction
w	Neuron weight
x	Neuron input
y	Neuron output
Z	Delay
z	Desired output
α	Weighing factor
Δw	Weight increment
σ	Parameter to control the spread of output
v	Neuron activation
γ	Performance ratio

Fuzzy Systems

Symbol	Meaning
A	Fuzzy subset
a	Membership function parameter
a_k	Crisp input
b	Membership function parameter
B	Fuzzy subset
c	Membership function parameter
d	Membership function parameter
H	Credibility level
L	Left reference
m	Central value
p	Consequent parameter
R	Right reference
X	Universe set
x	Element of a set
Y	Universe set
y	Element of a set
α	Alpha level of a membership function
α	Left spread
β	Right spread
σ	Spread
μ	Membership function
ν	Degree of fulfilment
$\square$	AND or OR or XOR operator

LIST OF ACRONYMS

1D	One-dimensional
2D	Two-dimensional
3D	Three-dimensional
ANFIS	Adaptive network based fuzzy inference system
ANN	Artificial neural network
APFM	Associated Programme on Flood Management
ARXFIS	Autoregressive exogenous input fuzzy inference system
ASCE	American Society of Civil Engineers
CE	Coefficient of efficiency
CFL	Courant-Friedrichs-Lewy number
DOF	Degree of fulfilment
DTM	Digital terrain model
FRBM	Fuzzy rule-based model
GIS	Geographic information system
HEC	Hydraulic Engineering Center
HN	Hydrodynamic numerical
IAHR	International Association of Hydraulic Engineering and Research
ISDR	International Strategy for Disaster Reduction
IKoNE	*Integrierende Konzeption Neckar Einzugsgebiet* Integrated Conception Neckar Catchment
IWK	*Institut für Wasserwirtschaft und Kulturtechnik* Institute for Water Resources Management, Hydraulic and Rural Engineering
LiDAR	Laser induced Detection and Ranging
LN	Linear network
MAE	Maximum absolute error
MC	Muskingum Cunge
MLP	Multilayer perceptron
NLN	Nonlinear network
PE	Peak error
R^2	Coefficient of determination
RBFN	Radial basis function network
RMSE	Root mean square error
TDL	Tapped delay line
TIN	Triangulated irregular network
USACE	US Army Corps of Engineers

LIST OF TABLES

LIST OF FIGURES

LEBENSLAUF

Name	Rajesh Raj Shrestha
Geburtsdatum	10.09.1971
Geburtsort	Kathmandu, Nepal
Nationalität	nepalesisch
Familienstand	verheiratet

Ausbildung

03.1977-06.1987	Grund- und Hauptschule an der Siddhartha Vanasthali Madhyamic Vidyalaya, Kathmandu, Nepal
06.1987	Abschluss: **School Leaving Certificate**
10.1987-03.1990	Abitur an der Amrit Science Campus, Tribhuvan University, Kathmandu, Nepal
03.1990	Abschluss: **Proficiency Certificate in Science**
03.1991-07.1995	Bauingenieurwesen Studium am Institute of Engineering, Tribhuvan University, Lalitpur, Nepal
07.1995	Abschluss: **B. E. (Civil Engineering)**
10.1998-09.2000	Aufbaustudium an der Universität Karlsruhe (TH)
09.2000	Abschluss: **M. Sc. (Resources Engineering)**
11.2000-01.2005	Doktorand am Institut für Wasserwirtschaft und Kulturtechnik, Fakultät für Bauingenieur-, Geo- und Umweltwissenschaften, Universität Karlsruhe (TH)

Berufstätigkeit

08.1995–02.1996	Bauingenieur an der Research & Study Centre, Kathmandu, Nepal
02.1996-07.1998	Wasserbauingenieur am Department of Irrigation, Ministry of Water Resources, Lalitpur, Nepal
11.2000-01-2005	Wissenschaftlicher Stipendiat am Institut für Wasserwirtschaft und Kulturtechnik, Fakultät für Bauingenieur-, Geo- und Umweltwissenschaften, Universität Karlsruhe (TH)
Seit 02.2005	Wissenschaftlicher Mitarbeiter am Department Hydrologische Modellierung, Umweltforschungszentrum Leipzig-Halle GmbH, Magdeburg

Bisher erschienene Mitteilungen aus dem
Institut für Wasser und Gewässerentwicklung
-Bereich Wasserwirtschaft und Kulturtechnik-

Bisher erschienene Mitteilungen aus dem Institut für Wasser und Gewässerentwicklung, Bereich Wasserwirtschaft und Kulturtechnik

Heft 154/1968

Ein Beitrag zur Erforschung von örtlichen Auskolkungen hinter geneigten Befestigungsstrecken in Abhängigkeit der Zeit; E. Mosonyi, B.Schoppmann
Institutsberichte über die Modellversuche seit 1962
Institutsberichte über die Exkursionen des Lehrstuhls für Wasserbau und Wasserwirtschaft seit 1965; E. Mosonyi, B. Schoppmann

Heft 155/1969

Kolkbildung in feinen oder leichten Sohlmaterialien bei strömendem Abfluß; J.W. Dietz

Heft 156/1969

Widerstandskräfte und Energiedissipation bei Verteilerklötzen im Wechselsprung; R. Muser
Schwebstofführung feinsandiger Wasserläufe; St. Bruk

Heft 157/1969 °

Widerstand schräg angeströmter Rechengitter; J. Zimmermann
Untersuchungen zur Durchströmung des Kraghammer Sattels an der Biggetalsperre nach neuentwickelten Methoden der Felshydraulik; W.Wittke, Cl. Louis

Heft 158/1970 °

Hydrodynamik der nichtstationären Dränung; G. Karadi, J. Gyuk, R.A.Williams
An Experimental Study of Thin-Sheet Flow over Inclined Surfaces; O.N Wakhlu
Schiffsträgheitskräfte als Indikator für die Güte von Schleusenfüllsystemen; E. Mosonyi, R. Muser
Schwall- und Sunkerscheinungen aus Schleusenbetrieb in Schiffahrtskanälen; Maßnahmen zur Sicherung des Schiffahrtsbetriebes; R. Muser, G. Meder
Beitrag zur Berechnung von Schleusenfüllungen; H.H. Bernhart
Spitzenmaßstab und L-O-Integrator, ein Gerät zur genauen Messung des Wasserspiegels in Modellversuchen; W. Götz, K. Schwedes
Turbulenzmessungen in Wasser mit Heißfilmanemometer; B. Schoppmann
Messung von Größe und Richtung der mittleren Geschwindigkeit in einem zweidimensionalen Strömungsfeld; K. Schwedes
Parameterfreie statistische Methoden zur Analyse von Datenreihen; H. Eggers
Dreidimensionale, anisotrope Kluftwasserströmung; W. Wittke

Heft 159/1972 °

Ein Verfahren zur Richtungs- und Betragsbestimmung von Vektoren mittlerer Strömungsgeschwindigkeit einer turbulenten Strömung; K.Schwedes, H. Weiher
Hydraulische Stabilität bei Wasserkraftanlagen; H. Berge
Land Reclamation Projects as Essential Elements of Economic Development Programmes; G.E. Papadopoulos
Institutsberichte über Modellversuche u. Forschungsarbeiten seit 1969
Institutsberichte über die Exkursionen des Lehrstuhls für Wasserbau und Wasserwirtschaft seit 1969

Heft 160/1973	*Das Widerstands-Kapazitätsnetzwerk zur Simulation instationärer Grundwasserströmungen; A. Widmer* *Der elektrolytische Trog zur Lösung stationärer dreidimensionaler Grundwasserströmungsfälle; U. Stentzel, K. Schwedes* *Standfiltermodelle mit und ohne Überströmung zur Untersuchung von Selbstdichtungsmechanismen an Gewässersohlen; S.G. van Riesen* *Anhang: Veröffentlichungen, Vorträge, Dissertationen der Abteilung für Kulturtechnische Untersuchungen (Lehrgebiet Landwirtschaftlicher Wasserbau) auf dem Gebiet der Grundwasserforschung*
Heft 161/1974	*Strömungs- und Transportmechanismen einer fortschreitenden Auskolkung; B. Schoppmann* *Water Resources Development in the U.A.R.; F. Nicola*
Heft 162/1974 °	*Dünnschichtabfluß auf stark geneigter Ebene; G. Karantounias* *Die Entwicklung der Sparschleusen des Main-Donau-Verbindungskanals mit besonderer Betrachtung der Sparschleuse Leerstetten; R.Muser* *Neuere Methoden für die Analyse hydrologischer Systeme; G.M. Karadi* *Die Impedenz eines axial oszillierenden Sphäroids in einem nicht zusammendrückbaren Medium; R.Y.S. Lai, G.M. Karadi*
Heft 163/1975 °	*Sekundärströmungen in aufeinanderfolgenden Gerinnekrümmungen; W.Götz* *Darstellung von skalaren Zustandsfeldern in beliebigen Kontrollräumen und ihre Nutzungsanwendung in der Hydrostatik mit Hilfe eines neuen Verfahrens der Vektoranalysis; M. Spielbauer* *Die Berechnung der Hochwasserwahrscheinlichkeit für deutsche Flußgebiete; D. Koberg, H. Eggers, W. Buck* *Drei Jahrzehnte operationelle Hydrologie; E. Walser*
Heft 164/1976	*Einfluß der Schließzeit auf die Druckstoßtransmission durch Wasserschlösser; H.H. Bernhart* *Verstärkung und Erhöhung von Betonstaumauern; E. Vallarino*
Heft 165/1976	*Die Auswahl des Bemessungshochwassers als ein Entscheidungsproblem unter Risiko und Ungewißheit; W. Buck*
Heft 166/1977	*Einfluß von Sickerströmungen auf den Geschiebetransport; K.E. Wedemann*
Heft 167/1979	*Der Einfluß seltener Ereignisse bei der Bestimmung der Hochwasserwahrscheinlichkeit; H. Eggers* *Statistisch erzeugte Serien von Hochwasserwellen; S. Weingärtner*
Heft 168/1982	*Strömungscharakteristiken in einem Kanal mit 180°-Krümmungen; W. Siebert* *Bestimmung des Bemessungshochwassers mit Hilfe der Clusteranalyse; W. Kiefer*

Heft 169/1982	*Entwurfskriterien zur Schleusenplanung; H.H. Bernhart*
Heft 170/1984	*Druckerhöhungenh durch instationäre Vorgänge in Schiffsschleusen mit großen Stufenhöhen; P.M. Schmelzle*
Heft 171/1984	*Beitrag zur Hydromechanik von Schwall- und Sunkwellen; N. Göbel*
Heft 172/1985	*Abschiedskolloquium zu Ehren von Herrn Prof. Dr.-Ing. Dr.rer.techn., Dr.sc.h.c., Dr.-Ing. E.h., Dr.sc.h.c., Dr.sc.h.c. E. Mosonyi*
Heft 173/1986 °	*Vor- und Nachteile des naturnahen Gewässerlaufes im Vergleich zu kanalisierten Fließgewässern; H. Willy*
Heft 174/1986	*Naturnahe Umgestaltung ausgebauter Fließgewässer. Beiträge zum Wasserbaulichen Kolloquium am 14.02.1986 in Karlsruhe*
Heft 175/1986 °	*Naturnahe Umgestaltung ausgebauter Fließgewässer Projektstudie; K. Kern, I. Nadolny*
Heft 176/1987 °	*Der Einfluß von Querströmungen auf ein Schiff bei beschränkten Fahrwassertiefen; F. Bakowies*
Heft 177/1988	*Zur Bemessung von Geschiebeabzügen; G.M. Kley*
Heft 178/1988	*Hydraulik der kontinuierlichen und intermittierenden Furchenbewässerung: ein hydrodynamisches Modell; M. Awwad*
Heft 179/1990	*Sturzwasserbewässerung. Bewässerung mit Niederschlagswasser ohne Zwischenspeicherung im Sahel; W. Klemm*
Heft 180/1991	*Beiträge zur naturnahen Umgestaltung von Fließgewässern*
Heft 181/1991 °	*Naturgemäße Bauweisen von Sohlenbauwerken und Fischaufstiegen zur Vernetzung der Fließgewässer; R.-J. Gebler*
Heft 182/1991	*Untersuchungen zum Stabilitätsverhalten von Gerinnesohlen; A.Dittrich, M. Rosport, O. Badde*
Heft 183/1993	*Der Einfluß der Belüftung auf die Kavitationserosion; N. Eisenhauer*
Heft 184/1993	*nur als Buch erhältlich bei Springer Verlag: Grundlagen naturnaher Gewässergestaltung. Geomorphol. Entwicklung von Fließgewässern; K. Kern*
Heft 185/1993	*Ausbauoptimierung dezentraler Wasserkraftsysteme; H. Hildebrand*
Heft 186/1994	*Turbulente, abgelöste Zweischichtenströmung über Sohlschwellen in einem offenen Rechteckgerinne; U. Kertzscher*
Heft 187/1994	*Untersuchung des Niederschlags- und Abflußgeschehens im westafrikanischen Sahel. Abschätzung des Wasserdargebots aus kleinen*

	Einzugsgebieten mittels stochastischer Methoden unter Verwendung von Satellitenbilddaten; W. Tauer
Heft 188/1994	*Bedarfsprognosen als Basis der Steuerungsoptimierung von Wasserversorgungssystemen; S. Ates*
Heft 189/1994	*Morphologie und Hydrologie naturnaher Flachlandbäche unter gewässertypologischen Gesichtspunkten - Gewässermorphologische und hydrologische Grundlagen für naturgemäßen Wasserbau und ökologische Gewässerentwicklung; I. Nadolny*
Heft 190/1994	*Ein Erosionsmodell mit räumlich und zeitlich veränderlicher Rillenmorphologie; M. Schramm*
Heft 191/1995	*Oberflächenabfluß und Bodenerosion in Kleineinzugsgebieten mit Mergelböden unter einem semiariden mediterranen Klima; D. Gomer*
Heft 192/1995	*Typologische und morphologische Untersuchungen an Bergbächen im Buntsandstein-Odenwald; G. Humborg*
Heft 193/1997	*Die Oberrheinkorrektion in Baden - Zur Umweltgeschichte des 19. Jahrhunderts; T. Löbert*
Heft 194/1997	*Erosionsprozesse auf Lößböden: Experimente und Modellierung; K.Gerlinger*
Heft 195/1997	*Synthese von biologischer und wasserbaulicher Analyse zur Bewertung von renaturierten Fließgewässern der Oberrheinebene; S. Kiene*
Heft 196/1997	*Fließwiderstand und Sohlstabilität steiler Fließgewässer unter Berücksichtigung gebirgsbachtypischer Sohlstrukturen; M. Rosport*
Heft 197/1997	*Ein Finite-Punkte-Verfahren für stationäre zweidimensionale Strömungen mit freier Oberfläche; C.J. Du*
Heft 198/1998	*Wechselwirkung Morphologie/Strömung naturnaher Fliessgewässer; A.Dittrich*
Heft 199/1999	*Entwicklung naturnaher Gewässerstrukturen - Grundlagen, Leitbilder, Planung; J. Scherle*
Heft 200/1999	*Zwei-Schichtenströmungen über Sohlenschwellen bei intern überkritischer Strömung; Y. Wang* *Hydraulic Design Considerations for Low- and High-Head Gates; E.Naudascher*
Heft 201/1999	*Numerische Simulation von Staustufenketten mit automatisiertem Betrieb; S. Theobald*
Heft 202/1999	*Der Einfluß von kurzen Gehölzstreifen auf den Hochwasserabfluß in Flüssen mit gegliedertem Querschnitt; K. Becker*

Heft 203/1999 *Typisierungskonzept zur Festlegung einer ökologisch begründeten Mindestwasser menge; M. Scherer*

Heft 204/1999 *Inseln und deren Widerstandsverhalten in Fließgewässern; A. Maryono*

Heft 205/1999 *Boden- und Wasserschutz in landwirtschaftlich genutzten Gebieten der Mata Atlântica Brasiliens; M. Kunzmann*

Heft 206/2000 *Nutzung von Landsat Thematic Mapper Daten zur Ermittlung hydrologischer Parameter; S. Belz (auch elektronisch unter:* http://www.ubka.uni-karlsruhe.de/eva/index.html)

Heft 207/2000 *Untersuchung der Rauheitsstruktur zur Bestimmung des Fließwiderstandes in Gebirgsbächen unter Klarwasserabfluß; J. Aberle (auch elektronisch unter:* http://www.ubka.uni-karlsruhe.de/eva/index.html)

Heft 208/2000° *Three Dimensional Computation of Turbulent Flow in Meandering Channels; V. T. Nguyen*

Heft 209/2001 *Sedimenttransportprozesse im Himalaya-Karakorum und ihre Bedeutung für Wasserkraftanlagen; S. Palt (auch elektronisch unter:* http://www.ubka.uni-karlsruhe.de/eva/index.html)

Heft 210/2002 *Die Identifikation hydrologischer Prozesse im Einzugsgebiet des Dürreychbaches (Nordschwarzwald); M. Casper (auch elektronisch unter:* http://www.ubka.uni-karlsruhe.de/eva/index.html)

Heft 211/2001 *Einfluß von Regelungsbauwerken auf die Wasserspiegellagen in Flüssen; F. Ritzert (auch elektronisch unter:* http://www.ubka.uni-karlsruhe.de/eva/index.html)

Heft 212/2001 *Konzept für einen ganzheitlichen Gewässerschutz; W. Hauck*

Heft 213/2002 *A Hydrodynamic-Numerical Model of the River Rhine; P. T. Minh Thu (auch elektronisch unter:* http://www.ubka.uni-karlsruhe.de/eva/index.html)

Heft 214/2002 *Zur hydraulischen Systemanalyse von Wasserversorgungsnetzen; J. Deuerlein (auch elektronisch unter:* http://www.ubka.uni-karlsruhe.de/eva/index.html)

Heft 215/2002 *Feststofftransport und Geschwindigkeitsverteilung in Raugerinnen; K. Koll (nur elektronisch unter:* http://www.ubka.uni-karlsruhe.de/eva/index.html)

Heft 216/2002 *Simulationswerkzeuge zur Bewirtschaftung von Staustufenketten; A. Celan*

Heft 217/2002 *Deutsch-Russisches Wörterbuch für Wasserwirtschaft; R. Krohmer, I.S. Rumjanzev*

Heft 218/2002 *Entwurfsoptimierung städtischer Abwasserentsorgungsnetze; I. V. Domínguez Talavera (auch elektronisch unter:* http://www.ubka.uni-karlsruhe.de/eva/index.html)

Heft 219/2002 *Kontrolle von Barrieren: Bestimmung der hydraulischen Leitfähigkeit an Hand des Bodenwassergehaltes; R. Schuhmann (auch elektronisch unter:* http://www.ubka.uni-karlsruhe.de/eva/index.html)

Heft 220/2003 *Langfristige, hydrologische Betrachtung der Grundwasserdynamik am Beispiel der Mittleren Elbe; P.-A. Burek (auch elektronisch unter:* http://www.ubka.uni-karlsruhe.de/eva/index.html)

Heft 221/2003 *Wassermengenbewirtschaftung im Einzugsgebiet der Ruhr: Simulation und Echtzeitbetrieb; T. Brudy-Zippelius (auch elektronisch unter:* http://www.ubka.uni-karlsruhe.de/eva/index.html)

Heft 222/2004 *Russisch-Deutsches Wörterbuch für Wasserwirtschaft; R. Krohmer, I.S.Rumjanzev*

Heft 223/2004 *Mobilisierung und Immobilisierung von mineralischen Feinstkorn-aggregaten an Gewässersohlen; J.-W. Kim (nur elektronisch unter:* http://www.ubka.uni-karlsruhe.de/eva/index.html)

Heft 224/2004 *Strömungsstruktur und Impulsaustausch in gegliederten Gerinnen mit Vorlandvegetation; I. Schnauder (nur elektronisch unter:* http://www.ubka.uni-karlsruhe.de/eva/index.html)

Heft 225/2004 *Towards Decision Support Models for Un-gauged Catchment in India, The Case of Anas Catchment; A. K. Singh (nur elektronisch unter:* http://www.ubka.uni-karlsruhe.de/eva/index.html)

Heft 226/2004 *Integrales Hochwasser-SimulationssystemNeckar – Verfahren, Werkzeuge, Anwendungen und Übertragungen; P. Oberle (auch elektronisch unter:* http://www.ubka.uni-karlsruhe.de/eva/index.html), noch nicht erschienen, Aug. 2005

Heft 227/2004 *Small Hydropower Plants Based Power Systems for Remote Regions; R. K. Maskey (nur elektronisch unter:* http://www.ubka.uni-karlsruhe.de/eva/index.html) noch nicht erschienen, Juli 2005

Heft 228/2004 *Spatial Time Domain Reflectometry and its Application for Monitoring Transient Soil Moisture Profile; R. Becker (nur elektronisch unter:* http://www.ubka.uni-karlsruhe.de/eva/index.html)

Heft 229/2005 *River Flood Prediction Systems: Towards Complementary Hydrodynamic, Hydrological and Data Driven Models with Uncertainty Analysis; R. Shrestha (auch elektronisch unter:* http://www.ubka.uni-karlsruhe.de/eva/index.html)

Heft 230/2005	*Empfehlungen zur naturnahen Gewässerentwicklung im urbanen Raum –unter Berücksichtigung der Hochwassersicherheit-; B. Lehmann (auch elektronisch unter:* http://www.ubka.uni-karlsruhe.de/eva/index.html)
Heft 231/2005	*Einfluß der Oberflächenströmung auf die permeable Gewässersohle; S. Vollmer (auch elektronisch unter:* http://www.ubka.uni-karlsruhe.de/eva/index.html)
Heft 232/2005	*Optimization of Internal Hydraulics and of System Design for PUMPS AS TURBINES with Field Implementation and Evaluation; P. Singh (auch elektronisch unter:* http://www.ubka.uni-karlsruhe.de/eva/index.html)

Bestellungen an:

Institut für Wasser und Gewässerentwicklung
-Bereich Wasserwirtschaft und Kulturtechnik-
Bibliothek
Universität Karlsruhe
Kaiserstr. 12
D-76131 Karlsruhe
Tel.: (0721) 608 6389
Fax: (0721) 60 60 46
e-mail: raskob@iwg.uka.de

° *vergriffen*